# Sutter Survey:
## Telescope Breakthrough Enables MicroSats to Map Accessible NEOs

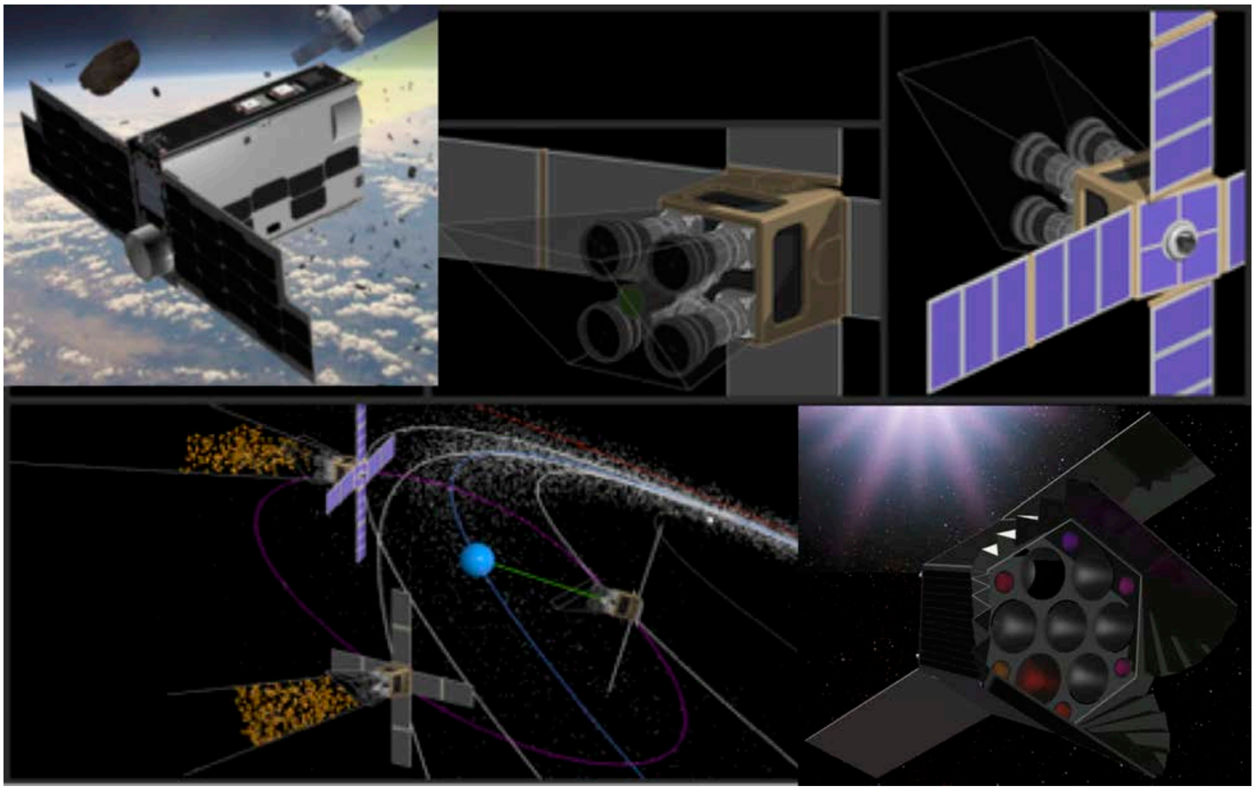

NIAC Phase I Final Report
14 February 2018

Joel C. Sercel, PhD
Principal Investigator
sercel@transastracorp.com

Trans Astronautica Corp.
Lake View Terrace, CA 91342

## Executive Summary

There are three primary reasons why it is important for NASA to develop better ways to locate and characterize Near Earth Objects (NEOs). First, NEOs are an impact hazard to the Earth and congress has mandated that NASA find 90 percent of all the Potentially Hazardous Objects (PHOs) over 140 meters by the end of 2020. NASA will fail to meet this mandate due to funding limitations and the cost and technical performance of current asteroid survey approaches. The Sutter Survey will solve this problem. Second, measuring NEO population distributions will unlock the answers to critical questions dealing with the formation and evolution of the solar system. Finally, NEOs are important targets for human exploration and they represent a virtually unlimited long term resource of valuable material for radiation shielding, propellant, and life support consumables that could make NASA's planned deep space human exploration program affordable.

In the past few years it has become increasingly clear that space exploration, commercialization, and colonization are not affordable as long as they are dependent on Earth for all of the resources involved. Even with the recent advances in launch vehicle cost reductions, the requirements for material (and particularly propellant) from Earth rapidly makes any ambitious program unrealistic, given the costs involved. However, lunar or asteroid resource extraction and utilization have the potential to radically reduce the need for large quantities of propellant and other resources from Earth, and to do so in a manner that makes economic and commercial sense as well.

Before asteroid In-Situ Resource Utilization (ISRU) can become a reality, the technology to find and track useful asteroids must be developed. Current Earth-based telescopes are not designed for this purpose and are limited by atmospheric considerations. Most asteroid detection efforts have been relegated to finding potentially hazardous object (PHOs) which, while important for the long term survival of humanity, is not suitable for finding targets for asteroid ISRU.

For every >140 m NEO, such as those targeted by the congressional mandate, there are about 200 intermediate sized (≈>20 meter class) objects. Going further down the size scale, for each 140 m object there are estimated to be over 1,000 ten meter sized objects and more than 8,000 objects five meters or larger. Due to their large numbers, these smallest of NEOs are the most likely to be highly accessible as space resource and human exploration targets. Because their size makes them easier to capture and work with using reasonably sized equipment, they are ideally suited as sources of ISRU space resources. Unfortunately, no sky surveys or methods currently being conducted or planned can find a significant fraction of these most plentiful and valuable but elusive small volatile rich targets. The energy requirements for accessing these NEO asteroids are less than half that required for lunar surface operations, which makes them a more attractive near-term solution, and could pave the way for later lunar surface missions.

The Sutter Survey approach applies new information processing capabilities and algorithms, small-satellite technology, and mission design concepts to create a series of affordable space missions that are specifically designed to identify these target asteroids and thus make their use for space resources a reality. This approach consists of an initial ground demonstration to verify the novel tracking software approach by using an existing telescope with an image plane and processing hardware that is similar if not identical to that planned for the following flight demonstration. The ground demonstration is then followed by a cube-sat implementation for an Earth orbiting mission to further refine the approach and provide additional evidence of intended performance. The full Sutter Survey mission, consisting of 3 small spacecraft, would then be launched into a novel heliocentric pseudo-Earth orbit that would keep the spacecraft with ~0.05 AU (approximately 7.5 million kilometers) of Earth and allow for identification and characterization of the most accessible and useful NEOs. At this point the use of the Sutter name becomes clear as it is anticipated that these resources will enable the equivalent of the California Gold Rush (triggered by the discovery of gold at Sutter's Mill) in space. A follow-on to the Sutter Survey mission, named Sutter Extreme, would continue to build on this approach and provide improved detection and characterization capabilities.

During this Phase 1 study, the Sutter Demo and Sutter Survey spacecraft and mission architectures have been examined in detail. The ground demonstration is described and is planned to be the subject of a Phase 2 proposal. The Sutter Demo spacecraft design is at a level that could allow it to be built and launched in the next two years for the cost of a few million dollars, and will likely be the subject of a Tipping Point proposal (or other similar opportunity) in the very near future. The Sutter Survey spacecraft design makes full use of available micro-sat technology, while including some advanced capabilities in microwave electro-thermal (MET) propulsion and laser communication. These designs and the supporting analyses are presented as part of this report. Additional definition of the Extreme mission has also been made, although not at the same level of fidelity as the Demo and Survey mission, as it is likely that additional technological innovations will be available in its later development timeframe.

The Sutter roadmap of missions provides a key capability in transforming space exploration. Coupled with developing technology for spacecraft capable of asteroid rendezvous and resource extraction, these missions can make asteroid ISRU not only practical but routine, opening up space to a more aggressive program of crewed space exploration to the lunar surface, other NEOs, and even Mars, as well as commercial exploitation and eventual colonization of space.

## Credits and Acknowledgements

The PI would like to acknowledge the contributions of the following individuals to this study and report:

Science Lead: Robert Jedicke, PhD
Systems Engineering: Craig Peterson
Astro-Digital Spacecraft support: Patrick Shannon
Tracking Software and Algorithms: Peter Gural
Illustrations: Anthony Longman

# Table of Contents

# 1. Introduction and Background

## 1.1 Overview of Report

This report contains the results of the NIAC Phase 1 study of the Sutter Survey concept. It is organized into 5 sections:

- Introduction and Background
- Innovations
- Sutter Mission System Architecture
- Path Forward
- Key Findings and Conclusions

The Introduction and Background section provides the rationale and motivation for the Sutter Survey approach. It specifies the problem and motivation for Asteroid Prospecting, the Requirements such a Prospecting System must meet, the corresponding System Design necessary to meet the requirements, an overview of the Sutter Survey Mission Roadmap as the best way to implement the required systems, and finally some descriptions of other related development efforts by TransAstra that support the goal of asteroid ISRU.

The Innovations section highlights some of the novel aspects of the Sutter Survey that make it feasible. The Sutter Mission System Architecture provides detailed information on the mission and spacecraft designs and supporting analyses that make up the Sutter Roadmap of missions including the newly developed near-term ground demonstration. The Path Forward describes the plan to continue to advance the Sutter Survey concept and roadmap missions beyond this study. The Key Findings and Conclusions section provides a summary of the major accomplishments achieved and conclusions drawn from this Phase 1 study.

A bibliography of relevant articles and references is also provided.

## 1.2 Problem and Motivation

There are three primary reasons why it is important for NASA to develop better ways to locate and characterize Near Earth Objects (NEOs). First, NEOs are an impact hazard to the Earth and Congress has mandated that NASA find 90 percent of all the Potentially Hazardous Objects (PHOs) over 140 meters by the end of 2020. NASA will fail to meet this mandate due to funding limitations and the cost and technical performance of current asteroid survey approaches. The Sutter Survey will solve this problem.

Second, measuring, instead of estimating, NEO population distributions will unlock the answers to critical questions dealing with the formation and evolution of the solar system.

Finally, NEOs are important targets for human exploration and they represent a virtually unlimited long term resource of valuable material for radiation shielding, propellant, and life support consumables that could make NASA’s planned deep space human exploration program affordable.

For every >140 m NEO, such as those targeted by the congressional mandate, there are about 200 intermediate sized (≈>20 meter class) objects. Because of their numbers, these intermediate sized objects are more likely to impact the Earth with detrimental effect but are not efficiently identified by current survey methods. One such example was the Chelyabinsk meteor which hit Russia in 2013 damaging 7,000 buildings and injuring 1,491 people.

Going further down the size scale, for each 140 m object there are over 1,000 ten meter sized objects and more than 8,000 objects five meters or larger. Due to their large numbers, these smallest of NEOs are the most likely to be highly accessible as space resource and human exploration targets. Because their size makes them easier to capture and work with using reasonably sized equipment, they are ideally suited as sources of ISRU space resources. ***Unfortunately, no sky surveys or methods currently being conducted or planned can find a significant fraction of these most plentiful and valuable but elusive small volatile rich targets.***

Finding several low ΔV, water rich asteroids will fundamentally enable a whole new asteroid mining industry. The inexpensive propellant harvested in space by this new industry will be made available to NASA at low cost *in space* to enable affordable human exploration missions to the Moon and asteroids. Performance modeling shows that Sutter Demo will find, track, and prospect, hundreds of new NEAs per year. Customers for Sutter Survey will include industrial asteroid mining companies, the science community, and NASA in its mission of planetary defense.

### 1.2.1 Background: Optical Mining of Asteroids

Optical Mining uses highly concentrated sunlight focused through a device called a “stinger” to heat the asteroid surface, resulting in a phenomenon know as spalling. Figure 1-1 shows how a mining spacecraft design by TransAstra called the Honey Bee (Sercel 2016) would be launched from Earth for an asteroid mining mission that would form part of a fleet capable of returning dozens of metric tons of extracted water and $CO_2$ annually to a convenient location near the moon. This can form the basis for a commercial company to provide resources in the cis-lunar area. Figure 1-2 illustrates and describes the basics of the spalling process on the surface of an asteroid. Figure 1-3 illustrates how this would occur using the conceptual mining spacecraft. Figure 1-4 provides an artist’s conception of the Honey Bee spacecraft capturing an asteroid for mining.

A detailed examination of the economics of such an approach to asteroid resource use is provided in a recent NASA Report “Stepping Stones: Economic Analysis of Space Transportation Supplied From NEO Resources“, available online. Laboratory experiments have been conducted to verify the effectiveness of the Optical Mining approach (Sercel 2016). Additional work is planned using an Optical Mining Testbed and a possible flight experiment using the International Space Station (ISS), currently being funded as a NIAC phase II study.

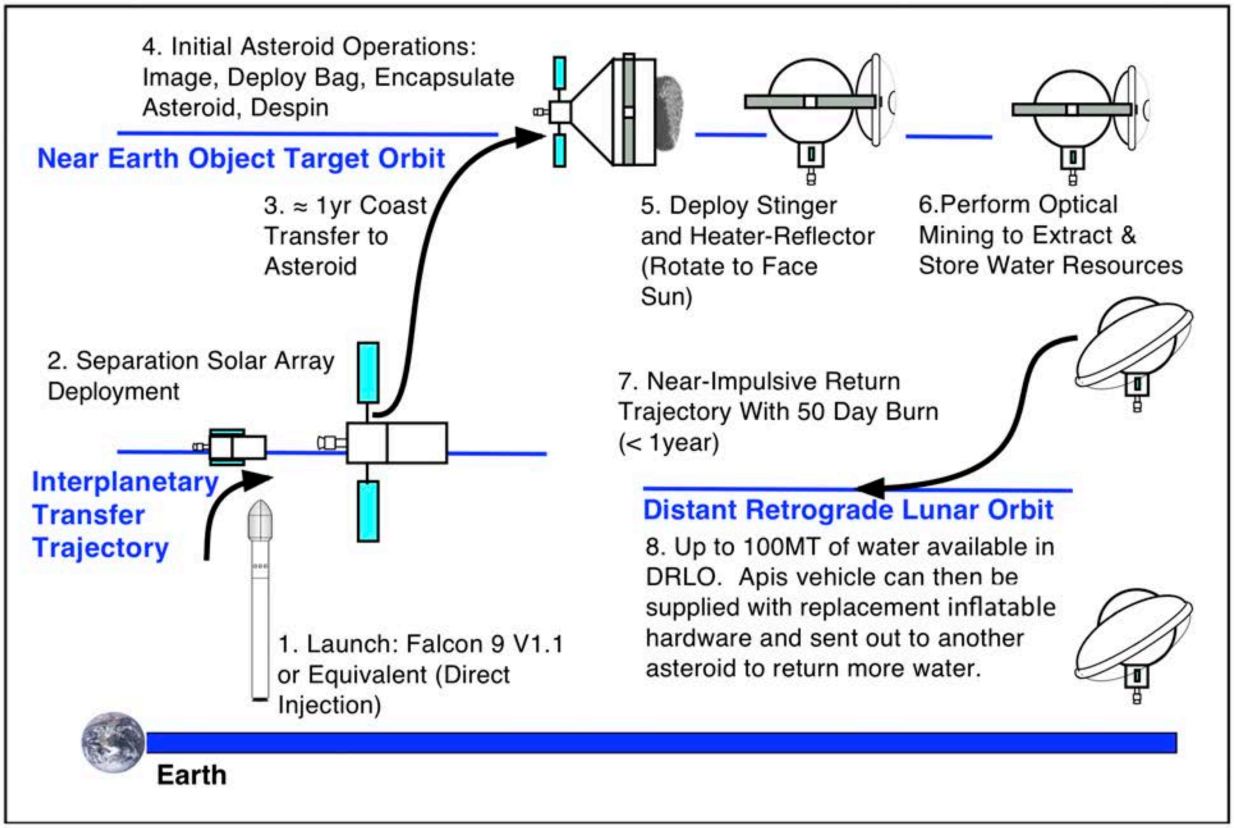


Figure 1-1 - Operational View of Asteroid mining mission.

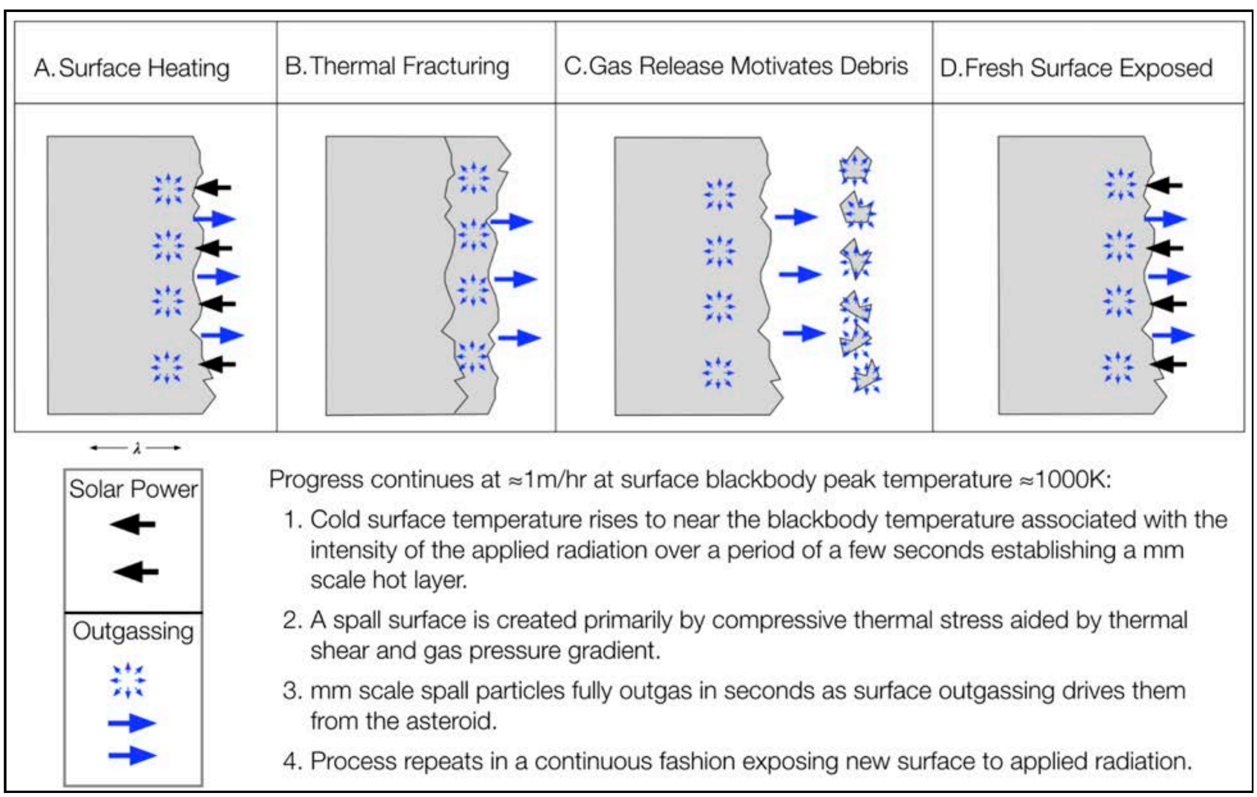


Figure 1-2: The Physics of Spalling in Optical Mining

1.2.2 Asteroid Prospecting Observing Requirements

*A key goal of Sutter Survey is asteroid prospecting*. In terrestrial mining prospecting is the search for mineral deposits in a place, especially by means of experimental drilling and excavation. This definition of prospecting is the standard in terrestrial mining because the Earth is a geologically differentiated planet and it is not obvious where a vein of ore might be by looking at the surface. Some large asteroids are thought to be geologically

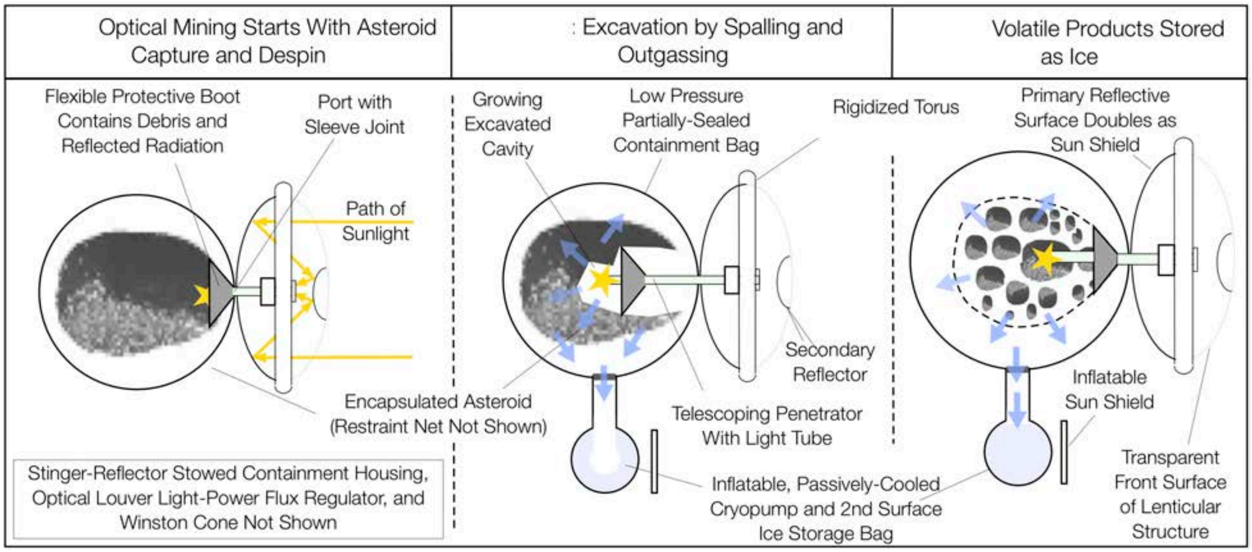


Figure 1-3: Application of Optical Mining to Asteroid mining.

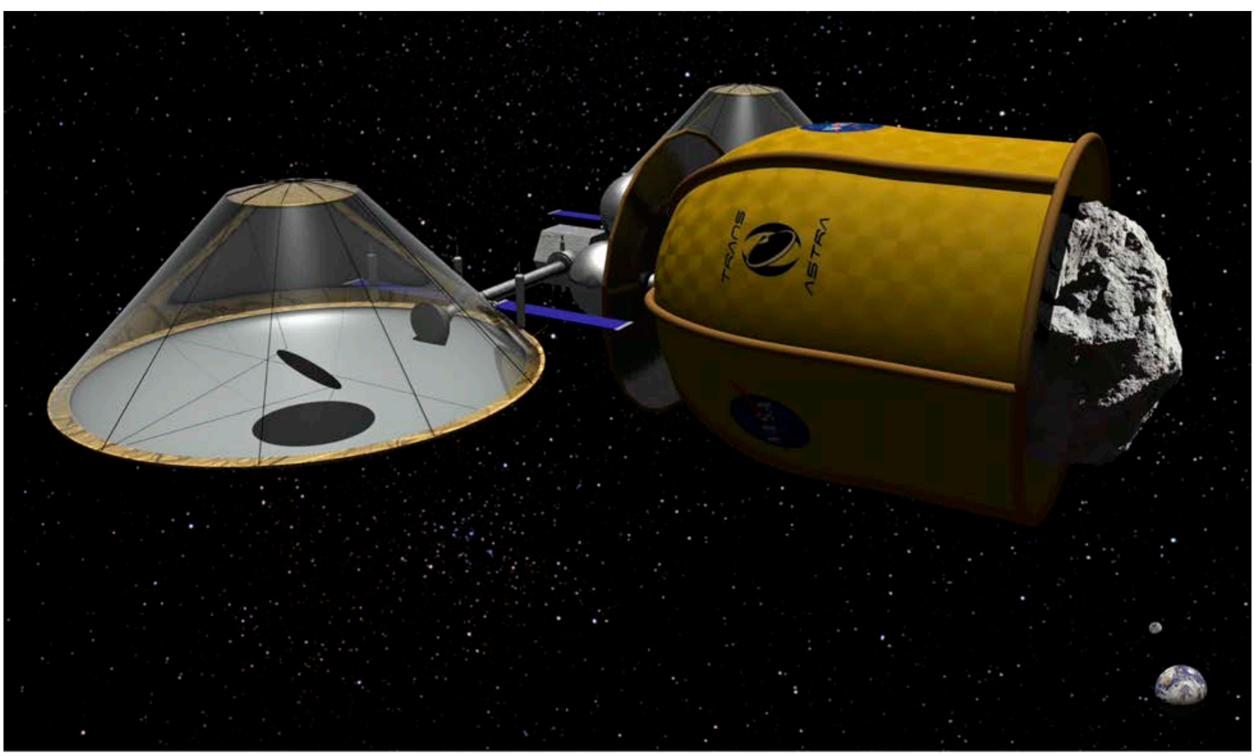


Figure 1-4: Illustration of Apis Spacecraft Capturing an Asteroid for Resource Extraction.

differentiated, but most small asteroids and virtually all of the water rich targets we are interested in are known from meteorite data and other observations to be primitive objects that are not geologically differentiated. This means that by normalizing for the surface effects of space weathering, measurements of the surface of these objects are good indicators of the body's composition.

Before making a decision to send an Optical Mining mission to a specific low ΔV asteroid, its orbital elements must be accurately predicted and it must be determined that it is a water rich target. It must also be ensured that is not spinning too fast and that its diameter is in a pre-specified range (between 5 m and 20 m). Given these needs, in the context of Optical Mining, *prospecting* means: 1) determining the target's spin state to screen out those that rotate too rapidly for practical resource harvesting, and 2) screening out those that either do not have high volatile content or are too difficult to distinguish from low volatile content bodies.

The screening process must be performed with very low false positive rates ensuring that mining missions seldom visit dry targets. Rapidly detecting the small, dark ISRU candidate objects on low ΔV orbits will require a system far more capable than any existing or planned asteroid survey on the ground or in space. Some of the most important requirements for the system, derived from the need to serve as a prospecting tool, are provided in Table 1-1. To place Table 1-1 in context the following paragraphs below describe the measurement requirements on the system in several different areas including photon flux, astrometry, taxonomic type, etc…

<u>Photon Flux</u>: The system must be able to accurately measure the calibrated photon flux from each source. The received photon rate is proportional to the asteroid's observed cross sectional area (related to its diameter), albedo, and the inverse-square of the object's heliocentric and topocentric distance. The flux should be measured to better than about 10% because the limiting factor for measuring the asteroid's diameter will be the knowledge of its albedo.

<u>Astrometry</u>: Measuring the apparent location of the target, astrometry, is the key to orbit determination. It requires the topocentric location of the observer to be known precisely. The Sutter system should be able to match typical asteroid surveys that obtain astrometric measurements at about the 0.1" level.

<u>Taxonomic Type</u>: An asteroid's mineralogy is correlated with its taxonomy and can be determined from low resolution spectra or a `sufficient' number of colors (equivalent to very low resolution spectroscopy). Taxonomic classification, specifically into one of C-complex asteroid sub-types, will be sufficient for identification of potential asteroid mining targets. We note that there are water rich taxonomic types that may be difficult to distinguish from water poor types. There are also water rich types that can be distinguished spectroscopically with high confidence. The good news is that we can reject targets with a high probability of taxonomic error for the purposes of asteroid prospecting because the

Table 1-1 - Concept Level Survey System Requirements

| Asteroid property | Notional requirement | Notional Survey System Requirement |
|---|---|---|
| Diameter | >5 meter and <10 meter | - Measure photon flux<br>- Measure albedo<br>- Measure topocentric distance<br>- Measure Heliocentric distance |
| Diameter uncertainty | +/- 50% | - Photon flux uncertainty <10%<br>- Albedo uncertainty <40%<br>- Topocentric distance <1%<br>- Heliocentric distance <1% |
| Shape | A:c < 2:1 (assuming triaxial ellipsoid a:b:c) | Photon flux uncertainty < 10% in 6 s<br>- 100 light curves over > 7days<br>> 10 deg phase angle coverage |
| Spin rate | < 1 rev/minute | - Time-resolved photometry in 6 s |
| Spin state | 90% of ang. Mom in principal axis | - Photon flux uncertainty < 10% in 6s<br>- 100 light curves over > 7days<br>> 10 deg phase angle coverage |
| Orbital uncertainty | $10^{-7}$ | - Astrometric uncertainty <0.5"<br>- Arc-length > 20 deg OR astrometry from >1 spacecraft over the course of >2 days |
| Return ΔV | < 3 km/s | - Targets are constrained to a torus with radius ~0.1 au centered on Earth's orbit |
| Water content | >= 10 wt% | - R (d-lambda/lambda) >10 spectrophotometry OR albedo determination |

cost of rejecting a candidate telescopically is low, but the cost of going to an asteroid for mining only to find it arid would be unacceptable high if it happened often enough.

Albedo: The fraction of sunlight that is reflected off an asteroid is critical to measuring the object's diameter and provides a first order approximation of the asteroid's taxonomy (and vice versa). Albedo can be estimated from the flux ratio in visible and near-IR bands or by a taxonomic classification. An albedo uncertainty of <40% should meet the diameter uncertainty requirement. In Sutter Survey we will infer albedo from taxonomic classification. In Sutter Extreme we plan to add an IR telescope to each spacecraft to obtain more accurate albedo measurements.

Topocentric and Heliocentric Distances: The distance between the detection system and the asteroid is known as the topocentric distance. It must be combined with accurate knowledge of the spacecraft's and the asteroid's heliocentric positions to determine the object's orbit, diameter, and other properties. These properties are derivable from many astrometric observations over the course of time. The longer the observation period is, the better the orbit determination.

Shape: Asteroid shapes can be derived from their light curves when they are observed over many rotation periods, over a long period of time, and at different aspect angles. Ground-based observations normally require years of observations to be 'inverted' to yield shape estimates.

Spin Rate: An asteroid's rotation rate can be measured from changes in its apparent brightness as a function of time. The asteroid's rotation causes the apparent brightness of the object to change in a periodic manner due to the shape of the object presenting different cross sections or because of surface albedo differences. Spin rate is not possible to measure in the unlikely event that the spin pole is pointed at the observer. Similarly, spin rate cannot be measured if the asteroid is close to being spherical and/or there are no surface albedo variations. The expected spin rate of asteroids in the 5 m to 10 m diameter range is less than once per minute (Farinella et al., 1998). See Figures 1-5 and 1-6 (next page) for current estimates of spin rates. Notice that Figure 1-6 shows a distinct cutoff in asteroid population statistics for spin rates above the speed at which a body with minimal tensile strength would pull apart due to centrifugal force. Note that this data suggests that very few large asteroids are solid bodies, but for targets in the size range under 100 m, there is reason to believe that some targets may be monolithic. Optical Mining is designed to handle this variation in composition.

Spin State: For asteroid mining and human exploration we need to know not only the spin rate, but also the spin *state* of the target body i.e. whether it is in a principal-axis rotation state or tumbling (rotating around multiple axes). Determining the spin state requires observations over many rotation periods with a set of observations separated in time such that the target can be viewed at aspect angles that vary over a wide range. This will be possible with the Sutter Survey mission design because the targets are expected to have rotation periods on the order of minutes and because the survey telescopes are relatively close to the targets. Thus, multiple ten minute duration observations over a period of several weeks should be adequate to determine spin state (and will also reduce the orbital element uncertainty).

Orbit Determination: The heliocentric path of an asteroid can, in principle, be determined with just two infinitely precise observations of an asteroid if the observations provide both the apparent position and apparent motion. In reality, most main belt asteroids need to be observed in at least 3 apparitions to have orbits that are sufficiently well-determined to be considered numbered. This is because most asteroids are far away and are only observed from ground-based locations.

Return ΔV: This parameter depends only on the ISRU candidate's orbital parameters and can be determined with sufficient accuracy even with an imprecise orbit determination.

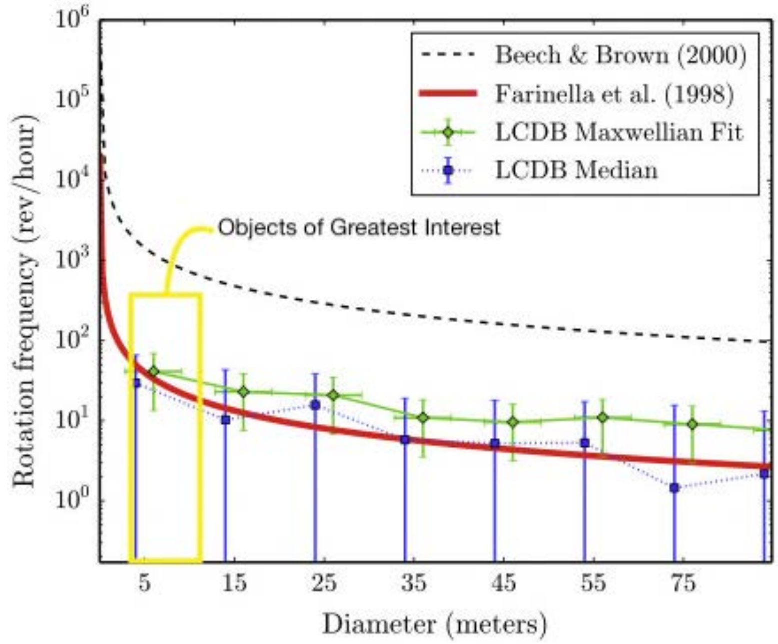


Figure 1-5 Rotation Frequency of Small Asteroids as a Function of Diameter. The data points joined by dotted lines represent the median of the data in 10 meter diameter bins from the Light Curve Database (LCDB).

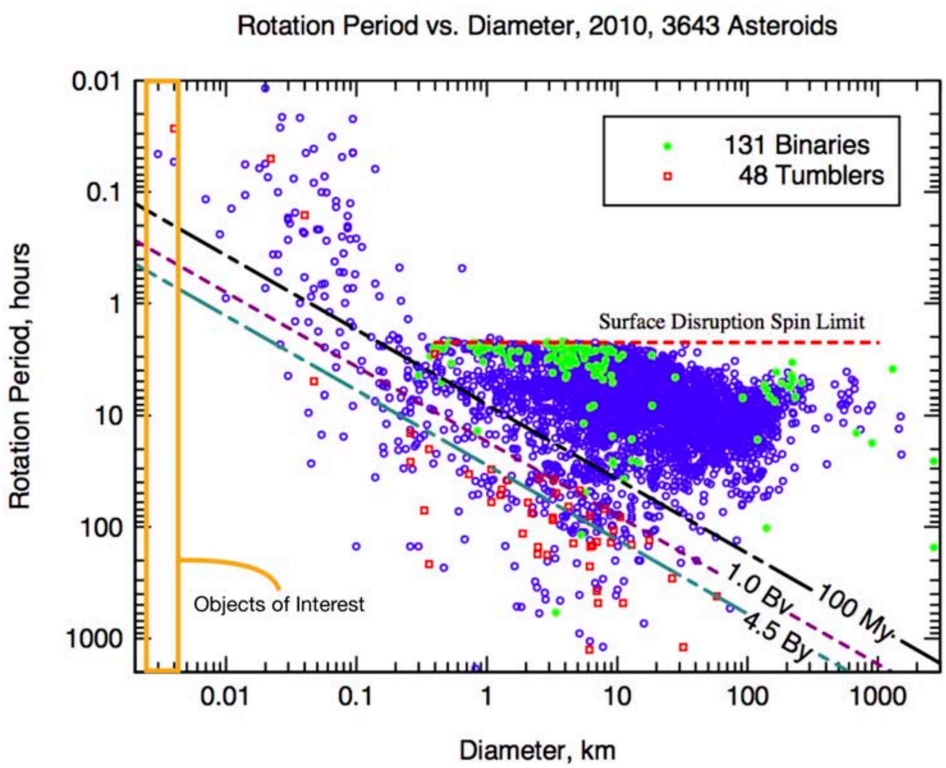


Figure 1-6 Rotation Period vs. Diameter [Sanchez]. Note that the surface disruption spin limit statistics suggest that asteroids larger than a few hundred meters exhibit minimal tensile strength suggesting rubble piles while smaller asteroids in the size range of our interest may be monolithic in some cases. Optical Mining is designed to handle either case.

Table 1-2 Physical Measurements Needed for Asteroid ISRU

| Asteroid property | Notional requirement |
|---|---|
| Diameter | >5 meter and <10 meter |
| Diameter uncertainty | +/- 50% |
| Shape | A:c < 2:1 (assuming triaxial ellipsoid a:b:c) |
| Spin rate | < 1 rev/minute |
| Spin state | 90% of ang. Mom in principal axis |
| Orbit | Uncertainty on each element <$10^{-7}$ |
| Return delta-v | < 3 km/s |
| Water content | >= 10 wt% |

Water Content: This is the most difficult asteroid property to measure and will rely on proxy measurements of the asteroid taxonomy rather than direct detection of spectral lines or band indicating mineralogically bound water on the asteroid. Measuring asteroid taxonomy requires spectrophotometry (d-lambda/lambda~10) or low resolution spectroscopy (d-lambda/lambda~100). The distinction between the two is imprecise but the former typically uses multiple images in different filters while the latter typically uses a prism or grating to obtain the entire spectrum in one image.

### 1.2.3 Notional Survey System Design

To meet the detection capabilities listed above and summarized in Table 1-1, the system must be able to make the measurements summarized in Table 1-2. We generated a realistic set of >~4,000 synthetic ISRU candidates with ΔV < 3 km/s (Jedicke et al., 2018) extracted from a realistic population of 5 m to 10 m diameter NEOs. These objects are all on Earth-like orbits located in a torus around the Sun (See Figure 1-7). Almost all the objects are always within about 0.2 au of Earth's orbit but can range from heliocentric distances of about 0.8 au to 1.3 au (See Figure 1-8). Thus, the goal of the Sutter Survey System is to efficiently prospect these objects.

The fundamental issue in the design of the Sutter Survey System is that 5 m to 10 m dark asteroids are difficult to detect under any circumstances. The water bearing C-complex asteroids in the main belt population are very dark with albedos of about 4% but C-complex objects in the NEO population are, unexpectedly, three times brighter with an albedo of about 13% (Thomas et al., 2011). For the purpose of this discussion we split the difference and assume the water-bearing asteroids have an albedo of 8% so that a 5 (or 10) meter diameter asteroid has a absolute V magnitude of $H_V$=29.9 (or 28.4).

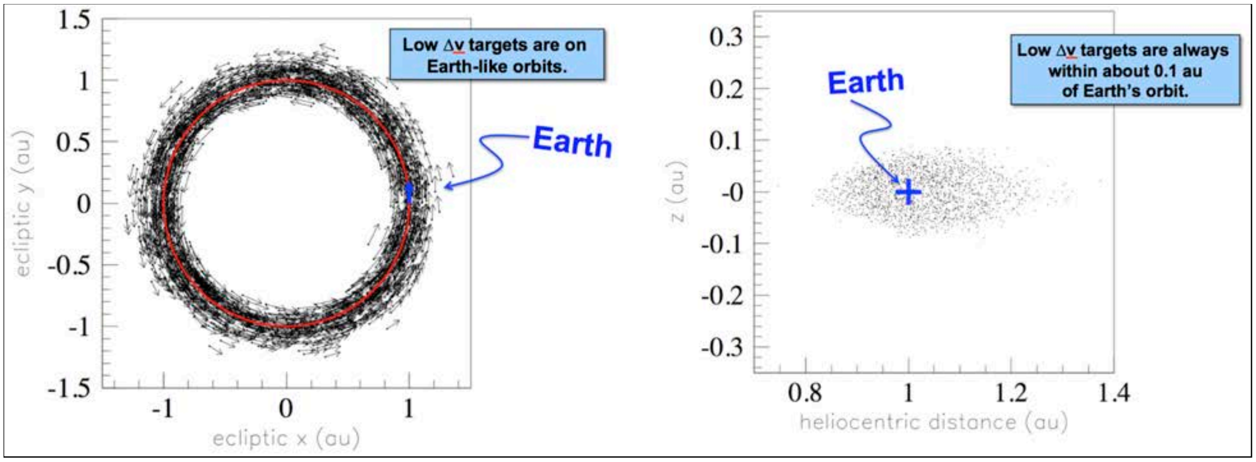


Figure 1-7 Distribution of Synthetic ISRU Candidates

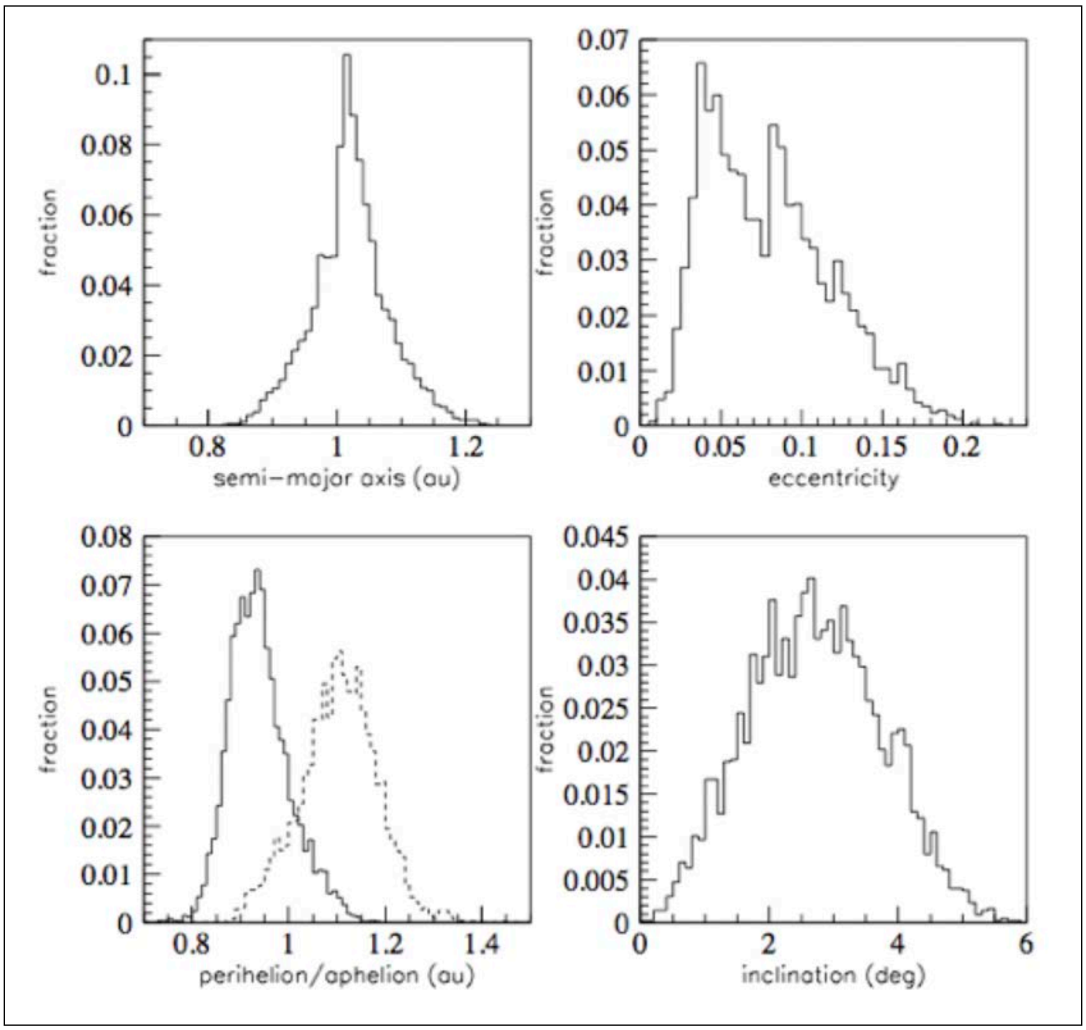


Figure 1-8 ISRU Candidate Orbital Elements. Incremental fractional (top left) semi-major axis, (top right) eccentricity, (bottom left) perihelion (solid) and aphelion (dashed) and (bottom right) inclination distributions of NEOs with a total Δ-V <3 km/sec. Residual binning effects that are particularly evident in the eccentricity pane are artifacts of the binning in the Granvik et al. (2016) NEO model.

A 10 m diameter object has V<23 at opposition if it is closer than 0.08 au from an observer and located about 1 au from the Sun while a 5 m diameter object would have the same brightness at half the distance. Our model predicts that there are roughly 7 low delta-v candidates with 0.08 au of the Earth at any time. These apparent magnitudes require long exposures or large apertures with ground-based telescopes. The problem with long exposures is that these objects can be moving so fast (Figure 1-9) that they spread their signal across many pixels on the imager, thereby reducing the apparent SNR. The billion dollar 8.4m diameter Large Synoptic Survey Telescope (LSST) will reach V~24.5 for stationary objects in ~10s exposures but the limiting magnitude will be reduced for objects moving faster than about 2.5 deg/day (See Figure 1-9). At these distances the object's

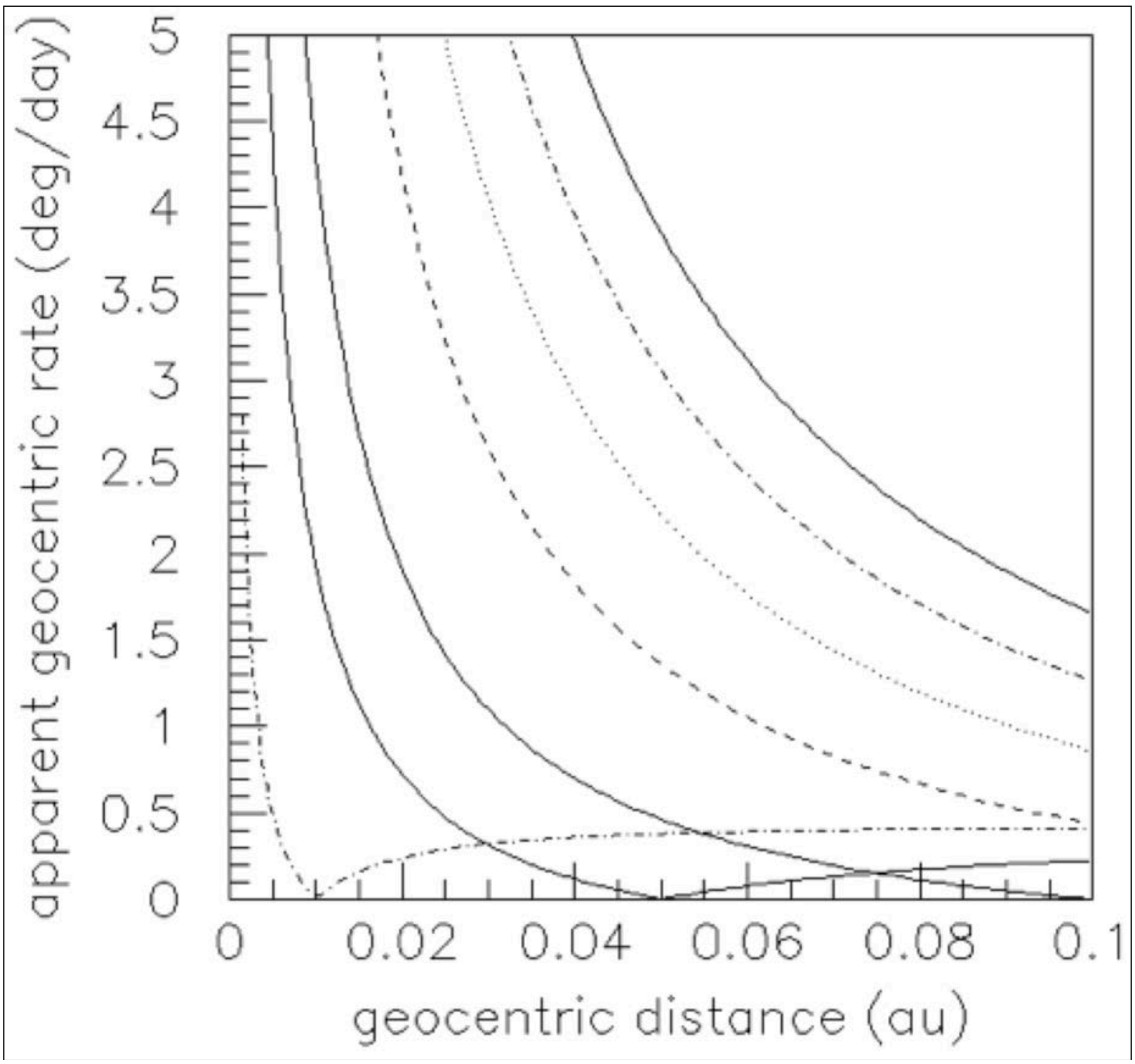


Figure 1-9 - Apparent Geocentric Rate of Motion of Objects vs. Geocentric Distance at Opposition and with the Object at Perihelion. The curves represent objects with eccentricities of 0.01, 0.05, 0.1, 0.2, 0.3, 0.4, 0.5 from bottom left outwards. i.e. the higher the eccentricity the faster the apparent rate of motion.

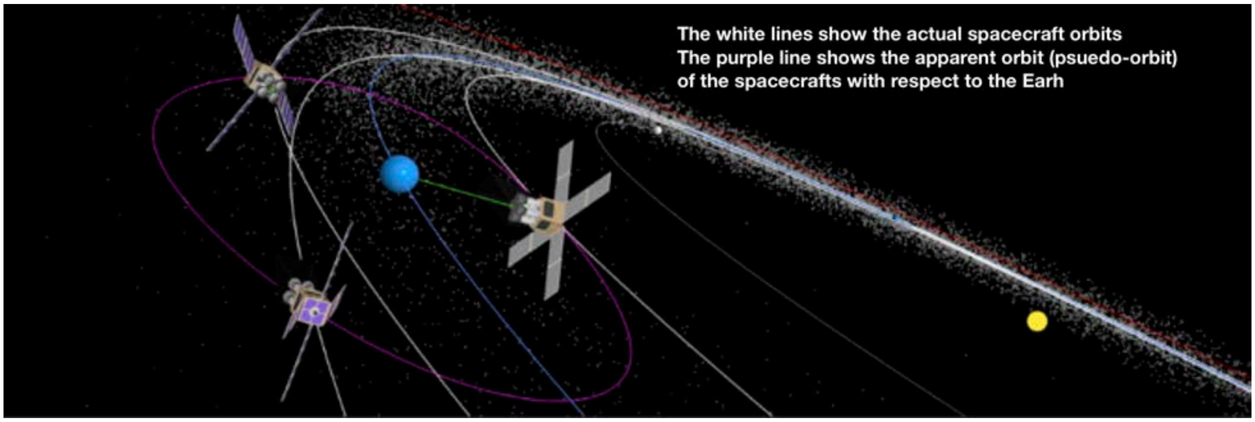


Figure 1-10 The Sutter Survey Approach

apparent rate of motion has a tremendous range from essentially stationary to tens of degrees per day (Figure 1-9). Thus, the Sutter survey system must be capable of detecting faint, rapidly moving objects.

These factors lead us to designing a space based system in Pseudo Geocentric Distant Retrograde (PGDR) Orbit with sCMOS detectors tied to graphics processor units running a Matched Filter Algorithm (MFA). These attributes of our missions architecture are discussed next.

<u>Multiple Spacecraft in Pseudo Geocentric Distant Retrograde (PGDR) Orbit</u>: A space-based detector system allows nearly 24 hour uninterrupted prospecting and provides a much deeper limiting magnitude at any given aperture size compared to ground-based surveying due to the elimination of sky background noise. An optimal location for surveying the volume within 0.08au of Earth would be a platform constantly located Sunward of Earth by 0.08 so that it could survey away from the Sun at all times and observe asteroids while they are fully illuminated (e.g. like full moon). This is not feasible from a dynamical standpoint without burning excess propellant for regular station keeping. Instead, we propose to have 3 or more Sutter Survey systems in heliocentric orbits that appear to be on pseudo-geocentric distant retrograde orbits as viewed from a geocentric frame (Figure 1-10).

These are stable orbits (e.g. Cyr et al., 2000; Stramacchia et al., 2016; Perozzi et al., 2017) requiring little station keeping because they are not near any massive body; the closest being the Earth that is roughly 8 Hill radii distant. The more spacecraft in the formation the more likely it is that one of them will be in the optimal location of 0.08 au towards the Sun for asteroid prospecting. With 2 or more spacecraft it is clear that one of them must always be interior to Earth's orbit where it can survey away from the Sun to detect asteroids. Spacecraft exterior to Earth's orbit may still be used for prospecting but with reduced efficiency or they can be used to obtain independent measurements of current ISRU candidates. The independent parallactic measurements of nearby ISRU candidates will accurately establish their orbits. Multiple observations of small objects, each for the period of many revolutions of rotation of the object, separated in time by a few weeks are needed to establish an object's rotation rate and state.

The survey system must be capable of very low resolution spectrophotometry yet suitable for eliminating ISRU candidates from consideration if they are not in the water bearing C-complex. Moderate resolution spectrophotometry may be capable of identifying particularly water-rich sub-types within the C-complex if we design and employ customized filters. (All astronomical surveys employ filters designed by astrophysicists for their purposes rather than filters optimized for asteroid characterization as we propose here). Table 1-3 summarizes the key requirements and the Sutter Survey System solution.

The Advantage of sCMOS detectors with Matched Filter Algorithm (MFA):

Infrared detectors such as those employed on NEOWISE (e.g. Mainzer 2011) and those planned for NEOCAM (e.g. Mainzer 2011), can reach the equivalent of faint limiting visual magnitudes and also benefit from reduced background confusion because stars tend to be faint in the IR while asteroids tend to be bright. But IR detectors require cooling have worse resolution, slower readout speed, and currently complicate implementing the matched filter algorithm (MFA). In addition, even passive cooling introduces extra complexity and cost. Visible-light, high frame rate, sCMOS detectors employing the MFA are a much better choice because, relative to IR detectors, they have better resolution, are cheaper, don't require cooling, and can implement the current MFA. With MFA they are not sensitive to trailing losses caused by high apparent rates of motion. A clutter suppression stage upfront of the MFA removes stationary objects from the images so there is little background confusion caused by high stellar sky plane densities. Furthermore, most of the 'background' asteroids will be main belt asteroids that will appear in each field with predictable directions and small rates of motion. The MFA can even be programmed to simply not detect main belt asteroids, thereby dramatically reducing the total number of asteroids that need to be considered in any manner. The rapid-readout sCMOS detectors also offer the additional capability of obtaining a series of short-exposure sequences for measuring rotational rates of even rapidly rotating asteroids.

## 1.3 The Sutter Development and Mission Roadmap

We propose a new type of low cost, high performance compound telescope, the Compound Matched Filter Algorithm (C-MFA) Telescope, for a series of increasingly capable space missions that make up the ***Sutter Roadmap Missions***, named after the Sutter's Mill discovery which led to the California gold rush. This approach is uniquely suited to detect and characterize near Earth Objects that are highly suitable for resource extraction and use. Like its namesake, the Sutter Survey will discover and characterize such valuable resources in space that it too will lead to a *gold rush:* this one in space.

### 1.3.1 Sutter Roadmap

The Sutter roadmap starts with Sutter Demo, a 6U, or potentially upgraded to a 16U, LEO CubeSat mission that demonstrates key technical aspects of the Sutter Survey. As

Table 1-3 Notional Survey System Requirement and Solutions

| Notional survey system requirement | Notional survey system solution |
|---|---|
| Targets are constrained to a torus with radius~0.1 au centered on Earth's orbit | Multiple platforms on roughly 0.08au DRO provide continuous surveying of the volume of space within about 0.1au centered on Earth. |
| Measure photon flux<br>Measure albedo<br><br>Measure topocentric distance<br>Measure Heliocentric distance | sCMOS detectors detect small rapidly rotating objects.<br>Use of multiple optimized filters for determining asteroid taxonomy that is correlated with albedo.<br>Multiple survey platforms in DRO allow rapid orbit determination with high accuracy from which these values are calculated. |
| Photon flux uncertainty <10%<br><br>Albedo uncertainty <40%<br><br>topocentric distance <1%<br>Heliocentric distance <1% | sCMOS detectors and MFA enable high SNR measurements of faint moving targets.<br>Taxonomic classification is correlated with albedo at about this level.<br>Multiple survey platforms in DRO allow rapid orbit determination with high accuracy. |
| Photon flux uncertainty < 10% in 6s<br><br><br><br>100 light curves over > 7days<br><br><br><br>>10 deg phase angle coverage | sCMOS detectors and MFA enable high SNR measurements of faint moving targets. Once an object is discovered the exposure time and MFA algorithm can be adjusted for optimal light curve coverage.<br>Typical rotation rates of 5-10m diameter asteroids is about 2 minutes so 100 light curves is only about 0.2% of the available observing time during a week. Only candidates that meet the delta-v requirement require these measurements.<br>Multiple platforms automatically provide >>10 deg phase angle coverage because each s/c is separated by roughly 120 deg (assuming nominal 3-system formation). |
| Time-resolved photometry in 6s | sCMOS detectors and MFA enable high SNR measurements of faint moving targets. Once an object is discovered the exposure time and MFA algorithm can be adjusted for optimal light curve coverage. |
| Astrometric uncertainty <0.5"<br><br><br>Arc-length > 20 deg OR astrometry from >1 s/c over the course of >7 days | sCMOS detectors and MFA enable good resolution and PSFs with many background stars in the same wide FOV for establishing the astrometric reference system.<br>Multiple platforms automatically provide parallactic detections of the same asteroid for accurate orbit determination. |
| R>10 spectrophotometry<br>OR albedo determination | System capability for multiple simultaneous customized filter measurements of the same object. Simultaneity avoids spatial color differences. Optimized taxonomic filters provide best ISRU candidate triage. |

depicted in Figure 1-10, after Sutter Demo, the first operational mission involves a constellation of three SmallSats in heliocentric space in an innovative new type of asteroid survey orbit called a Pseudo Geocentric Distant Retrograde (PGDR) orbit. We estimate that this entire constellation can be built for less than $150M, launched as piggy back payloads, and perform like the billion dollar, 8 m aperture, Large Synoptic Survey Telescope (LSST) ground based telescope at finding and tracking small dark asteroids.

More than just finding and tracking, because of the unique features of CMFA, Sutter Survey will also prospect the targets it finds screening for water rich targets in specified ranges of diameter and rotation rate. After the deployment of the initial constellation, an even more capable *Sutter Extreme* mission can be launched to increase total asteroid discovery rate by more than an order of magnitude providing beyond flagship level mission performance at a price point well below the flagship level.

### 1.3.2 Low ΔV ISRU target orbit distribution

Jedicke et al. (2018) generated 200 million synthetic NEOs according to the Granvik et al. (2016) NEO model orbital element distribution. That is roughly the total number of NEOs larger than about 5 m diameter. They then used a simplified technique to estimate the maximum return-trip ΔV (i.e., the required ΔV to travel from the asteroid back to cis-lunar space) and selected only objects with return-trip ΔV < 3 km/s (see Figure 1-11).

The resulting sample of about 4,000 objects is probably an underestimate of the population because the number of available candidates increases as the cube of the ΔV and their technique methodically over-estimated the ΔV. (Subsequent careful analysis suggests that there may be 3x more objects.) The 3 km/s ΔV represents an important energy limit in that it presents a significant energy savings (>50%) over obtaining resources from the lunar surface, such as may be found in permanently shadowed craters.

They also calculated that roughly 20% of those objects are likely water-bearing objects in the asteroid C-complex so, for the purpose of argument, we work with a nominal value of 1,000 water-bearing low ΔV asteroids. These objects are on Earth-like orbits and spend 90% of their time in the heliocentric distance range from 0.895 au to 1.18 au. Nearly 30% of the low ΔV candidates have semi-major axis within 0.02 au of Earth's orbit so that they have long synodic periods. Furthermore, ~11% of the synthetic targets have aphelion distances less than 1 au so they are always interior to Earth's orbit (IEO; Zavodny et al., 2008) Their orbits make them difficult or nearly impossible to detect from Earth's surface at night because they only appear close to the Sun in twilight just before sunrise or after sunset. The combination of the difficult-or-impossible-to-detect IEOs and the long synodic period objects account for 40% of the low Δ-V NEO population.

### 1.3.3 Asteroid Detection Projections

The system discovery rates are estimated (Table 1-4 Annual Discovery Rates) in a manner consistent with our current understanding of the system’s concepts of operations. First, we generated a synthetic population of ISRU candidates and potentially hazardous objects

(PHO) with 10x the statistics of the actual population and calculated their position and velocity at one instant in time.

We could then assign any diameter and albedo to any (or all) objects in the population and determine the sky-plane density of objects from one of the populations at a particular size. Next, we combined that information with a reasonable size-frequency distribution for the

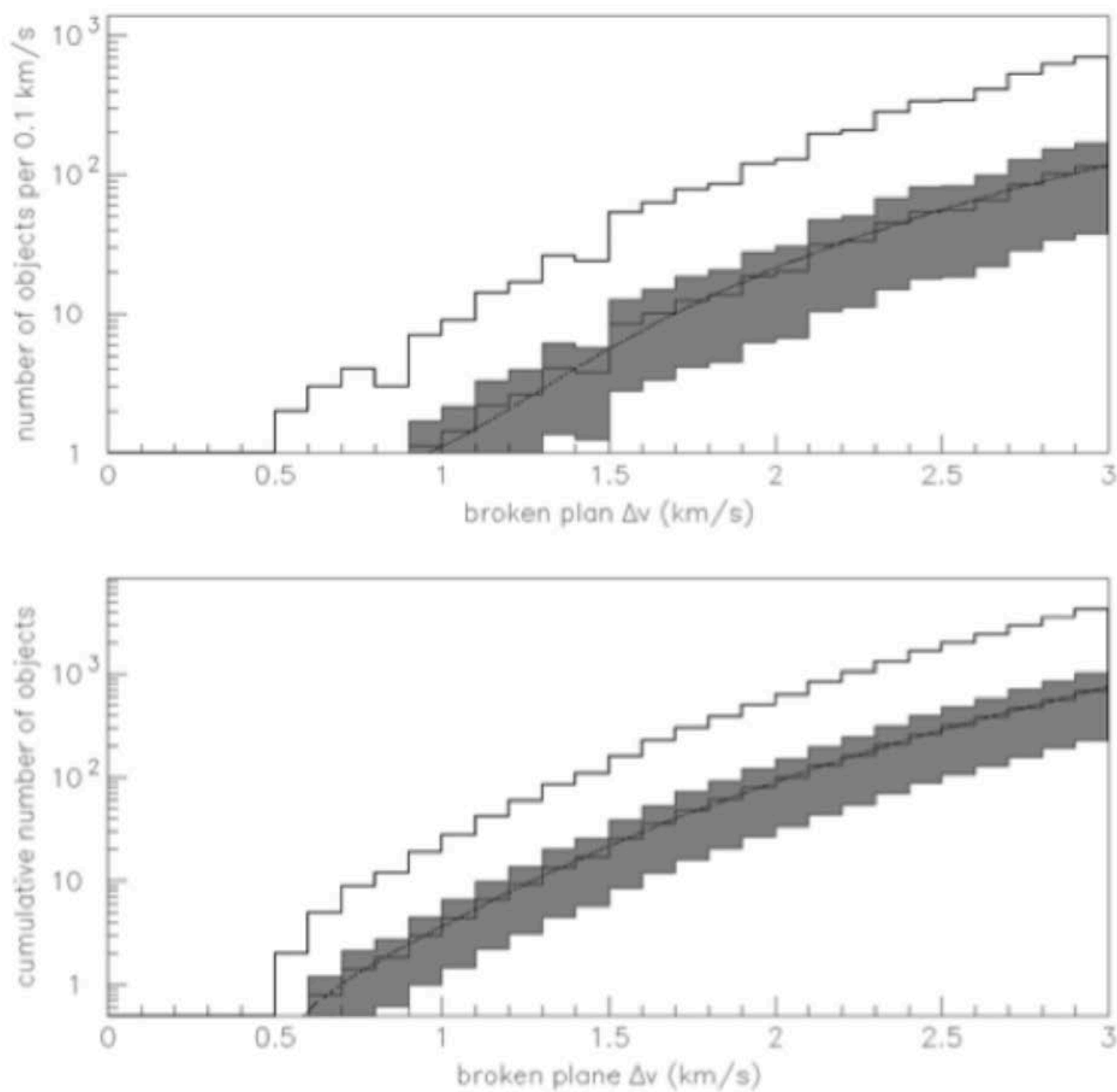


Figure 1-11 Δ-V Distribution of Targets of Interest: Incremental (top) and Cumulative (bottom) number of NEOs with diameter between 5 and 10 m per 100 m/sec bin. The topmost solid line in both panels represents all objects. The gray region in both panels represents a 50% uncertainty on the number of NEOs with the nominal value represented by the histogram in the gray region. The fitted curve through the incremental distribution is a 3rd order polynomial and the one through the cumulative distribution is a 5th order polynomial. There are more than 1,000 objects with a return Δ-V < 3 km/sec.

Table 1-4— Annual discovery rates

| Asteroid Type | Sutter Ground Demo | Sutter Space Demo (1 LEO) | Sutter Survey (3 Helio) | Sutter Extreme (3 Helio) |
|---|---|---|---|---|
| Bright NEOs > 5m Diameter with return ΔV < 3 km/s | 30 | 35 | 1,500 | 7,500 |
| Dark NEOs >5m Diameter With Return ΔV < 3 km/s | 15 | 20 | 900 | 3,600 |
| Total Water-Rich Return ΔV<3 km/s ISRU Targets | 3 | 4 | 150 | 600 |
| Total PHOs Relative to Current | 0.2x | 0.2x | 9x | 24x |

asteroids and a phase function that accounts for the geometry of the observations to calculate each object's apparent brightness. Finally, we determined the apparent rate of motion of each object. Combining all these data together allowed us to determine the total number of objects larger than a given diameter and brighter than a given limiting magnitude per square degree towards opposition.

The FOVs of the Sutter systems and the rates of motions of the objects are such that they can continuously survey towards opposition and the survey region will 'refresh' with new asteroids. Thus, the number of discovered objects is the product of the area of surveyed sky and the sky-plane density of objects in the direction of opposition. At this time we assume the surveys are surveying 100% of the time (i.e., we do not yet account for down time e.g. data transmission, candidate followup, etc.) Some of our assumptions break down with the more capable Sutter systems (i.e., they can survey so much that the sky does not necessarily 'refresh' with asteroids) but the comparisons provide a good assessment of the relative system power.

### 1.3.4 Implications for asteroid mining

Assuming parallel development of optical mining spacecraft, aka Honey Bees, initial missions will be sent to harvest "low-hanging fruit", i.e., lowest Δ-V targets with option to redirect if initial target does not pass close examination or otherwise provides unexpected difficulties. Difficulties include excessive irregularity, unmanageable spin rate, etc.. Assuming 50% of identified water-rich targets turn out to be useful, 2500 tonnes of water could be extracted annually for at least 20 years based on the detections expected up through the end of the Sutter Extreme missions.

Extended mission lifetimes or additional missions after Sutter Extreme would increase the total number of targets over time, although it may not be in a linear fashion as candidate asteroids move in and out of the near Earth vicinity. Also additional low-Δ-V targets may be detected that increase the round-trip time, requiring fielding of additional optical mining spacecraft to maintain the returned resource rate. Development of optical mining spacecraft with increased capacity (Queen Bees) will allow use of larger targets and greatly increase the total amount of resources that can be extracted and returned.

## 1.4 Related Work by TransAstra

The Sutter Survey is designed to usher in a "gold rush" in space by finding and prospecting a large number of low ΔV asteroid mining and ISRU targets. In addition to Sutter, TransAstra is developing other technologies and missions for finding and prospecting these targets designed to bring about the large scale utilization of asteroid resources. In one such effort, we have designed a novel new thruster called Omnivore™ Thruster, capable of using almost any liquid as a propellant and utilizing concentrated sunlight for solar thermal propulsion. This thruster development effort is the subject of a NIAC phase II proposal.

There are currently plans and proposals that would pave the way for development of the Apis Honey Bee Mining spacecraft. A Baseline Honey Bee vehicle design massing approximately 4000 kg and capable of capturing a 10 m diameter asteroid has been developed (Sercel 2016), along with the concept for a 250 kg Mini-Bee demonstration vehicle (Sercel 2017) compatible with a SmallSat launch vehicle. The Honey Bee is estimated as having the capability to return ~100 metric tons of water and $CO_2$ ices per asteroid resource extraction mission. An increased capacity version, Queen Bee, has also been the subject of conceptual development (Skelton, 2017). The Queen Bee would not only be capable of extracting much larger volumes of water, but could also be used to bring back processed regolith for potential use as shielding material for human habitats.

Figure 1-12 illustrates the various steps of the proposed Mini-Bee Mission. The Mini-Bee is conceived as a SmallSat mission which would demonstrate capture of a simulated asteroid, extract material (water) from the simulated asteroid, and use it for demonstration of solar thermal propulsion, thus showing proof of the Honey Bee concept.

A precursor mission to the Mini-Bee is a standalone Optical Mining experiment that could be performed at the International Space Station (ISS). Figure 1-13 illustrates the sequence of operations of the Optical Mining Experiment Module (OMEM) that would demonstrate use of an inflatable concentrator to perform optical mining on a simulated asteroid and allow for the processed sample to be returned to Earth for analysis.

Other uses of asteroid material are also being explored and evaluated. Under TransAstra sponsorship, Dr. Otis R. Walton is evaluating micro-gravity techniques and granular mechanics required for fabricating radiation shielding from leftover asteroid regolith in space. This shielding is planned for use by long duration crewed missions and human habitats and is designed to easily wrap around existing structures. Figure 1-14 shows the

Ancilia approach for creating radiation shielding from the leftover regolith. Figure 1-15 shows the rotating funnel that is a key component of the Ancilia approach. This approach applies granular dynamics in a micro-gravity environment to move the regolith into extendable tubes for fabrication of the shielding. In collaboration with the TransAstra team, Dr. Christopher Dreyer of the Colorado School of Mines is studying laboratory techniques

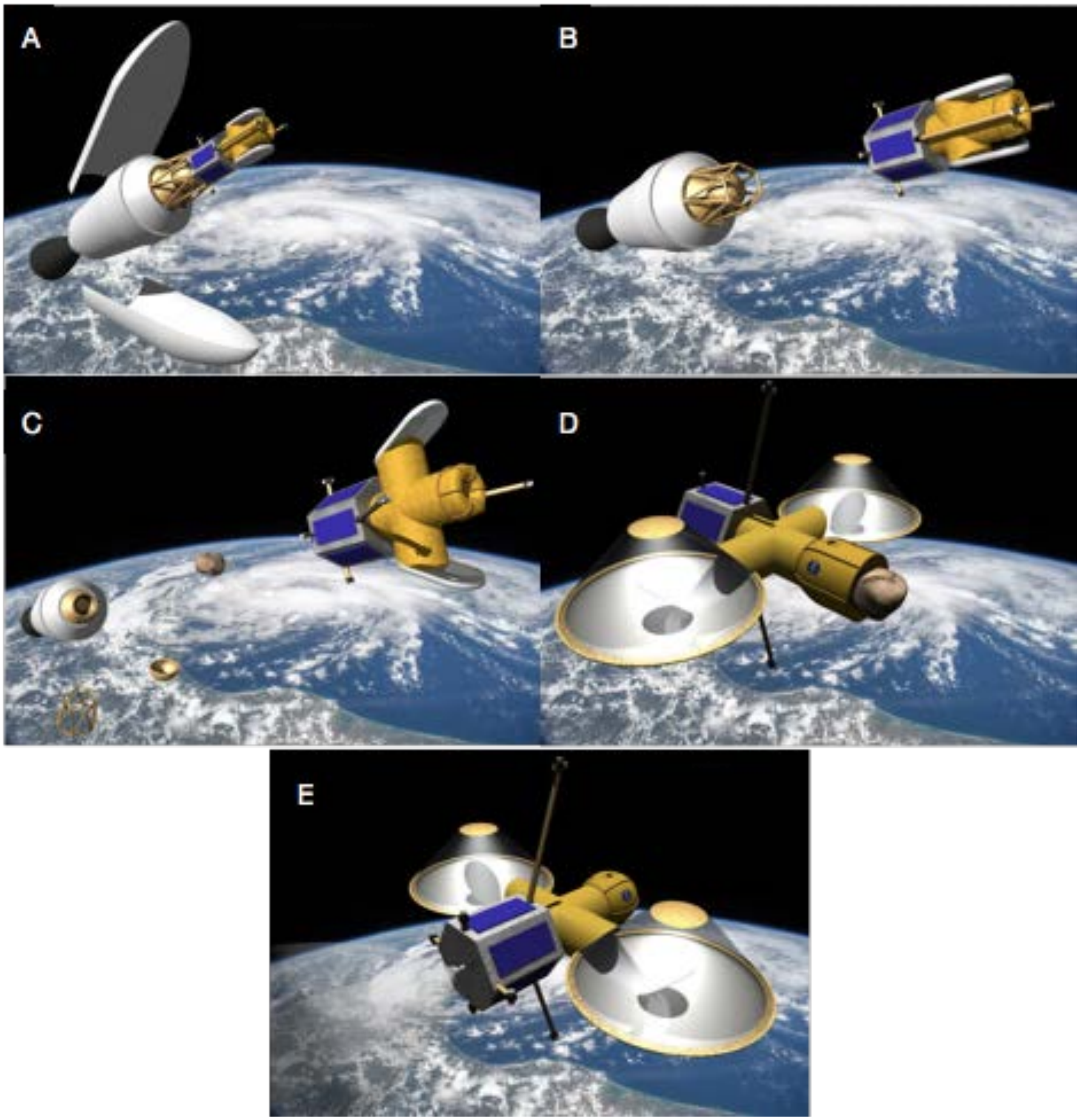


Figure 1-12 Mini-Bee Tech Demo Mission: Launch On A SmallSat Launcher (eg Launcher One) B ) Mini Bee Separation C) Synthetic Asteroid and Structures Deployment D) Synthetic Asteroid Capture and Optical Mining Demonstration E) Demonstration of Solar Thermal Rocket Maneuvering With Mined Propellant

to verify the utility of these approaches. One such experiment that could be performed by astronauts at the International Space Stations (ISS) is illustrated in Figure 1-16. In a related research effort, TransAstra recently built a prototype of this apparatus under SBIR Phase 1 funding and has proposed a flight version to the SBIR Phase 2 program.

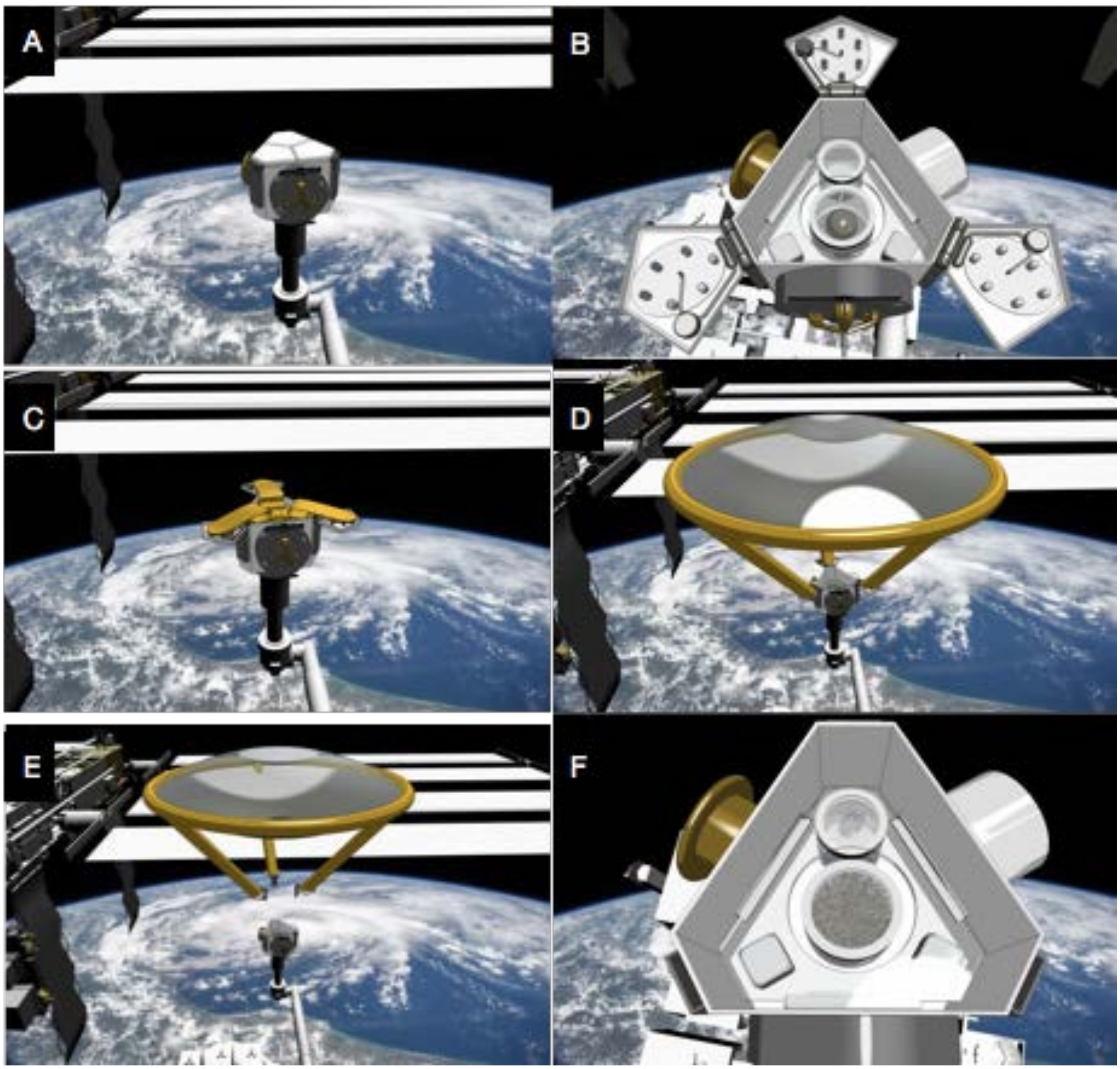


Figure 1-13 A) Optical Mining Experiment Module (OMEM). B) OMEM Interior Cutaway C) OMEM Inflatable Deployment D) OMEM Optical Mining Demonstration E) Inflatable Structure Separation and Deployment F) Interior Cutawav Prior to Return to Earth

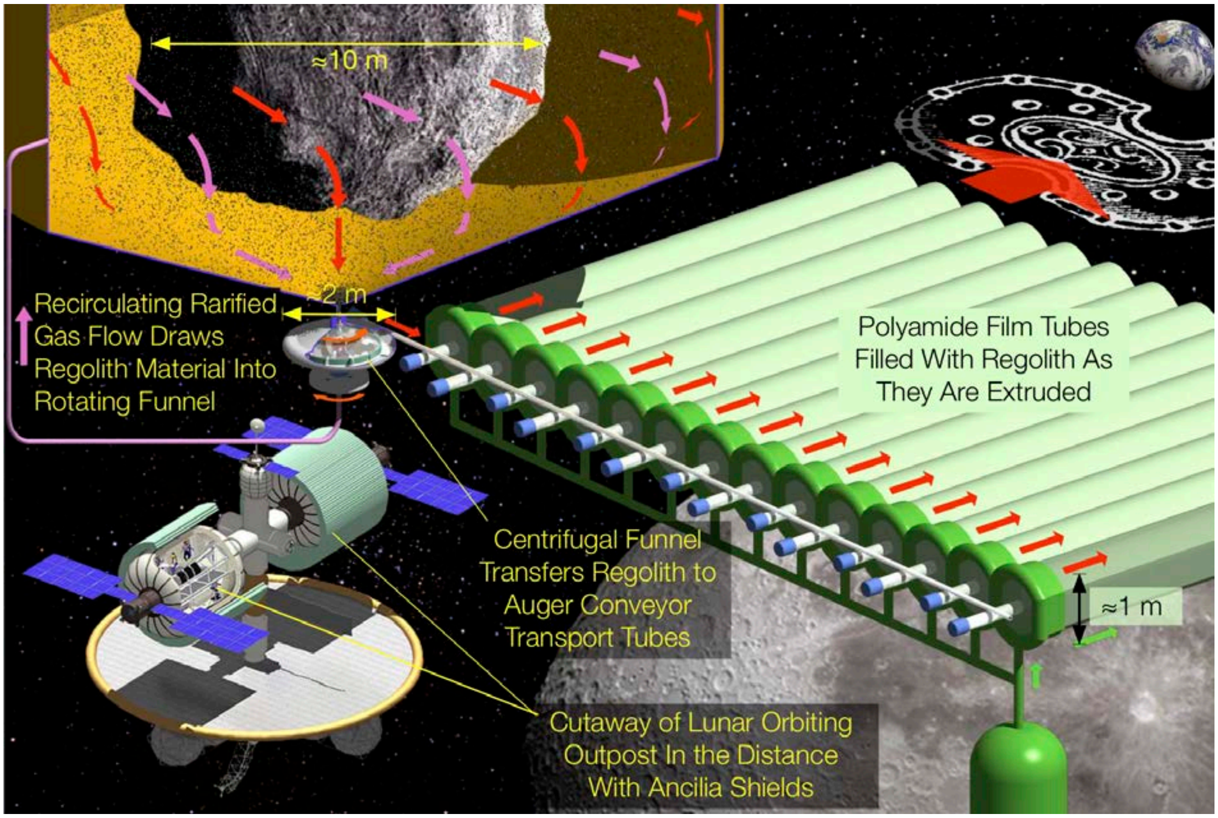


Figure 1-14 Ancilia: Radiation Shield from Leftover Regolith for use in Surrounding Habitats

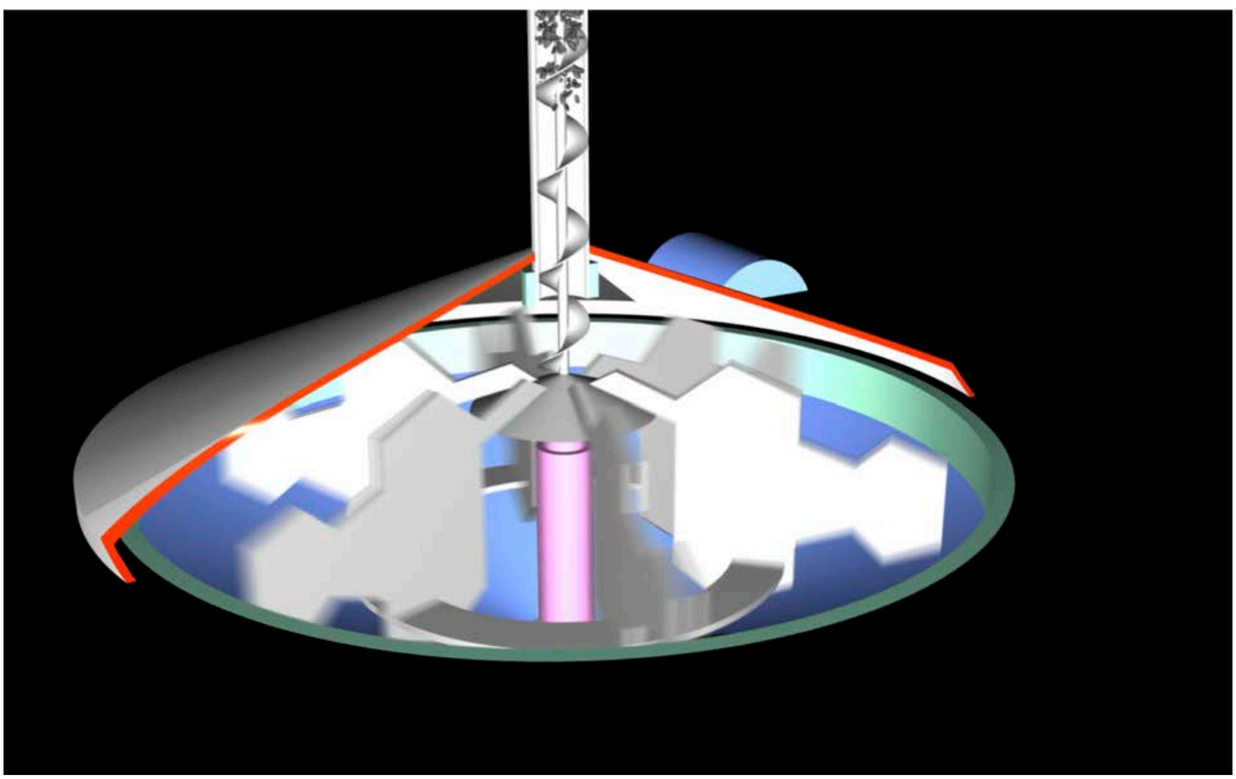

Figure 1-15 Ancilia: Rotating Funnel

## 2.0 Completed Sutter Research and Development

Planetary astronomers who study small bodies of the solar system have operated under the tyranny of the astrophysicists's filters rather than using filters optimal for planetary science. For the purpose of discovering asteroids the system should maximize Signal to Noise (SNR). Doing so for a ground-based detection system becomes complicated mostly because the Moon changes the spectrum of the background sky but there are also atmospheric and scattered light issues. Thus, a wide-band filters optimal for detecting asteroids would have a different design based on the presence or absence of moonlight (See Figure 2-1 for an example of such a Wideband filter.) Similarly, the filter design could be optimized for a particular taxonomic type or complex.

The background for a space-based system is dominated by zodiacal light consisting of small dust particles in the plane of the solar system that reflect sunlight in the ecliptic. We will explore the design of a filter or potentially use no filter at all, to maximize the SNR for detecting the small, dark, C-complex asteroids against the zodiacal background given the sCMOS detector spectral response.

Once a low-ΔV ISRU candidate has been discovered the next step is physical characterization: taxonomy, rotation rate, rotation state and shape. The fastest parameter to measure is probably taxonomy. Filters will be designed with passbands that provide optimal discrimination of water-bearing asteroids from other asteroid classes given the sCMOS detector's spectral response, the asteroid spectra, and the spectrum of the zodiacal light (See Figure 2-2).

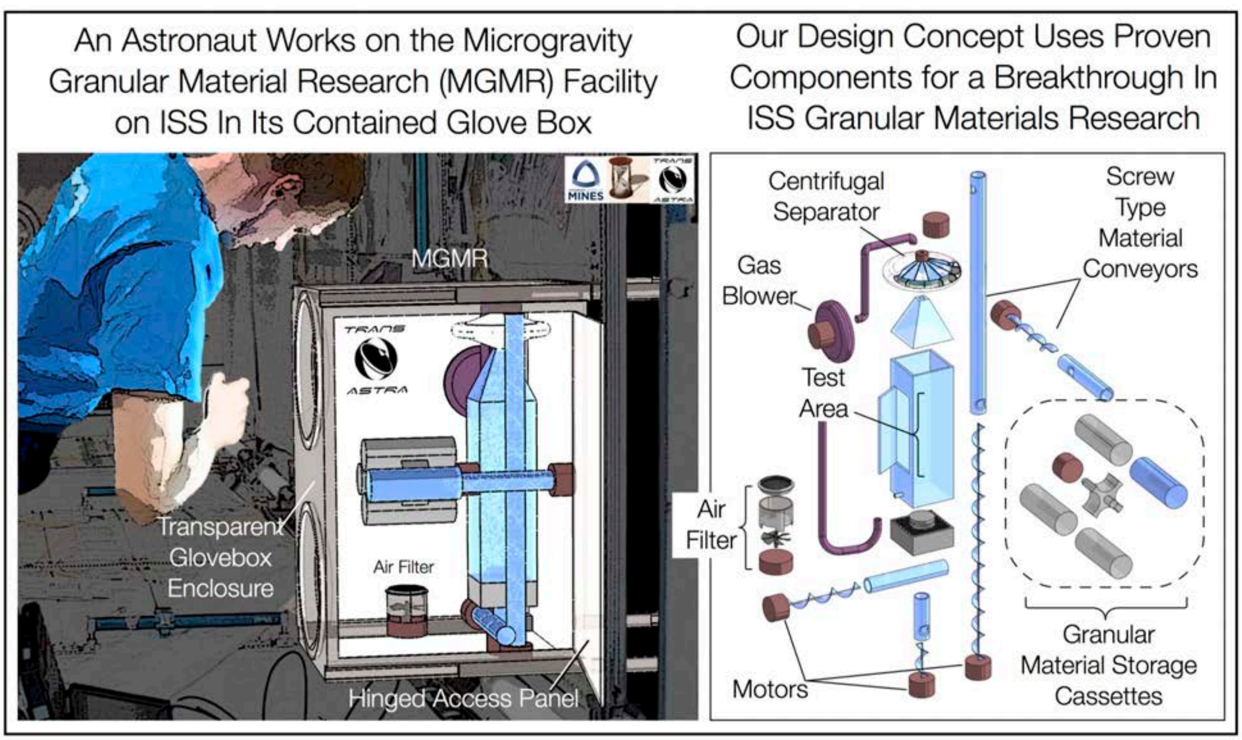


Figure 1-16 Ancilia Demonstration (Pending NASA Phase 2 SBIR Proposal)

It may be possible to introduce an R~100 fiber-fed prism spectrometer in future Sutter systems. Figure 2-2 provides a best guess (not a calculation) at the optimal bandpasses for separating the water-bearing C-complex asteroids from the dominant S-complex asteroids. In this scenario the first Sutter systems may employ just three filters to separate the S- and C-complex objects while the ability to call out the particularly water rich Ch sub-type depends entirely on the SNR available in the band centered at about 0.7um. Sutter Extreme will include an IR channel to take advantage of the separation between the C and Ch types in the IR that is in the opposite sense of the separation in the 0.7um band. i.e. the 1.3um/0.7um flux ratio is different for generic C-complex asteroids and the water rich Ch sub-type.

Along with the application of effective filtering strategies described above, recent innovations in Matched Filter Algorithm (MFA) Asteroid detection, coupled with a novel mission architecture (pseudo-Earth orbit) provide the basis for the novel series of Sutter Missions proposed in the roadmap. Application of an even more advanced Compound

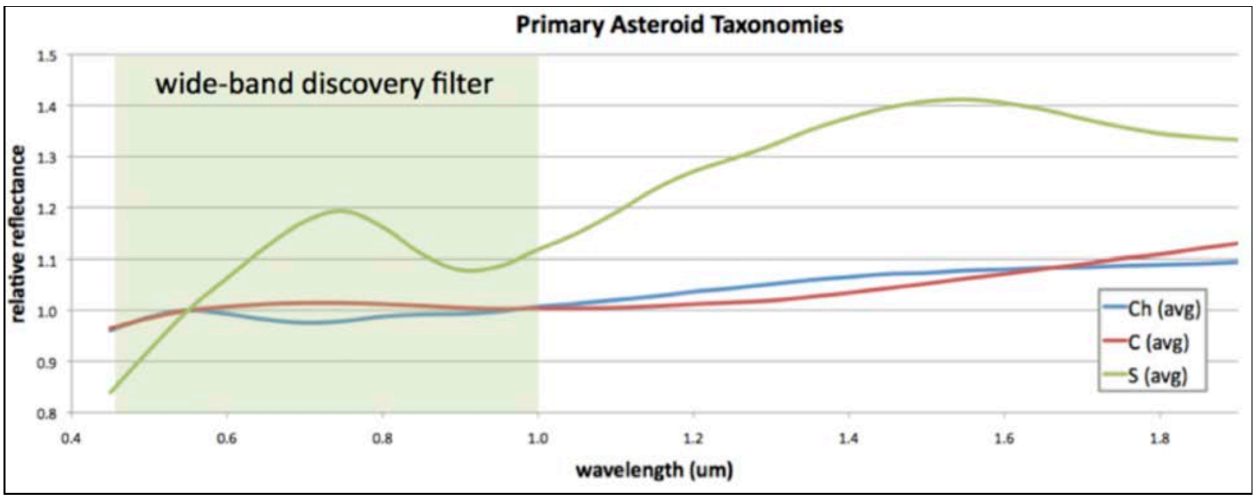


Figure 2-1 Wideband Filter

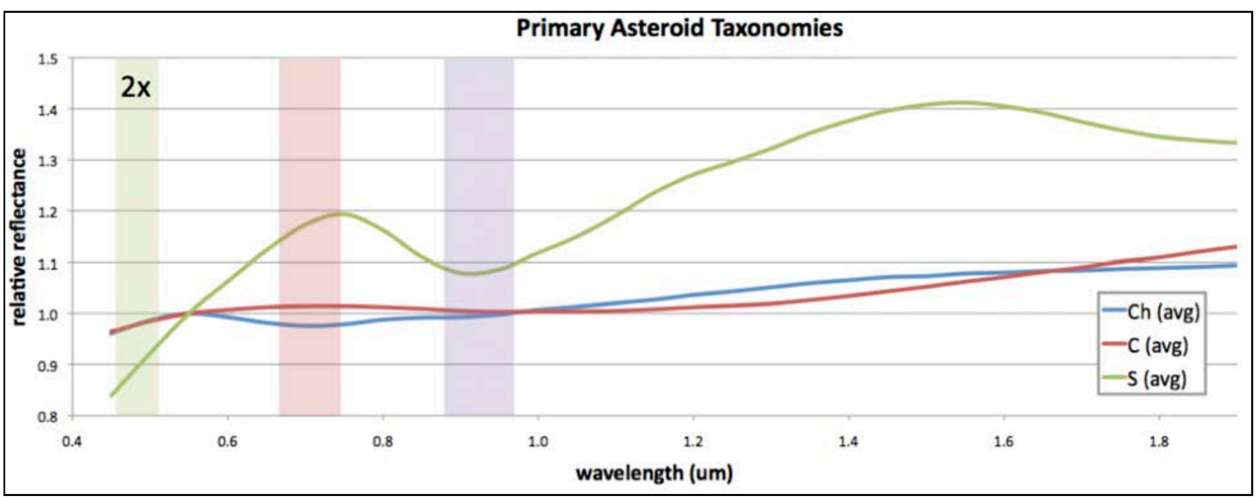


Figure 2-2 Taxonomic Filters

MFA (C-MFA) approach will provide additional improvements in Sutter system capability. These innovations are described in more detail below.

## 2.1 Matched Filter Algorithm Asteroid Detection

Recent innovations in the field of asteroid detection algorithms and processing hardware are directly applicable to all phases of Sutter deployment. Drawing on these innovations, we propose to use matched filtering techniques to provide ISRU detection capability down to the noise background of a single imaged star field. Within the bounds of the Sutter collection, CONOPS, the application of matched filtering techniques in real-time, has become practical as Moore's law has finally caught up to the algorithm's large computational load requirements. With modern graphical processing units (GPUs), the fundamental operations of matched filtering are built directly into the hardware and typically yield a twenty fold improvement in run-time costs over single core CPUs. This coupled to the fact that the required processing capability is available onboard a modern cube-sat, alleviates the need for large downlink bandwidth for ground processing of imagery.

Historically, asteroid motion detection approaches used in ground and space based surveys break into two major categories. The first is the traditional "detect-before-track" methodology and is most commonly used by the asteroid community due to its very fast processing throughput. The method also goes by the name of moving target indicator or velocity matching. The basic concept (see Figure 2-3) is that each frame of a collection sequence is thresholded independently, all star-like objects found, and their centroid positions tagged with the associated frame number.

Common objects across frames, such as stars and stationary objects, are identified and tossed out, while unique objects, like asteroids and artifacts, are identified between frames. Given the timing between frame collections, an object from the first frame and an object from the second frame provides a motion velocity vector that can be used to predict where the object should appear in the third, fourth, etc. frames. If the object is found at the predicted location(s), then detection is declared. The major drawback with the method is that rejection of common star areas, can result in loss of co-located asteroid positions and thus missed detections. This is the reason most ground asteroid surveys avoid the galactic plane.

The second methodology is referred to as "track-before-detect" because it performs the thresholding operation after a multi-frame signal integration gain is computed. A template of the target motion across the focal plane is hypothesized and correlated to the space-time imaging cube [(see Figure 2-4). This is often referred to as matched filtering, template matching, or multiple hypothesis testing and has been applied to space imagery (Mohanty 1981, Pohlig 1995, Sanders-Reed 1998; Stokes et al 2000; Gural et al 2005, Shucker et al 2013; Dawson et al 2016).

For unresolved moving point sources, as commonly experienced in asteroid detection surveys, the matched filter operation is equivalent to a translation of each image (shift) followed by a sum of the shifted images (stack). The shift-and-stack operation reviewed in

(Parker and Kavelaars 2010) provides a multi-frame integrated signal-to-noise gain prior to thresholding on the maximum likelihood estimate (MLE) detection statistic. The matched filter is often coupled to a clutter suppression stage up front to remove stationary objects (mean removal) and suppress noisy pixels (whitening via covariance estimation).

A subset of matched filtering is synthetic tracking, which performs the same unresolved point source shift-and-stack operation, but under more restrictive collection requirements (Shao et al., 2014; Zhai et al., 2014; Heinze et al 2015). In synthetic tracking, the integration time per frame is limited to be short enough to ensure that the fastest expected focal plane motion of an asteroid does NOT result in any smear in a given frame. This ensures no trailing loss and maximum signal-to-noise gain when numerous short integration exposures are aggregated together in the matched filter. This does impose a requirement on employing very fast read-out sensors to minimize total collection dwell time on a star field and thus maximize total sky coverage. The Sutter missions will meet this fast image collection cadence requirement through the use of the Fairchild CIS2521imaging sensor chip.

The processing for asteroid detection has been done almost exclusively at ground facilities. Surveys such as Spacewatch, CSS, LONEOS, NEAT, and LINEAR, all used fast detect-before-track algorithms on processors sited with the telescopes. LINEAR discussed switching to matched filtering (Stokes et al 2000) but it was not adopted for routine processing. Spacewatch considered the option in 2004, but the processing loads required and the high-end CPU cooling issue of running at altitude, limited application at the time. The Canadian NEOSSat space based asteroid survey mission was set up to use matched

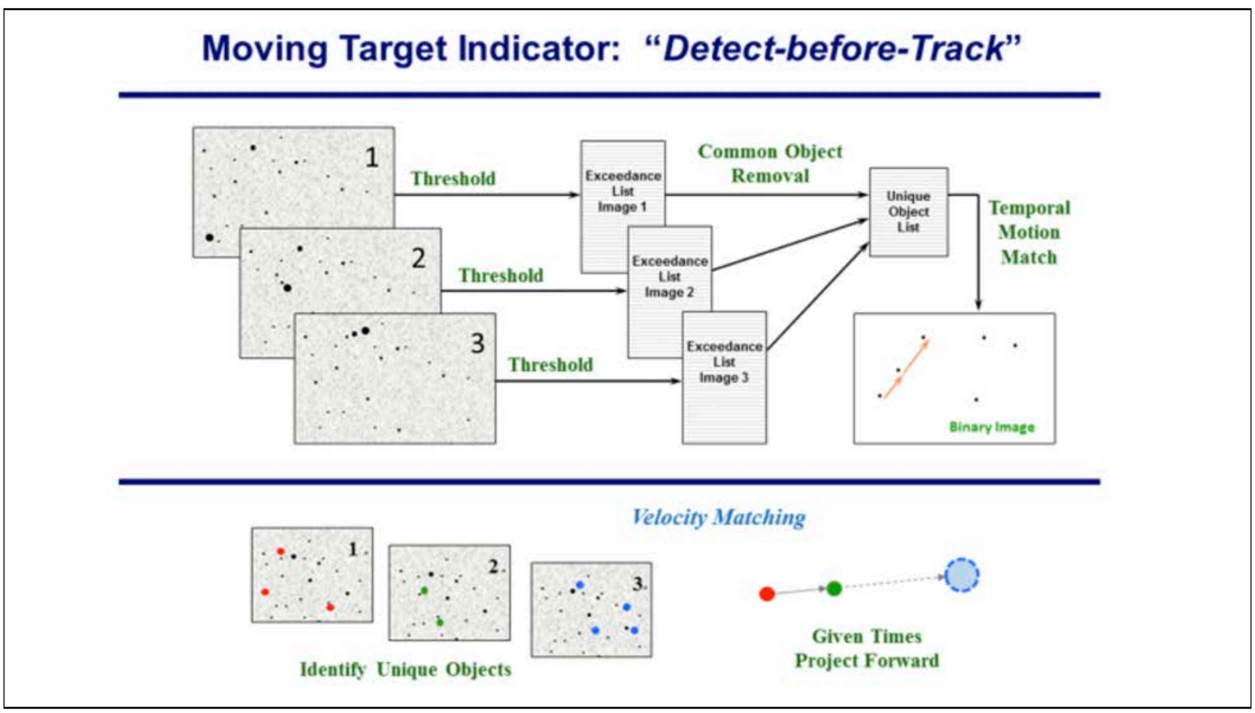


Figure 2-3 Moving Target Indicator

filtering with parallax induced motion hypotheses (zig-zag shift-and-stack) on imagery downlinked and processed at their ground facility. Another space-based asteroid search program associated with IR imagery collected by the WISE spacecraft, also downlinked data to the ground, and applied the faster detect-before-track technique to the image sets. Thus the Sutter system will be a pioneer in performing matched filter detection directly onboard the spacecraft.

It is important to emphasize that the Sutter mission processing hardware can handle the computational load of the large number of motion hypotheses generated in a matched filter application. We know this because under the NEOSSat mission development of the Software Algorithmic Testbed for Asteroid Detection (SALTAD) suite of software, one task was to migrate the most computationally loaded aspects of matched filtering, namely the shift-and-stack operation, onto a GPU. One of the Co-Is on our Phase II proposal developed this software which is available to our team at no cost to NASA for use on the Sutter missions. The shift-and-stack process is essentially a binomial interpolation operation applied to an array. Figure 2-5 shows the GPU implementation as used in SALTAD. The code uses GPU texture memory, which means that a single pixel fetch gives one an interpolated shift-and-stack pixel value for “free” just by doing the fetch. Coupling that to only 4000 hypotheses, the 30 Sutter image frames remaining resident in GPU memory while looping through hypotheses, very low input bandwidth per motion hypothesis, and a fast compaction (threshold aggregation) kernel, results in highly efficient processing ideally suited to a GPU architecture.

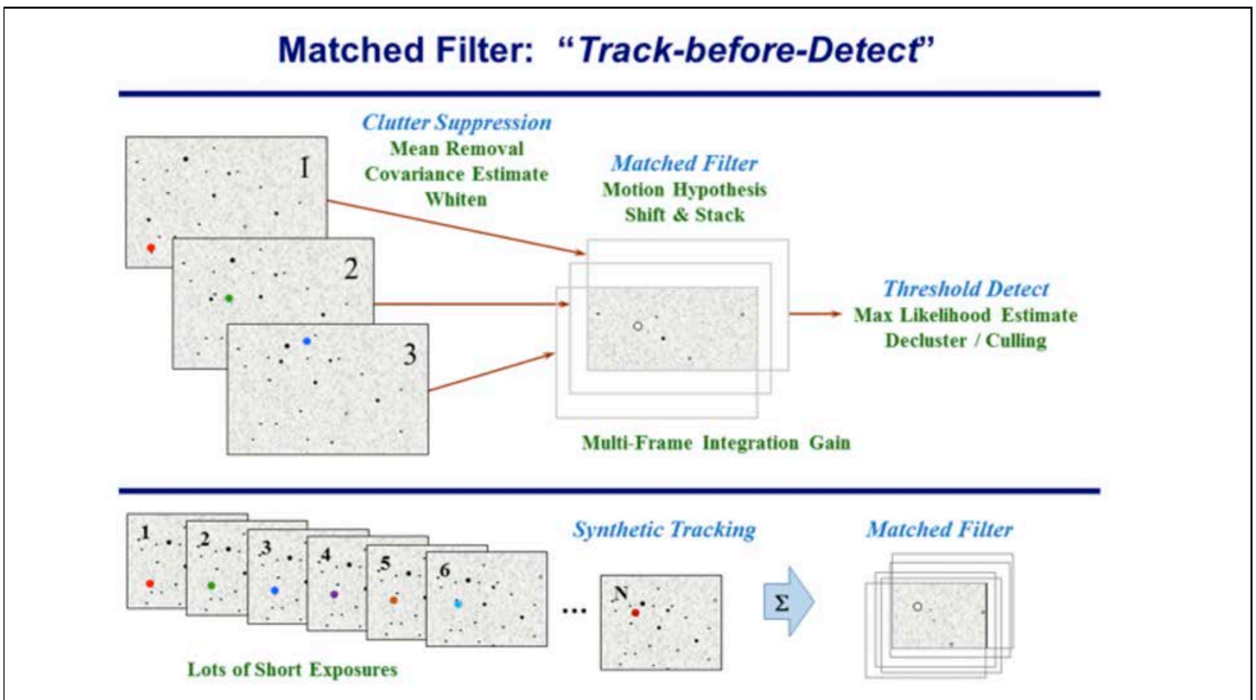


Figure 2-4 Matched Filter Approach

Thus, given that the matched filter coupled to a GPU code base is available, the detection image processing can be deployed on a cube-sat and not rely on a full imagery down-link to the ground. Looking at Figure 2-6, an analysis was done comparing a ground based computer system using a single i7 CPU core and Tesla K80 GPU, to space qualified CPUs (Cortex A15 and A57) and GPUs (Mali T604 and Tegra TX2). Timing was broken up into CPU sub-functionality and the primary GPU load of shift-and-stack. For a nominal 4 megapixel Sutter image, taken every 10 seconds for 300 seconds (30 frames), the ground based timing numbers were extrapolated to the space qualified systems based on flops/second scaling. Clearly the Tegra TX2 class GPU can meet the real-time requirement of 300 seconds of processing between each 30 frame set collected (note there is a small extra margin for move and settle of the Sutter spacecraft onto the next star field). Thus, computational performance is achievable for the Sutter Demo, which is planned for low Earth orbit (LEO), but will be first tested on the ground with the Tegra TX2 during the phase II Sutter Ground experiment. Note that for Sutter Survey and Extreme, the GPU will be replaced with FPGAs.

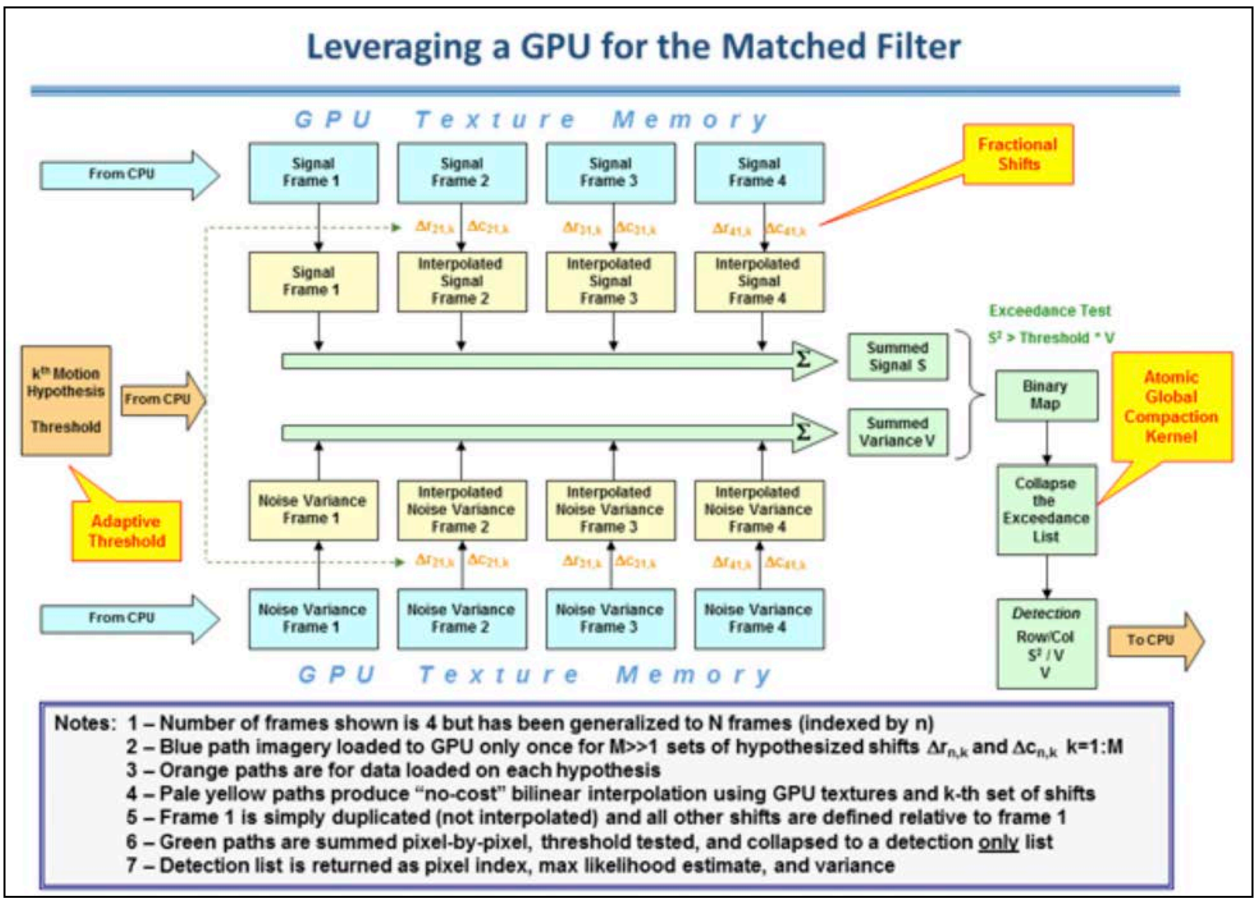


Figure 2-5 Leveraging a GPU for the Matched Filter

## 2.2 New Mission Trajectory for Sutter Survey & Sutter Extreme

As discussed above (and illustrated in Figure 1-10), the following mission concept for prospecting for ISRU candidates was determined to be most effective:

- Three spacecraft on heliocentric orbits that appear to be in distant pseudo-geocentric distant retrograde orbits around Earth through a careful selection of their orbital elements (Cyr et al., 2000; Stramacchia et al., 2016; Perozzi et al., 2017).
- They all have semi-major axis ~1 au, small inclinations, and eccentricities~0.075 so that their geocentric distances are typically about 0.075 au (about 11 million km, nearly 8x the distance to the Earth-Sun L1 and L2 points).
- These are stable orbits because they are well outside Earth's Hill sphere.
- There is always at least one spacecraft inside Earth's orbit.
- All three spacecraft are normally operating in survey mode searching for new ISRU candidates.
- Optimizing the orbit is part of the Phase II study but we envision that:
  - spacecraft interior to Earth's orbit will survey towards opposition (directly away from the Sun) to take advantage of the full phase illumination of the NEOs in that direction, and
  - spacecraft exterior to Earth will survey at an angle with respect to opposition that optimizes ISRU candidate discovery based on their spatial number density and phase function with respect to the spacecraft.

**Sutter Image Processing Timing Estimate**

Target motion ≤ 0.6"/sec → 180" in 300 seconds (30 x 10 sec frames)
Pixel angular extent = 5" → Moves 36 pixels in 30 frames
Square raster grid with circular limit of 36 pixels → 4072 hypotheses for 1/30 pixel per frame step, 1 pixel 30 frame resolution

| Process | i7-4810 MQ 3.7 Gflops / core | Tesla K80 1 GPU 2.8 Tflops single prec | Cortex A15 0.9 Gflops / core | Mali T604 GPU 72 Gflops single prec | Cortex A57 1.2 Gflops / core | Tegra TX2 GPU 1.5 Tflops single prec |
|---|---|---|---|---|---|---|
| Image Size → | 2004 x 1336 x 9 | 4K x 4K x 3 | 2K x 2K x 30 | 2K x 2K x 30 | 2K x 2K x 30 | 2K x 2K x 30 |
| Star Localization | 0.15 | | 3.2 | | 2.4 | |
| Registration | 0.10 | | 2.1 | | 1.6 | |
| Apply Dark & Flat | 0.07 | | 1.5 | | 1.1 | |
| Background Equalize | 0.02 | | 0.4 | | 0.3 | |
| Mean / Demean | 0.27 | | 5.8 | | 4.4 | |
| Covariance / Whiten | 0.06 | | 1.3 | | 1.0 | |
| PSF Convolution | 0.16 | | 3.4 | | 2.6 | |
| Noise Variance | 0.29 | | 6.2 | | 4.7 | |
| Shift & Stack | | 35 | | 6790 | | 163 |
| Total CPU or GPU | 1.12 | 35 | 24 | 6790 | 18 | 163 |
| | | | 6814 seconds | | 181 seconds | |

Blue = Guesstimate

Figure 2-6 Sutter Imaging Processing Timing Estimates

- Once an ISRU candidate is discovered by one spacecraft and has a good enough orbit then the other two spacecraft can provide targeted observations to triangulate on its position and rapidly collapse the orbital elements.

### 2.3 Compound Matched Filter Algorithm (C-MFA) and Telescope Concept

A new type of low cost, high performance compound telescope is proposed which will require application of a Compound Matched Filter Algorithm (C-MFA). This concept uses multiple telescopes as proposed for the Sutter Survey and Sutter Extreme missions to obtain image frames with a shared field of view that can then be jointly processed to identify and track objects that might be missed when processing the frames from a single telescope alone. It also provides for increased detail in the characterization of a target body by combining either identically filtered imagery or differently filtered images simultaneously and in the case of the Sutter Extreme spacecraft, near-InfraRed (near-IR) imagery as well.

### 2.4 Performance and Benefits Analysis

The innovations described in the previous paragraphs have increased the confidence that the candidate asteroid targets can be detected as predicted and that the focus of the detection effort will be on those most energetically accessible for near term mining missions. A side benefit of the mission architecture is early detection of asteroids that may pose a threat to Earth including asteroids smaller than those posed by the class of PHOs currently of greatest interest. Further analysis is the subject of a Phase II proposal.

## 3.0 Sutter Mission System Architecture

### 3.1 Mission System Architecture Overview

The sequence of Sutter Missions in the overall architecture constitute increasingly capable small spacecraft that provide the means to identify and characterize potential targets for asteroid ISRU. The design of each spacecraft in the road map is evolving, providing a platform for the telescope[s] and data processing elements required to meet the requirements of each mission (See Figure 3-1). While some new technology is envisioned for use in the later missions, the majority of the spacecraft and payload elements are Off the Shelf. Each will be able to detect, track, and characterize target asteroids in the near Earth environment in heliocentric space. While the initial Sutter Demo mission will be limited in capability and lifetime, it will make clear the utility of the concept which can then be fully implemented in the Sutter Survey mission. Using the novel Pseudo Geocentric Distant Retrograde (PGDR) Orbits that were developed in this study, the Survey mission spacecraft will be ideally situated to track and characterize numerous potential targets for asteroid resources. The Sutter Extreme mission will greatly expand this capability to continue to find and characterize the wealth of objects waiting for use in near-Earth space.

The first mission is an inexpensive cubesat spacecraft, designed to take advantage of ride-share launch opportunities and demonstrate the Sutter detection approach from Earth orbit. The NASA phase of this mission is short, with an extended commercial phase of up

Table 3-1 Launch Vehicle Capacity for Demo, Sutter, Extreme

| Mission | Launch Opportunities | Payload Capacity | Margin | Estimated Price |
|---|---|---|---|---|
| Sutter Demo (10kg) | 6U Cannisterized Rideshare to 550 km | 12 kg | 2 kg | $500K |
| Sutter Demo (10kg) | Devoted Launch on Vector-R to 550 km | 20 kg | 8 kg | $1.2M |
| Sutter Survey (120kg) | ESPA Class Rideshare to GTO | 180 kg | 60 kg | ~$9M |
| Sutter Extreme (830kg ea.) | All 3 together on single Falcon 9 non-expendable (reusable) to C3 > 0 | 2,800 kg | 310 kg | ~$63M |

to at least a year. See Table 3-1 for an overview of launch opportunities and costs for the roadmap missions. The second Sutter Survey mission consists of three much more capable spacecraft with 4 larger telescopes each, launched into novel Pseudo Geocentric Distant Retrograde (PGDR) orbit designed to keep the spacecraft within 0.08 AU of the Earth, for a cost estimated at less than $150 million. Finally, the Sutter Extreme mission will provide substantially increased detection and prospecting capabilities by providing three

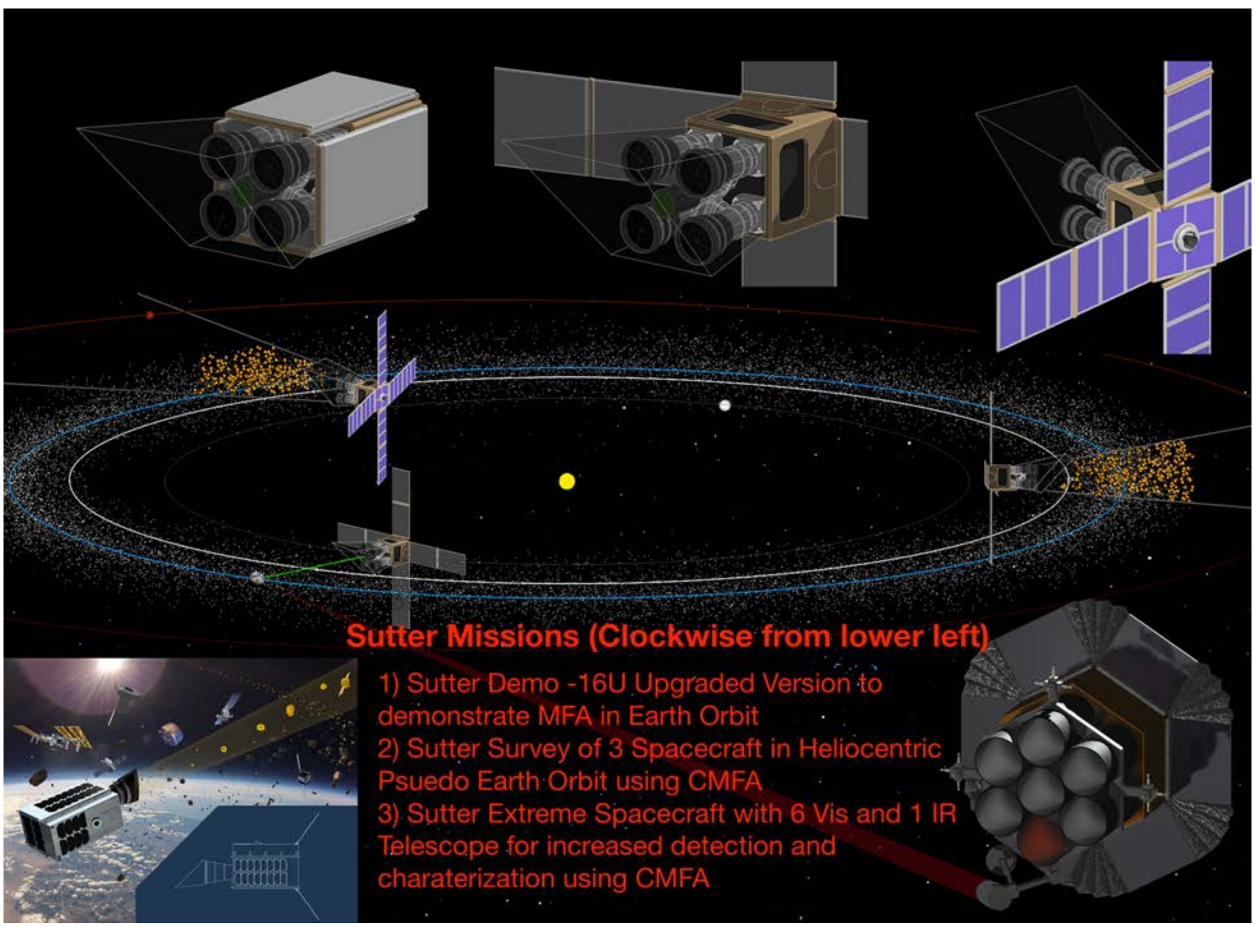


Figure 3-1 Artist's Illustration of the Three Sutter Roadmap Missions

spacecraft each with six visible and one IR telescope, each with 50 cm apertures at a cost less than a New Horizons class mission.

### 3.2 Sutter Demonstration Mission

The Sutter Demonstration Mission is a low-cost cubesat scale mission with a single small aperture telescope that will demonstrate the basics of the Sutter approach in Earth orbit (see Figure 3-2). This mission was previously proposed by TransAstra and competitively selected by NASA but could not be funded when one of the partners was unable to follow through on their portion of the proposal. The mission has since been replanned with new, more technically capable partners. This mission will cost less than $5 million. An upgraded version (16U with a 14 cm aperture telescope) is currently being proposed to the NASA Tipping Points opportunity. In particular, it will verify the detection and tracking capabilities of the matched filter algorithm (MFA) by not only detecting new objects during it's relatively short mission life, but also by allowing for reproduction of the results by processing

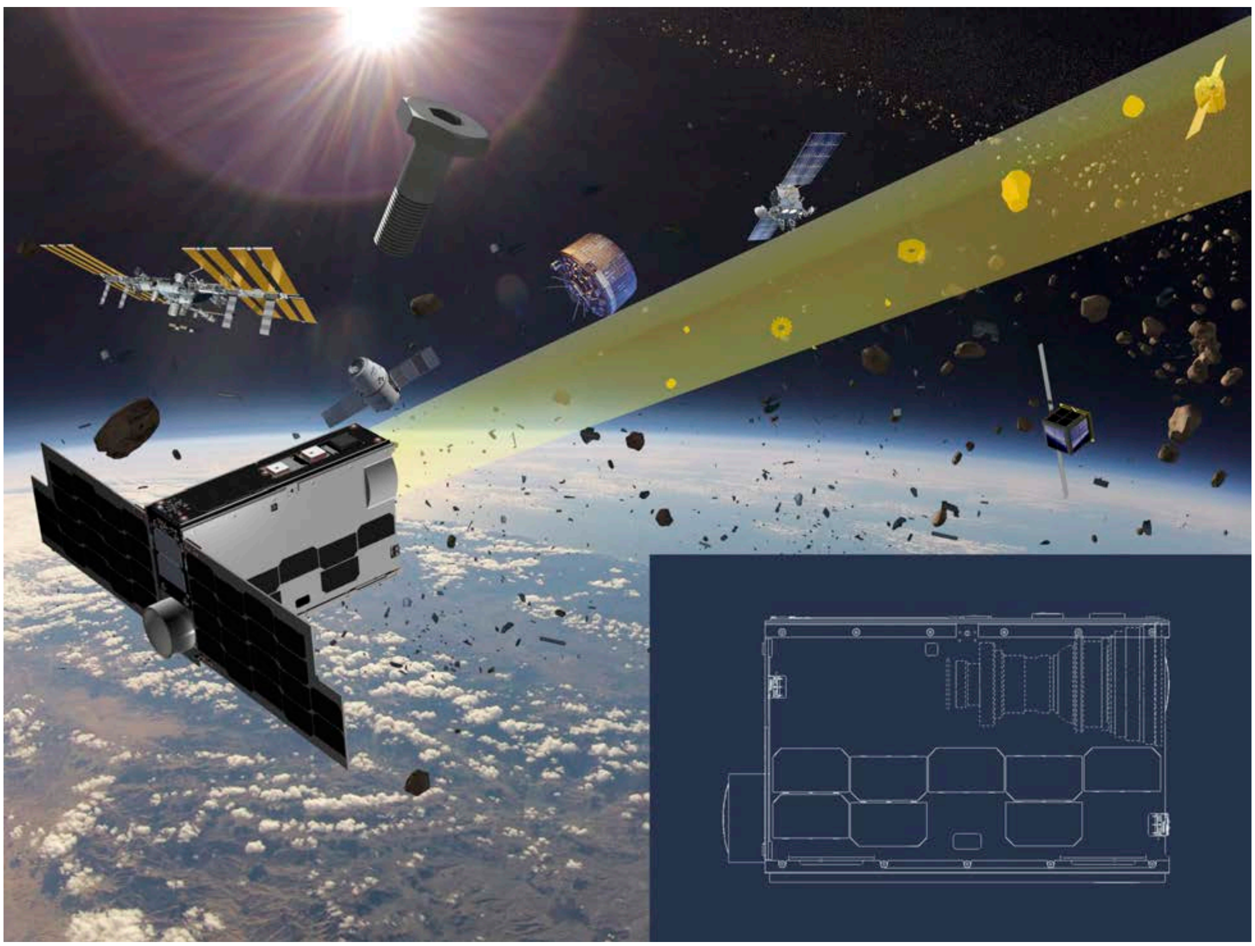

Figure 3-2 Sutter Demonstration Mission Illustration. Nominally the spacecraft would be pointing away from the sun for prospecting, but it is capable of pointing less than 90 degrees to the sun if desired or required for downlinking data to Earth. Concept shown is for a 6U implementation with a total cost including launch of under $3M.

selecting image sets, data cubes, on the ground using the same matched filter software as used on the spacecraft.

The Sutter Demonstration mission is envisioned as a short term mission of a few months for NASA, but an extended commercial mission will continue until the spacecraft de-orbits.

### 3.2.1 Sutter Demonstration Mission Design

The Sun-synchronous polar orbit for Sutter Demo provides continuous access to the opposition region (away from the Sun) where asteroids are fully illuminated and therefore brightest (e.g., full moon). The Moon will be an issue but the survey region can be modified with care taken to eliminate internal reflections due to the Moon's proximity. LEO provides fast data transmission to Earth.

The small ISRU targets will have to be close to be detected. An average angular speed of 10 deg/day is projected (see Figure 1-9). Their motion will be predominantly in the ecliptic because the candidates have small orbital inclinations. Expanding on the legacy of decades of ground-based asteroid detection systems (e.g. Denneau et al., 2013) five detections over the course of 5 hr are required to create a track during which the typical object moves about 2º. A LEO Sun-synchronous orbit suitable for triaging ISRU candidates is optimal.

The current design for the Sutter Demo Field of View (FOV) is about 4.8 $deg^2$ equivalent to about 2.2 deg x 2.2 deg. With 300 s/stack and five stacks/track Sutter Demo can observe about 58 fields/day but we assume 50 here to allow time for data transmission to the ground station and other overheads.

The Sutter Demo Field of Regard (FOR), the entire sky survey area in one survey pattern, will be centered on opposition because objects are brightest towards opposition where they are nearly fully illuminated (0 deg phase angle, the angle between the Sun and spacecraft as observed from the target). Figure 3-3 illustrates the nominal survey pattern with these assumptions. Sutter Demo images 50 fields in a 25x2 field pattern in a single day. The daily pattern is shifted each day for a total of five days after which the entire process begins again. The fields can be re-imaged at this time because the region will have been 'refreshed' with new objects. On each day Sutter Demo will obtain five visits at each FOV in about a five hour time period to obtain enough observations to calculate a preliminary orbit. Details of the observing strategy will be refined and optimized in Phase II or in the Tipping Points Missions.

### 3.2.2 Sutter Demo Flight System Description

#### 3.2.2.1 Payload Hardware

The matched filter algorithm tracking telescope is derived from COTS components that are high-TRL and the majority of which are flight-proven. The optical front end is derived from the COTS 10 cm or 14 cm aperture telephoto Canon system (See Figure 3-4) ruggedized for flight (which principally involves replacing the chassis with low-TML and low-CVCM, high-stability chassis materials.) The detector—the Fairchild Imaging CIS2521—is a large format, ultra-low-noise CMOS image sensor intended for applications requiring high quality imaging under extremely low light conditions. The device features an array of five transistor (5T) pixels on a 6.5μm pitch with an active imaging area of 2560(H) x 2160(V) pixels. This sensor supports user-programmable row start/stop control for region of interest (ROI) readout. These features, combined with 5.5 megapixel resolution and 100 fps imaging rates, make the CIS2521 an imaging device ideally suited for a variety of low light-level camera applications.

#### 3.2.2.2 Sutter Demo Payload Software

The Sutter demonstration will include the first deployment of asteroid detection onboard a satellite. To achieve that goal the satellite will require significant hardware computing resources since the plan is to use clutter suppression and matched filter detection processing. The required hardware has been identified and described in section 3.2.2.1 above. The requirements for detection limits, target motion expectations, and processing time line have been folded into the overall hardware and software system design of Sutter Demo and beyond. This section describes the software components necessary for matched filter detection of moving asteroids in a sequence of imagery. The goal is to perform these operations in real-time, which we will define as completion of the processing of the previous 300 second imagery set during the next 300 second collection. The move and settle time of the spacecraft prior to next star field collection, will be treated as extra margin.

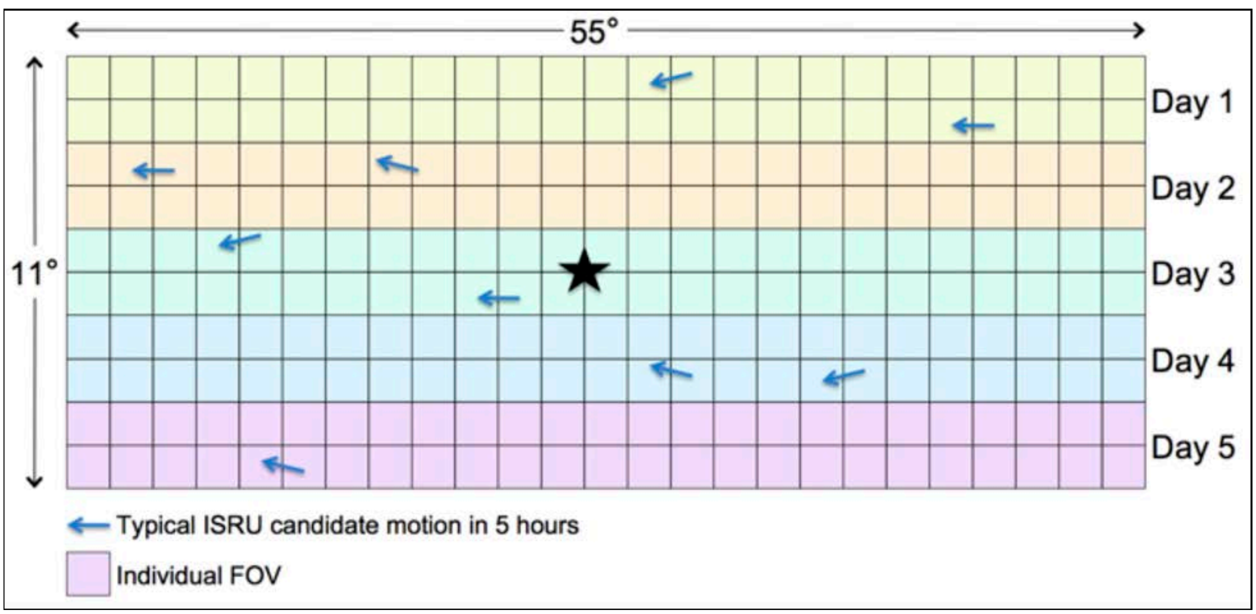


Figure 3-3 Survey Field of Regard - The field of regard for a 5 day survey period with Sutter Demo. Each color represents a single day and the entire pattern is repeated every 5 days. All FOVs are acquired at a constant offset with respect to opposition that is represented by the black star at the center of the figure.

It should be noted that a distinction needs to be made between onboard and ground station processing modules. The primary responsibility of the software onboard the satellite is to provide to the ground as complete a detection list of candidate ISRUs as feasible, which may include both real asteroid detections as well as false alarms. The satellite software will also transmit support metadata such as star positions, dark and flat field files, and image chips around the detected objects. For the Sutter demo satellite stationed in LEO, since the downlink bandwidth is sufficient, full image frames will also be transmitted to the ground on an as needed basis. The ground processing will consist of post detection processing such as astrometric and photometric calibration, culling of false alarms, refinement of the asteroid track, and orbital parameter estimation of the ISRU. This is more fully discussed in section 3.2.3.1 and 3.2.3.2.

Figure 3-5 is the block processing diagram consisting of the onboard software components of Sutter Demo. Most items depicted in the figure will have been embedded in the SALTAD software suite and tested on the target CPU/GPU during the phase II Sutter ground experiment. One goal of Sutter Demo is to validate the processing functionality onboard an orbiting satellite and address any image processing issues or artifacts not encountered during the Sutter ground collections.

The onboard software suite includes separate processing applications for dark image formation, flat field estimation, registration, and matched filter detection processing. The dark image will be computed as an average of multiple dark frames collected with cover closed. The flat field will be generated from sample imagery over the previous day that involve different spacecraft attitudes (various star fields), processed to exclude stars, and estimate the relative background sky responsiveness of each pixel. Each frame will have the dark removed and resultant image flat fielded. The registration will be done by first

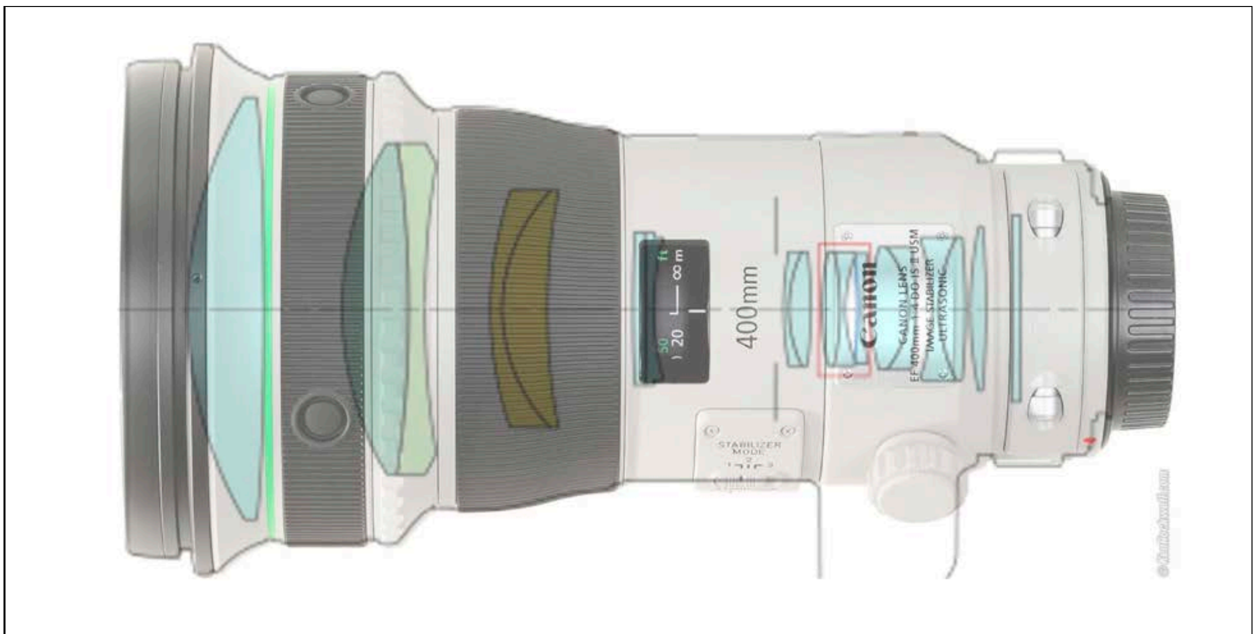


Figure 3-4 Cutaway of Canon Optics for 10 cm Aperture Telescope

extracting star locations in each frame and estimating their centroid positions (via SourceExtractor). The chip out of regions around each star will be packaged for transmission to the ground. The next step is to perform frame-to-frame relative registration within the 30 frame collection sequence. The registration will use a translation-only estimator based on a fast tie-point phase correlation method using the star centroid positions.

The main detection processing components are implemented as described in SALTAD. The registered frames are equalized, so that a fixed level global background is maintained across the 30 frame sequence. A mean and covariance estimate is made for each pixel assuming no spatial dependence of the noise statistics (covariance is diagonal). Note that this will require special handling for very slow moving objects that look almost stationary. The mean is removed (subtracted per frame) and the imagery is whitened (via inverse of the covariance applied to each frame). A spatially invariant point spread function (PSF) is assumed and applied across the whitened image sequence. In addition, a noise estimate of a donut region around each pixel is also estimated for use in the later CFAR (constant false alarm rate) detector downstream.

These previous processing steps are expected to be run on the A57 Cortex CPU. The next phase of processing, namely the shift and stack operation of the matched filter, will be run on the Tegra-X2 GPU. A hypothesis list of shift vectors will be defined given maximum expected motion of the target ISRUs within the defined field of view and actual per pixel angular resolution. This is expected to be on the order of 4000 motion vectors. Each 30 frame whitened and PSF convolved imagery set, along with the trial hypothesis list, will be pushed onto the GPU, the detection kernels processed, and asteroid positions in focal

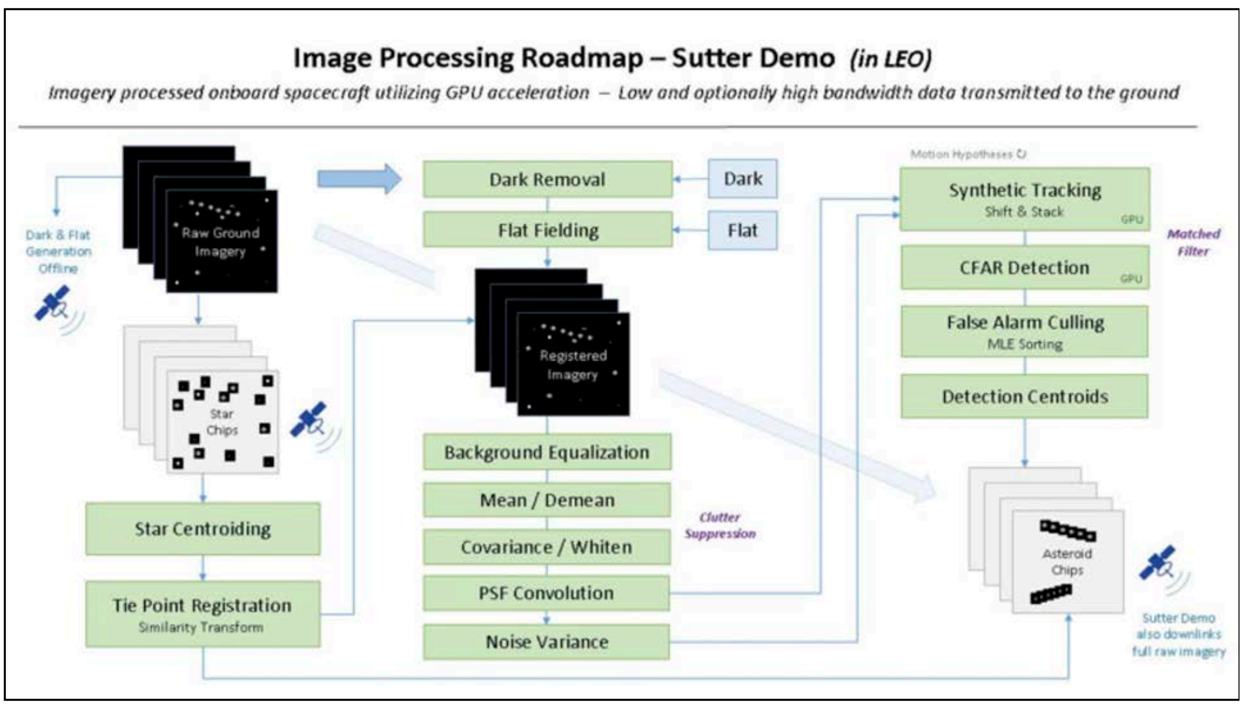


Figure 3-5 Image Processing Block Diagram for the Sutter Demonstration Mission

Table 3-2 Corvus 6 Platform Specifications

| Corvus-6 Platform Specifications | |
|---|---|
| Flight Computer | ARM Cortex A8 running Linux 3.2 |
| UHF Transceiver | 19.2 kbps TT&C |
| Battery Capacity | 48 watt-hours |
| Baseline Attitude Control Knowledge | <100 arcsec |
| Baseline Attitude Control Accuracy | ≈ 2 arcsec |
| Position Knowledge | <100 meters, System Level |
| Available Interfaces | CAN, Ethernet, I2C, SPI, UART, USB |
| Available Payload Volume | ~3U |
| Sun Pointing Power Generation | 34 watts |
| Max Continuous Payload Power | 10 watts, 100% duty cycle |
| Peak Payload Power | 35 watts |
| Platform Mass (no payload) | 7.5 kg |
| Compatible Deployers | ISL, NASA, Tyvak |
| Environments Testing | NASA GEVS-STD-1700 |
| Payload Transmitter Option | Easy integration of either AKaT-2 (37 Mbps) or AKaT-3 (320 Mbps) |

plane coordinates sent back to the CPU along with maximum likelihood estimates and integrated SNR. Image chips will be extracted per frame around potential detections and transmitted to the ground for further processing. Note that only in Sutter Demo, will the option exist to also transmit full frame imagery sets to the ground for validation processing in a non-real-time environment.

#### 3.2.2.3 Sutter Demo Spacecraft 6U Design

The Corvus-6 Platform was originally developed to support the Landmapper-BC constellation and designed to collect multi-spectral Earth imagery at a resolution of 22 meters. This platform is now available to support any payload up to 3 liters in volume. The platform utilizes a star tracker, magnetometers, sun sensors, an inertial measurement unit (IMU), reaction wheels, and magnetic torque coils for precision 3-axis pointing. A dual-band GPS receiver and on-board orbit propagator provide accurate positional knowledge at all times. Telemetry and command are accomplished with a UHF half-duplex radio and a backup S/L band radio, with a Ka-Band transmitter for high speed data transfer to the ground. Electrical power is generated using both body-mounted and deployable solar arrays. Power is distributed with a custom Electrical Power System (EPS) which includes 48 watt-hours of lithium-ion battery energy storage capacity.

The Corvus-6 Platform is a 6U CubeSat bus designed to accommodate a wide range of Earth-orbiting payloads. “6U” refers to the number of 1000 cm3 CubeSat “Units” of volume that the spacecraft occupies in a standardized launch vehicle deployer; in this case

Table 3-3 Spacecraft Design Characteristics

| Spacecraft Design Characteristics | |
|---|---|
| Redundancy Architecture | Single String, Functional |
| Primary Solar Array | Body Mounted and Fixed Deployable Panels with Triple-junction Cells |
| Keep-Alive Solar Arrays | Body Mounted Panels |
| Bus Voltage | 3.4 – 3.95 V Unregulated |
| Communications | 320 Mbps Ka-band payload transmitter<br>19.2 kbps UHF telemetry and command transceiver |
| Attitude Determination | 3-axis; 2 Star Trackers, Rate Sensors, Sun Sensors |
| Attitude Control | 3-axis; Reaction Wheels, Torque Coils |
| Position Determination | GPS Receiver, On-orbit Propagator |
| Flight Heritage of Hardware and Flight Software | Perseus-M1, Perseus-M2, Landmapper-BC1, Landmapper-BC2 |

a 30 x 20 x 10 cm total volume. The primary benefits of using these standardized dimensions/deployers is a drastic increase in launch opportunities, a greatly simplified launch vehicle interface, and faster, cheaper, “New Space” design cycle.

Based on the Corbus-6 platform (see Figure 3-6), the Sutter Demo key components of the Sutter Demo platform (solar arrays, battery, propellant, and thermal control surfaces) are sized for a three-year mission in a worst-case orbit. All quoted margins are with respect to worst-case conditions at end-of-life. Thus, there is significant design margin and robustness overall, which can be exploited for much greater performance until EOL.

The proposed satellite platform for the Sutter Demo mission uses as little new technology as possible. This allows the team to minimize risk, as well as leverage designs that have formed the backbone of several dozen prior satellites to the maximum extent practical.

Table 3-2 provides the key spacecraft bus platform specifications of the Corvus-6 as adapted for the Sutter Demo spacecraft. Table 3-3 lists the Spacecraft Design Characteristics, while Table 3-4 provides the Mass Equipment List for the Sutter Demo spacecraft design. Table 3-5 provides the detailed power budget analysis, while Table 3-6 shows the Duty Cycle per Sutter Demonstration Orbit.

Mechanical Design and Payload Accommodation: The Corvus-6 platform consists of the Data and Power Module, Attitude Control Module, Smart Solar Panels, and the spacecraft structure. With these subsystems installed, a full 3U of payload volume is available to the developer. Figures 3-6 and 3-7 illustrate current concept level design configurations. Various data and control interfaces are available, including CAN, Ethernet, I2C, SPI, UART, and USB. With the spacecraft in “sun pointing” mode (orienting its broad face towards the sun), the solar panels generate 34 watts of power at End Of Life (EOL). If the spacecraft remains in sun pointing mode throughout the daylight portion of its orbit, 42 watts of continuous power is available for sensors or transmitters. The available power increases as the duty cycle is reduced, and decreases as the available sun pointing time is reduced.

Table 3-4 Mass Equipment List (MEL)

| Item | CBE Mass per Unit (kg) | Qty | Current Best Estimate Total Mass (kg) | Component Contingency | Predicted Mass (kg) | Comments/Heritage/Method of Estimation |
|---|---|---|---|---|---|---|
| **Payload** | | | | | | |
| Telescope | 0.71 | 1 | 0.71 | 20% | 0.85 | Canon EF 400 mm, 10cm Optic |
| Imager | 0.30 | 1 | 0.30 | 20% | 0.36 | Fairchild Imaging CIS2521 + Electronics & Enclosure |
| Payload Processor | 0.40 | 1 | 0.40 | 20% | 0.48 | Nvidia Tegra X1 GPU 400 mm, 10cm Optic |
| | | | | | | |
| **Structures** | | | | | | |
| Structural Panels | 3.88 | 1 | 3.88 | 10% | 4.26 | Based on 7.5kg Standard Bus Mass - Called Out Subsystems |
| Separation System | 0.00 | 1 | 0.00 | 10% | 0.00 | None, Not Included in Launch Mass Allocation |
| | | | | | | |
| **Power** | | | | | | |
| Solar Panels Fixed | 0.00 | 0 | 0.00 | 10% | 0.00 | Included in Structure Mass Above |
| Solar Panels Deployed | 0.00 | 0 | 0.00 | 10% | 0.00 | Included in Structure Mass Above |
| Batteries | 0.00 | 0 | 0.00 | 10% | 0.00 | Batteries Included in DPM Mass |
| | | | | | | |
| **Avionics and ACS** | | | | | | |
| Reaction Wheels | 0.19 | 3 | 0.56 | 0% | 0.56 | Sinclair Interplanetary 30 mNm Reaction Wheels (RW3-0.03) |
| Star Tracker | 0.19 | 2 | 0.37 | 0% | 0.37 | Sinclair Interplanetary (ST-16-R2) |
| DPM | 1.90 | 1 | 1.90 | 10% | 2.09 | AD Space Standard DPM, Corvus-6 Based |
| Payload Data Transmitter | 0.80 | 1 | 0.80 | 5% | 0.84 | AD Space AKAT-3 |
| | | | | | | |
| **Propulsion** | | | | | | |
| Thruster | 0.00 | 1 | 0.00 | 0% | 0.00 | No Propulsion on Sutter Demo |
| Tank | 0.00 | 1 | 0.00 | 0% | 0.00 | |
| Propellant | 0.00 | 1 | 0.00 | 0% | 0.00 | |
| **System Total - DRY** | | | **8.905** | **10.1%** | **9.804** | |
| **System Total - WET** | | | **8.905** | **10.1%** | **9.804** | |

Table 3-5 Detailed Power Budget Analysis

| | | | | | Mode Power (W) | | | | | | |
|---|---|---|---|---|---|---|---|---|---|---|---|
| **Module** | **Component** | **Power (W)** | **Quantity** | **Total Power (W)** | **Detumble** | **Safe Mode** | **Nominal** | **Imaging** | **Processing** | **UHF Downlink** | **Ka Downlink** |
| Panels | Sun Sensors | 0.0200 | 5 | 0.1000 | 0.10 | 0.10 | 0.10 | 0.10 | 0.10 | 0.10 | 0.10 |
| | Magnetorquers (detumble = 30% duty cycle) (magnetic pointing = 20% duty cycle) (momentum dump = 5% duty cycle) | Panel Dependent | 5 | 9.6530 | 2.90 | 0.00 | 0.48 | 0.00 | 0.48 | 0.48 | 0.00 |
| | Magnetometer | 0.0026 | 7 | 0.0185 | 0.02 | 0.02 | 0.02 | 0.02 | 0.02 | 0.02 | 0.02 |
| | Panel Processors | 0.0211 | 5 | 0.1056 | 0.11 | 0.11 | 0.11 | 0.11 | 0.11 | 0.11 | 0.11 |
| | I & V Monitors | 0.0033 | 5 | 0.0165 | 0.02 | 0.02 | 0.02 | 0.02 | 0.02 | 0.02 | 0.02 |
| | Panel Regulators | 0.0013 | 5 | 0.0063 | 0.01 | 0.01 | 0.01 | 0.01 | 0.01 | 0.01 | 0.01 |
| | Temperature Sensors | 0.0040 | 7 | 0.0277 | 0.03 | 0.03 | 0.03 | 0.03 | 0.03 | 0.03 | 0.03 |
| | H-Bridge | 0.0010 | 5 | 0.0050 | 0.01 | 0.01 | 0.01 | 0.01 | 0.01 | 0.01 | 0.01 |
| | Measured Inefficiencies | 0.3700 | 1 | 0.3700 | 0.37 | 0.37 | 0.37 | 0.37 | 0.37 | 0.37 | 0.37 |
| | Panels Total | | | | **3.55** | **0.65** | **1.13** | **0.65** | **1.13** | **1.13** | **0.65** |
| FCS | Avionics Board | 2.0000 | 1 | 2.0000 | 2.00 | 2.00 | 2.00 | 2.00 | 2.00 | 2.00 | 2.00 |
| | Reaction Wheels | 0.2000 | 3 | 0.6000 | 0.00 | 0.00 | 0.60 | 1.80 | 0.60 | 0.60 | 1.80 |
| | GPS Receiver | 1.1000 | 1 | 1.1000 | 0.00 | 0.00 | 1.10 | 1.10 | 1.10 | 1.10 | 1.10 |
| | UHF Radio Tx (beacon = 10% duty cycle) | 1.0000 | 1 | 1.0000 | 1.00 | 1.00 | 1.00 | 0.00 | 1.00 | 10.00 | 0.00 |
| | UHF Radio Rx | 0.2000 | 1 | 0.2000 | 0.20 | 0.20 | 0.20 | 0.20 | 0.20 | 0.20 | 0.20 |
| | Globalstar Tx | 3.1500 | 1 | 3.1500 | 0.00 | 0.00 | 0.00 | 0.00 | 0.00 | 0.00 | 0.00 |
| | Globalstar Rx | 1.0500 | 1 | 1.0500 | 0.00 | 0.00 | 0.00 | 0.00 | 0.00 | 0.00 | 0.00 |
| | Aquila Radio S-band Rx | 0.1000 | 1 | 0.1000 | 0.00 | 0.00 | 0.00 | 0.00 | 0.00 | 0.00 | 0.00 |
| | Aquila Radio UHF Tx | 10.0000 | 1 | 10.0000 | 0.00 | 0.00 | 0.00 | 0.00 | 0.00 | 0.00 | 0.00 |
| | Star Tracker | 0.4000 | 1 | 0.4000 | 0.00 | 0.00 | 0.40 | 0.40 | 0.40 | 0.40 | 0.40 |
| | FCS Total | | | | **3.20** | **3.20** | **5.30** | **5.50** | **5.30** | **14.30** | **5.50** |
| Imager | Imaging Sensor | 1.0000 | 1 | 1.0000 | 0.00 | 0.00 | 0.00 | 1.00 | 0.00 | 0.00 | 0.00 |
| | Analog to Digital Converter | 1.7000 | 1 | 1.7000 | 0.00 | 0.00 | 0.00 | 1.70 | 0.00 | 0.00 | 0.00 |
| | FPGA | 5.3000 | 1 | 5.3000 | 0.00 | 0.00 | 0.00 | 5.30 | 0.00 | 0.00 | 0.00 |
| | mSATA SSD | 1.5000 | 1 | 1.5000 | 0.00 | 0.00 | 0.00 | 1.50 | 1.50 | 0.00 | 1.50 |
| | Processor | 6.0000 | 1 | 6.0000 | 0.00 | 0.00 | 0.00 | 6.00 | 6.00 | 0.00 | 6.00 |
| | Payload Total | | | | **0.00** | **0.00** | **0.00** | **15.50** | **7.50** | **0.00** | **7.50** |
| Ka-band | Modulator Chip | 3.3250 | 1 | 3.3250 | 0.00 | 0.00 | 0.00 | 0.00 | 0.00 | 0.00 | 3.33 |
| | Oscillator/Upconverter | 3.2000 | 1 | 3.2000 | 0.00 | 0.00 | 0.00 | 0.00 | 0.00 | 0.00 | 3.20 |
| | Ka FPGA | 5.8000 | 1 | 5.8000 | 0.00 | 0.00 | 0.00 | 0.00 | 0.00 | 0.00 | 5.80 |
| | High Power Amplifier | 8.0000 | 1 | 8.0000 | 0.00 | 0.00 | 0.00 | 0.00 | 0.00 | 0.00 | 8.00 |
| | Ka-band Transmitter Total | | | | **0.00** | **0.00** | **0.00** | **0.00** | **0.00** | **0.00** | **20.33** |
| Total - before EPS efficiency | | | | | 6.75 | 3.85 | 6.43 | 21.65 | 13.93 | 15.43 | 33.97 |
| EPS | Battery Charging Regulator Efficiency | | | | 91.00% | 91.00% | 91.00% | 91.00% | 91.00% | 91.00% | 91.00% |
| | Power Distribution Module Efficiency | | | | 90.00% | 90.00% | 90.00% | 90.00% | 90.00% | 90.00% | 90.00% |
| | EPS Total Power Dissipation | | | | 1.83 | 1.04 | 1.74 | 5.87 | 3.78 | 4.18 | 9.21 |
| Margin | 5% Uncertainty Margin | | | 5.00% | 0.34 | 0.19 | 0.32 | 1.08 | 0.70 | 0.77 | 1.70 |
| **Total (W)** | | | | | **8.57** | **4.89** | **8.18** | **27.52** | **17.71** | **19.61** | **43.18** |

Table 3-6 Demo Orbit vs. Duty Cycle

| LTAN | Eclipse Time [min] | Available Payload Operations [min] |
|---|---|---|
| 06:00 hrs | 0 | 51 |
| 08:00 hrs | 23 | 43 |
| 10:00 hrs | 33 | 35 |
| 12:00 hrs | 35 | 33 |

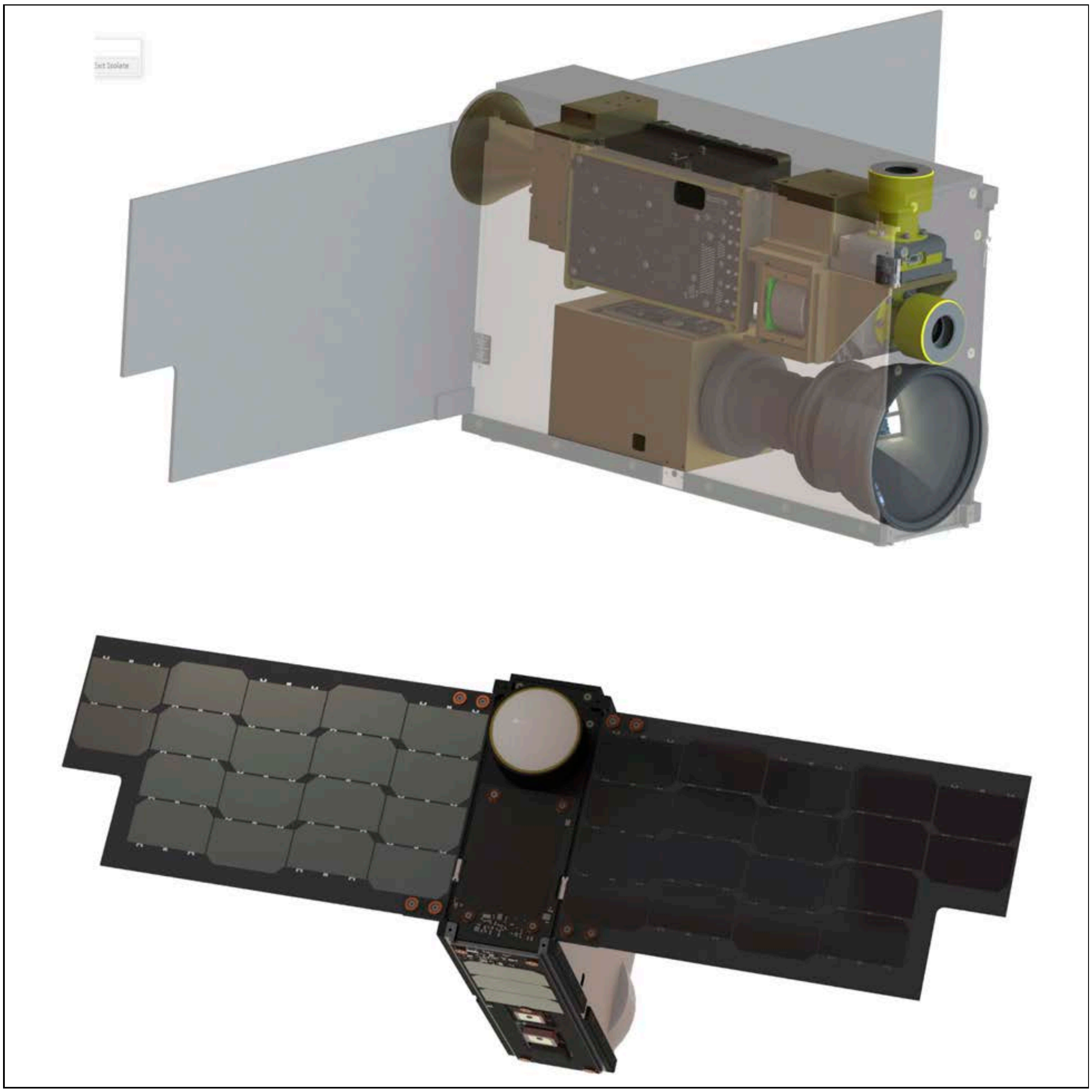

Figure 3-6 CAD Views of the Sutter Demo Spacecraft. Deployed

Figure 3-7 CAD View of 6U Spacecraft Stowed With 10 cm Telescope

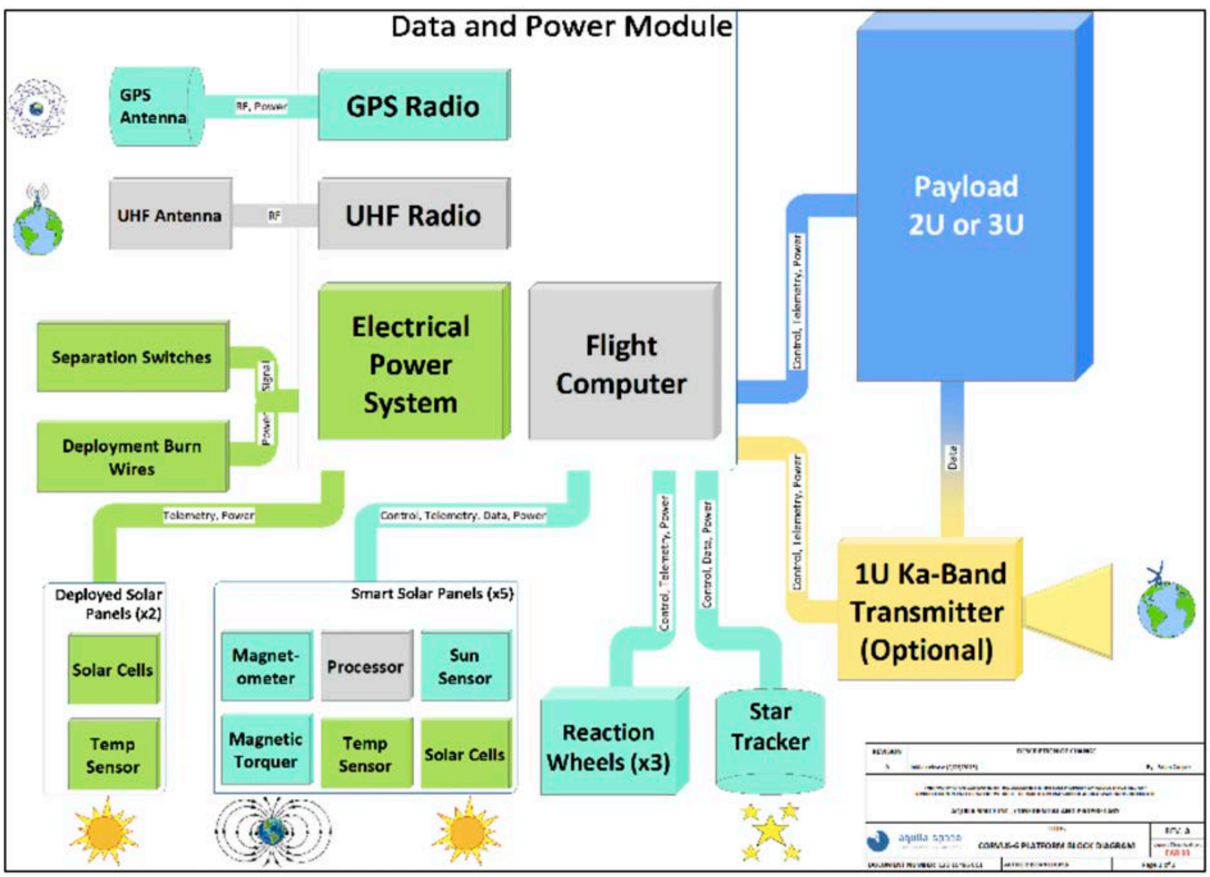


Figure 3-8 Data and Power Module Block Diagram

Electrical Architecture: The Corvus-6 Data and Power Module (DPM) combines many of the control and housekeeping functions of the spacecraft into an easily accessible single integrated unit and is illustrated in Figure 3-8 below.

The DPM consists of the following “cards”:

- Electrical Power Subsystem (EPS) on four separate cards:
  - Battery Board: 48 watt-hour lithium ion, 18650 form factor
  - Power Board: Voltage regulation and switching
  - Charging Board: Solar conversion and EPS central computer
- Flight Computer:
  - Cortex-A8 32 bit ARM running Linux
  - Integrated magnetometer and IMU with large selection of external interfaces
- Novatel OEM615 GPS Receiver:
  - Includes a distributed portion of the EPS with two 3.3V switches controlled by the Charging Board
- AstroDev Lithium UHF Transceiver:
  - Custom watchdog included
  - ‘Firecode’ functionality to force a system-wide hard reboot from the ground
- Backplane board, routing all circuits to external spacecraft modules as required.

The Data and Power Module also includes a breakout connector to route control and debugging signals to the outside of the spacecraft for development and testing on the ground. Each card can be easily installed and removed, allowing for quick assembly and test. All interfaces are alodined, providing excellent thermal dissipation and electrical grounding for all cards. Ruggedized connectors between the Backplane and each card are qualified to greater than 100 mate/demate cycles. Control signals and power lines are routed out to external system modules through aerospace-grade Glenair Nano-D and Micro-D connectors. The full DPM was successfully vibration tested to NASA GEVS levels both as with no adverse effects observed.

The EPS is capable of supporting up to 50 watts peak discharge power. It includes four (4) peak-power tracking battery charge regulators, all four (4) of which can support up to 22 watts each. The low power battery charge regulators support up to 12 watts. Each battery charge regulator measures the input current and voltage to monitor total solar power input. 48 watt-hour batteries provide continuous power throughout eclipse and the Charging Board can be set to completely customizable battery “full” and “empty” voltages. The baseline operation of the EPS is between 3.4 and 3.95 Volts to extend the life of the battery. The Battery Board is designed with an all-parallel cell design, the benefits of which include: cell failure tolerance, high regulation efficiency to low voltage units, and guaranteed cell charge balancing. A fail-safe watchdog system is designed into the EPS with a systems perspective to prevent downtime and safeguard against loss-of-mission. The EPS includes an “Inhibit” signal. When Inhibit is shorted to ground, the EPS disables all power outputs and enters an extremely low-power consumption mode (<100 microamps). Inhibit can be shorted to ground through external micro-switches or through the Flight Computer umbilical connector.

Two modes of Peak Power Tracking (PPT) are possible with the EPS. The first is "temperature programmed" PPT, in which the temperature of the solar panel is used to set the input to the PVCs to a value based on the well characterized inverse linear relationship of the voltage at maximum power (Vmp) to temperature. This is open-loop PPT, and requires minimal work on the part of the processor. The system is also capable of "perturb and observe" PPT (sometimes called hill-climbing PPT). In this mode the processor changes the PVC input set point and waits to see if the power delivered goes up or down. If it goes up, it takes a further step in that direction; otherwise it goes in the opposite direction, trying to find the peak power point. The choice between these may depend on other system factors.

The battery has multiple levels of safety. During normal operations, the primary safety is the associated EPS microprocessor, which monitors all critical voltages and currents and is able to connect or disconnect any loads. Additionally, the processor can disconnect cells individually or in groups. It is the responsibility of the EPS processor to keep the cells from becoming over-discharged or over-charged. In the event of power emergencies, the processor is able to remove loads to protect the battery. The second level of protection is hardware based. Each cell has its own monitoring circuit, and should the cell voltage become too high or too low, the cell will automatically be disconnected to prevent damage. There is also current monitoring to prevent damage from short circuits or anomalous charge currents. Finally, there is a safety inhibit which can be installed which disconnects all cells and puts them in the lowest possible discharge mode, for storage, shipment, or while attached to the launch vehicle. Thus, as far as the launch vehicle is concerned, the battery has triple safety protection features.

The EPS STM32F4 microprocessor runs a bare metal version of Python 3, referred to as MicroPython. This allows for easy customization of all battery protection features, especially considering the large open source support community for MicroPython. The Astro Digital source code for the microprocessor is open source, and mission-specific modifications are supported. The EPS microprocessor could potentially serve as the main flight computer for a simple spacecraft thanks to this extremely flexible design.

The Astro Digital Flight Computer provides telemetry storage, spacecraft operational control, and attitude control. It runs Linux OS on a Cortex-A8 processor to allow for straight-forward customization. For Astro Digital missions, Python is used extensively for simple scripting and easy debugging. All functional data handling, attitude control calculation, and event timing for the spacecraft is performed on the Flight Computer. The Flight Computer includes an onboard magnetometer, gyroscope, and Inertial Measurement Unit (IMU). The IMU is a single-chip magnetometer, gyroscope, accelerometer, and temperature sensor.

The GPS receiver card consists of a Novatel OEM615 GPS receiver and a small breakout board for power regulation and switching. The breakout board includes a 3.3 volt regulator with two switched outputs. The outputs are controlled by the Charging Board via an I2C connection to the GPS Card. One output is used to power the GPS, and the second output is routed to the Backplane Board to provide a spare 3.3 V output for use at the system level. The GPS card includes a coax connector for routing to an externally mounted active receive patch antenna. The GPS receiver also provides a calibrated “Pulse Per Second” signal. This allows for extremely precise timing accuracy as required by the bus or payload.

The UHF card includes an AstroDev Lithium UHF radio and a custom Astro Digital daughterboard. The daughterboard funnels switched transmit power and “always-on” receive power to the UHF radio. A One-Shot Reset Circuit is included to allow the EPS to momentarily power cycle the radio in order to clear any potential errors. After a reset, the One Shot Reset Circuit will prevent any further resets for a duration of 60 seconds. This allows the spacecraft operator to issue a command as necessary to prevent the spacecraft from entering a reset loop. The baseline setting for the UHF radio is in the ~400 MHz band, although it can be adjusted between 130-450 MHz. The radio is connected to a calibrated and matched monopole whip antenna which is deployed from the spacecraft after launch. The UHF radio includes a “Firecode” pin, which is toggled high when the radio detects a short, user-defined radio burst. In Corvus-BC, this pin is routed to a reset circuit on the EPS which power cycles the entire spacecraft, thereby clearing any system-level errors.

The 1U Ka-band Module will provide a capability of 120 GB data download per day, of which only 5 GB per day is required to provide full unprocessed data download.

The DPM is designed to be easily reconfigurable. New cards can be added to the DPM with a re-spin of the relatively simple Backplane board. Existing cards can be replaced, or the DPM structure can be elongated to accommodate more card slots. The Backplane board includes very limited circuitry, such as data bus buffers, which results in a fairly straightforward redesign process. Assembly and disassembly is extremely easy thanks to the “server rack” style design; only 2 screws are needed to secure each DPM card. Card-specific keying prevents accidental mis-mates and also provides mechanical interlocking for connector strain-relief.

The Attitude Control Module (ACM) shown in Figure 3-9 consists of three Sinclair Interplanetary 30 millinewton-meter-second reaction wheels and two 10 Hz sample-rate Sinclair Interplanetary star trackers. This enhanced hardware implementation for the Sutter Demo Mission allows for low jitter 3-axis attitude control with a pointing knowledge of better than 100 arcsec in all axes (including system level jitter and propagation errors) better than the baseline platform. The reaction wheels provide a nominal torque of 2 millinewton-meters, which enables full 180 degree maneuvers in less than 30 seconds. These enable a pointing accuracy of better than 2 arcsec in all axes which enables sub-pixel control during 10 second matched filter algorithm tracking frames. All Sinclair products are put through rigorous environmental and functional tests to qualify them for launch and operations.

All three of the reaction wheels are controlled with a single UART RS-232 port. They consume 1.8 watts each at 5 volts when generating maximum torque, dropping down to 0.1 watts at steady state low speed rotation. The Star Tracker is controlled with an RS-485 port, and consumes 0.4 watts of power at 12 volts while active. Quaternions are provided at a maximum rate of 10 solutions per second, allowing for spacecraft attitude control with only a simple MEMS inertial measurement unit. The basic Corvus 6 design has been modified by adding a second star tracker and the star tracker manufacturer consulted with to upgrade its performance. By making this change and improvements in the control algorithm, the 2 arcsec pointing control over a ten second image frame requirement is achieved. Figure 3-9 shows a current configuration of the Attitude Control Module with only one star tracker.

The Astro Digital Smart Solar Panels serve as attitude control sensors and actuators and can be fitted with any solar cells that use the standard 26.62 cm2 Spectrolab form factor. In the Landmapper-BC configuration, the +X and –X panels (defined as the panels on the UHF Antenna and Star Tracker faces respectively) each have 4 cells. The body-mounted Y axis panels have 18 cells each, and the deployed Y panels have 20 cells each. The –Z

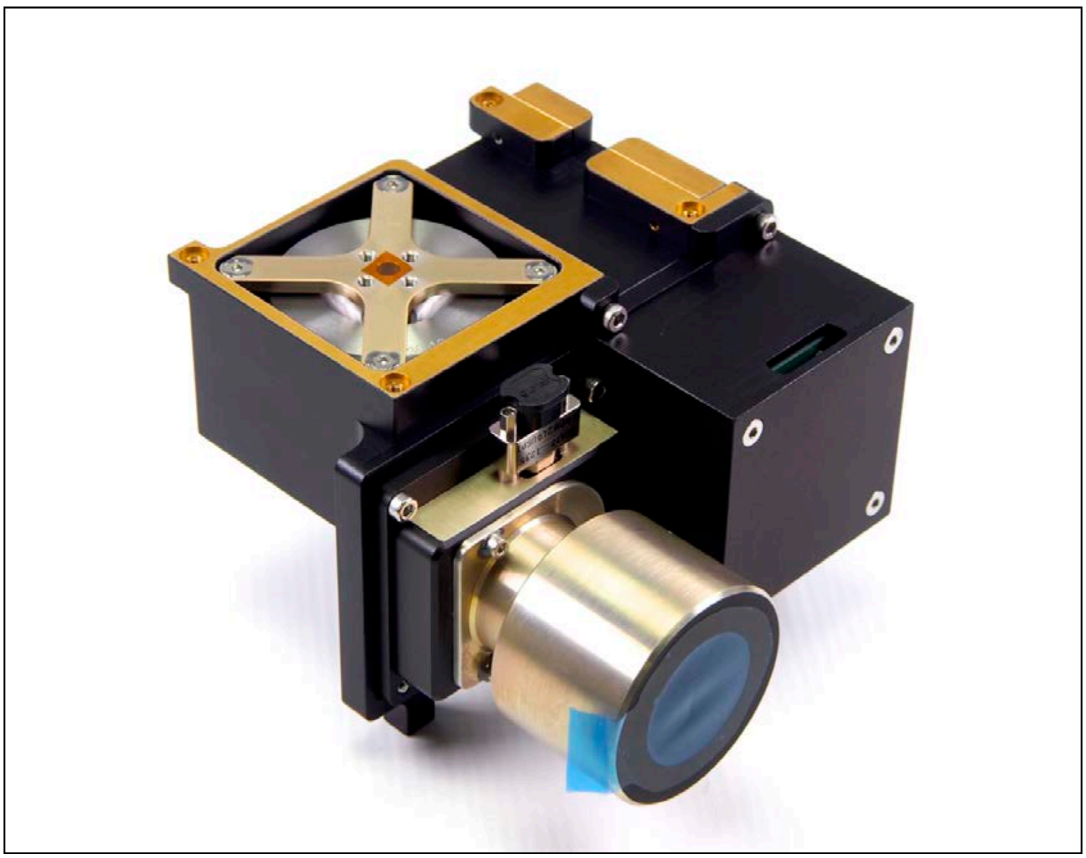

Figure 3-9 Attitude Control Module

panel, which is the face opposite of the cameras, has 3 cells. The baseline solar cells are Spectrolab UTJ cells with 28.3% efficiency. Higher efficiency solar cells are available.

All body-mounted panels include a 2-axis sun sensor with sun intensity measurement, a 3-axis magnetometer, a temperature sensor, an embedded magnetic torque coil, current/ voltage monitors for torque coils, and a micro-controller for telemetry collection and command distribution. The X axis torque coils each have a dipole moment of 31 mA*m2, the Y axis torque coils have 115 mA*m2, and the Z axis torque coil has 114 mA*m2. These moments are all derived from a 5 volt solar panel digital power supply, which is the minimum allowable voltage, as well as the voltage used in the Corvus-BC system design. The dipole moment increases linearly with supply voltage. All panel micro-controllers are controlled with a common I2C bus, and the temperature sensors are controlled using a “1-Wire” bus. The fixed Y panels are designed with the intent for structural grounding to be used as a return path for solar panel output power. All panels utilize a 9 pin Nano-D connector for control signals, digital power input, and solar power output.

### 3.2.3 Sutter Demo Ground System

#### 3.2.3.1 Sutter Demo Ground Station and Telemetry

In support of the Sutter Demo mission, TransAstra proposes to utilize the existing Astro Digital software, facilities, and infrastructure previously developed for the Landmapper Constellation. This suite of capability includes a satellite operations center in Santa Clara California, UHF ground stations, and previously configured Ka-band ground stations in Svalbard. The operations center is shown in Figure 3-10.

Advanced Solutions Inc. is the heritage provider of both Flight Software and Ground Software for Astro Digital’s Corvus-6 and 16 platforms. (See Figure 3-11 above for display images) The operations software is a modified version of the open source COSMOS suite from Ball Aerospace. Ongoing advancement of this software stack is under development funded internally by Astro Digital in support of the Landmapper constellation. Sutter Demo will benefit from ongoing investment, development and lessons learned on the 11 Astro Digital spacecraft to launch ahead of Sutter Demo.

All Astro Digital Corvus spacecraft are controlled from the Astro Digital Quad-Yagi UHF ground station located in Santa Clara, California as shown in Figure 3-12. The antenna transmits with 300 Watts of output power and 24 dB of gain. The open source satellite tracking program, Gpredict, is used for pass prediction and antenna pointing control. The spacecraft can be commanded to immediately execute activities and maneuvers from the UHF ground station, or schedules can be uploaded with planned future maneuvers. Our proposed TT&C ground station provision includes as many UHF TT&C passes as available (2-4 per day) with additional potential capability as needed provided by a third party provider in Norway.

Payload data to include TLEs and Imagery Stacks are downlinked via Ka-band transmitter to a 2.4 meter ground station located in Svalbard, Norway shown in Figure 3-13. This

Figure 3-10 Space SOC Photographs Multi-view

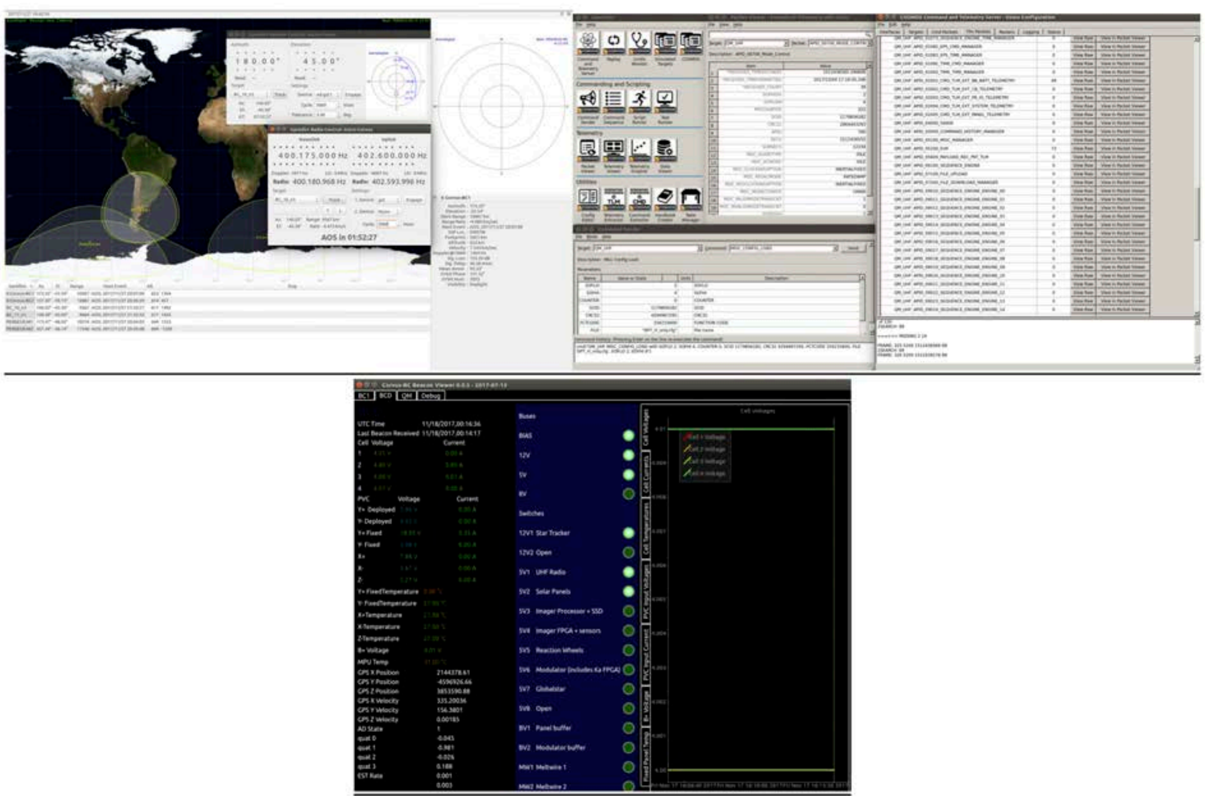

Figure 3-11 ASI Operations Software Display Images

station, operated by Konsberg Satellite Services is provided as a turn-key service for delivering the payload data directly from the antenna to their customers, or to the cloud. This ground station was developed with Astro Digital to specifically support the Landmapper constellation and was commissioned in the summer of 2017. The station has excess capacity to support Sutter Demo and it is expected that one pass per day will be enough to downlink all anticipated payload data.

Figure 3-12— UHF Ground Station Mountain View

3.2.3.2 Sutter Demo Science Data Processing and Distribution

Once imagery has been collected and initially processed onboard the Sutter systems, any potential detections and their associated metadata (star image chips, asteroid image chips, darks, flats, registration offsets, spacecraft telemetry) are downlinked to a ground station for higher fidelity processing. As depicted in Figure 3-14, this can involve several steps to obtain the final asteroid characterization. The ground station would have a high end workstation or server to manage the downlinked data, archive it, and perform post-detection processing.

Figure 3-13 - KSAT Ka-band Ground Station

The first step would be to improve the frame-to-frame registration over that used in the Sutter Ground Test or Sutter Demo. This would move from a purely translational alignment to a higher order (at least cubic) warping function across the focal plane to better align the image chips for an asteroid chip-out sequence. This would employ a star centroid estimation that is a more computationally heavy and robust algorithm than that used onboard the spacecraft. The asteroid chips would then be fed into a matched filter refinement process to fine tune the starting position and velocity vector measurement, obtain a revised MLE and SNR, and determine if the onboard detection was a false alarm. The refinement process will use a particle swarm optimizer to obtain sub-pixel accuracy on the matched filter template fitting.

The star centroids will also be used to obtain an improved astrometric plate solution for one frame in the collection sequence. All other frames will be aligned after the frame-to-frame registration. This will be based upon the latest star catalog obtainable. The astrometry combined with the refined asteroid positions will yield the asteroid line-of-sight coordinates which when coupled to the spacecraft's heliocentric position provides measurements that make up a tracklet, which in turn can be used for estimating the ISRU candidate's orbital elements. The orbit can then be sent to Sutter tasking control for re-imaging the ISRU candidate with the same or another survey instrument.

In addition to these steps, the satellite camera's photometric calibration can be done on known standard stars that have been imaged and aperture photometry performed on the asteroid chips to obtain light curves and filter band information to define taxonomy. Together these processes produce a complete ISRU characterization for Sutter mining mission operations.

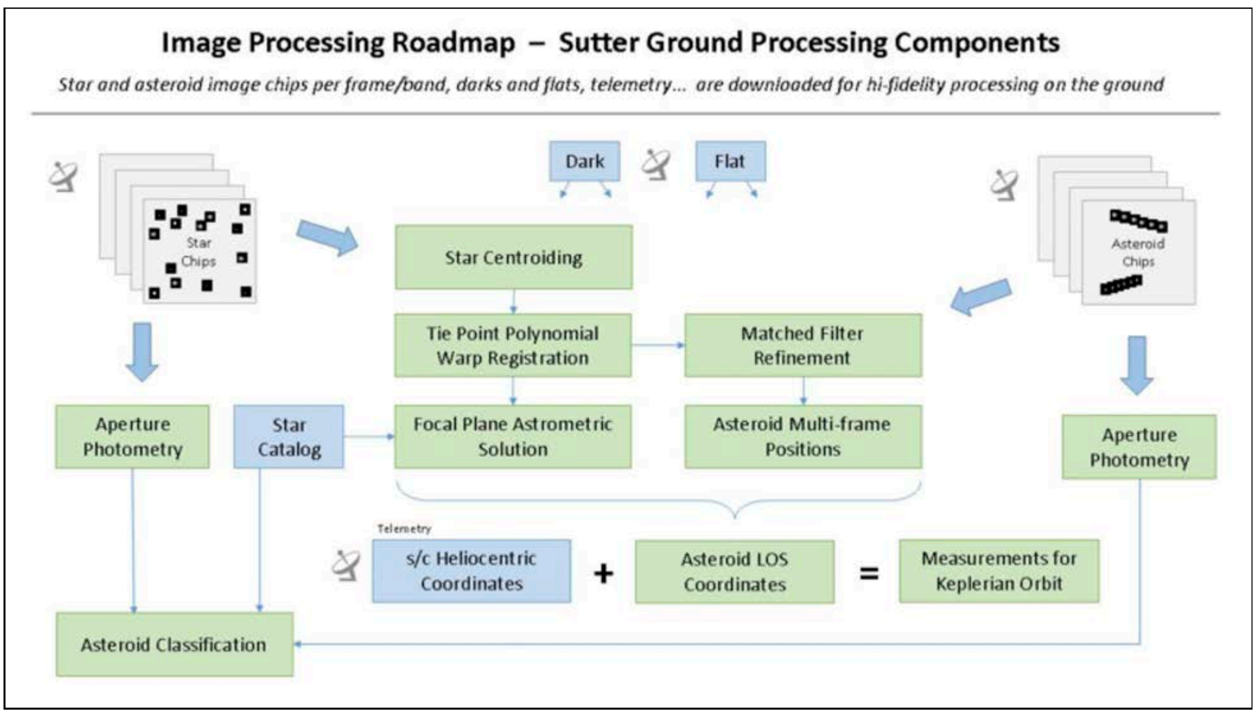


Figure 3-14 Image Processing: Ground Processing

Although the primary purpose of the Sutter Demonstration mission will be to prove the MFA approach in a space telescope for NASA, additional science data products may be produced from new detections. Commercial funding is expected for an extended mission to continue to make detections for the life of the spacecraft. All data including asteroid photometry & astrometry, colors from the different filters (if available) and identification of any PHOs or asteroids detected will be compiled and submitted to the appropriate object databases.

### 3.3 Sutter Survey Mission

The Sutter Survey is the first complete realization of the Sutter approach to asteroid prospecting and consists of 3 spacecraft, each with 4 telescopes capable of initial characterization (prospecting) of high value targets. The Mission is further described in detail below.

#### 3.3.1 Sutter Survey Mission Design

This Sutter Survey prospecting strategy will evolve as understanding improves based on the ground-based demo and Sutter demo results. However, there are some considerations that are already understood that provide a general idea of the surveying strategy.

First, the 3 spacecraft are on Earth-like heliocentric orbits so much of the understanding of ground-based asteroid surveying can be applied to Sutter Survey. The apparent behavior of the ISRU candidates will be similar to ground-based observations of close approaching asteroids. See Figure 1-10 for an illustration of the Sutter Survey Mission Design.

Second, the spacecraft interior to Earth's orbit will have most ISRU candidates outside their orbit and these objects will be brightest at opposition. Conventional wisdom suggests that surveying towards opposition where the asteroids are nearly 100% illuminated provides optimal discovery capability.

Third, the spacecraft exterior to Earth's orbit will have most of the ISRU candidates interior to them but in this observing scenario the objects will be back lit and difficult to detect and observations would have to be performed looking towards the Sun. These spacecraft will survey in the general direction along the Earth's orbit where the ISRU candidates will appear to be moving slowly because most of the motion is along the line-of-sight.

An average phase angle of 90 deg will cause these objects to be fainter but this effect may be mitigated by their slower apparent rate of motion. While these spacecraft may be sub-optimally located for prospecting their locations provide excellent opportunities to provide completely different observations of desirable ISRU candidates. A candidate's orbit will be quickly and accurately determined with observations acquired by the 'exterior' spacecraft. Furthermore, the acquisition of light curves from the different spacecraft all observe different aspect angles on the candidates and should allow rapid determination of an object's rotation rate, state, and even shape.

### 3.3.2 Sutter Survey Flight System

The Sutter Survey spacecraft is a 90 kg platform, roughly of ESPA class, custom designed to support a 5 year compound telescope match filter asteroid survey mission. The platform utilizes commercial grade satellite subsystems with custom modifications to support affordable interplanetary operation, while leveraging the heritage and experience of Astro Digital's Corvus-XL LEO Platform. It has a peak power generation of 185 watts and implements a Microwave Electrothermal Thruster (MET) primary propulsion system providing 2 km/s of total delta-V.

The Sutter Survey spacecraft implements redundant communication systems for command and control as well as payload data downlink consisting of a 20 Watt Eridium Laser Comm terminal with a 10 cm optic and an X-band DSN link. The payload consists of four 14 cm optical telescopes with partially overlapping fields of view, with low light panchromatic sensors and an FPGA image processing computer for identification and tracking of NEOs. Figure 3-15 shows the spacecraft from several angles, while figure 3-16 provides a cutaway view of the internals of the spacecraft from two angles. Figure 3-17 provides a functional block diagram of the spacecraft systems.

#### 3.3.2.1 Sutter Survey Payload Hardware

The compound matched filter tracking payload is an evolution of the Sutter Demo payload and likewise derived from COTS components that are high-TRL. The optical front end

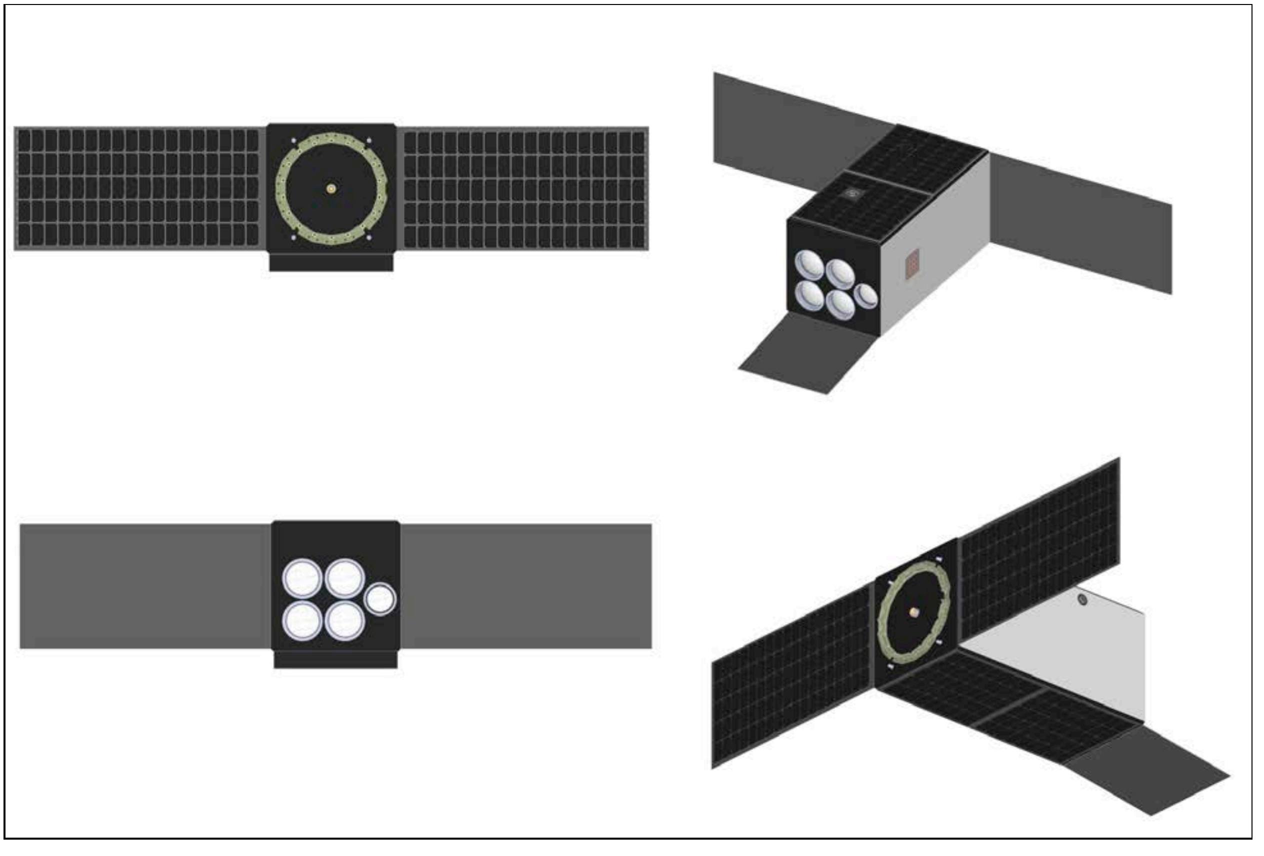

Figure 3-15 - Sutter Survey Spacecraft 3-View consists of four independent telescopes, derived from COTS Canon telephoto lenses ruggedized for flight. The ruggedization process principally involves replacing the chassis with low Total Mass Loss (TML) and low Collected Volatile Condensable Materials (CVCM), high-stability chassis materials, the process of which was initially developed for AD's Landmapper constellation and will have also been previously implemented on Sutter Demo. The chosen 14 cm F/5.4 COTS Canon optics each provide a 0.55 X 0.60 deg^2 field of view and combined in an array, the four optics provide an aggregate 1.05 X 1.17 deg^2 field of view. See Figure 3-18 for an illustration of the telescope layout. The optics' individual FOVs will be partially overlapped to support a taxomonic imaging mode, which will provide a simultaneous multispectral imaging capability of select and known NEOs. See Figure 3-19 for a graphical representation of the overlapping FOVs.

Each optic is paired with its own focal plane and detector electronics to support simplified box level assembly, integration, and testing. The detector—the Fairchild Imaging CIS4000—is a large format, ultra-low-noise CMOS image sensor intended for applications requiring high quality imaging under extremely low light conditions. The device is an evolution of the CIS2521 sensor baselined for Sutter Demo and features an array of 5 transistor (5T) pixels on a 6.5μm pitch with an active imaging area of greater than 4000(H) x 4000(V) pixels.

This sensor supports user-programmable row start/stop control for region of interest (ROI) readout. These features, combined with 17 megapixel resolution and 100 fps imaging rates, make the CIS4000 an imaging device ideally suited for a variety of low light-level camera applications, like Match Filter based NEO discovery and tracking. An initial sensor noise budget is presented in Table 3-7 The current requirement for S/N is 7. Passive thermal control of the sensors will be required to maintain a sensor temperature of 0ºC to achieve the required dark noise levels. The combined optic sensor pairing provides a angular resolution of 1.5 arc-seconds per pixel, compliant with the algorithms two-line element derivation requirements.

The Sutter Survey payload also contains a payload computer responsible for command and housekeeping activities of the payload and the match filter processing previously

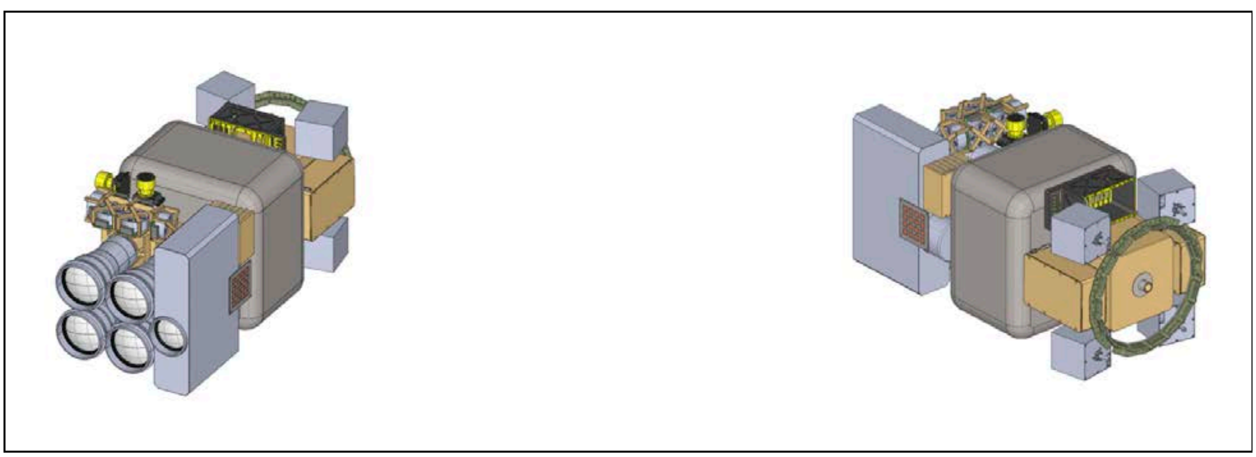

Figure 3-16— Sutter Survey Spacecraft Cutaway

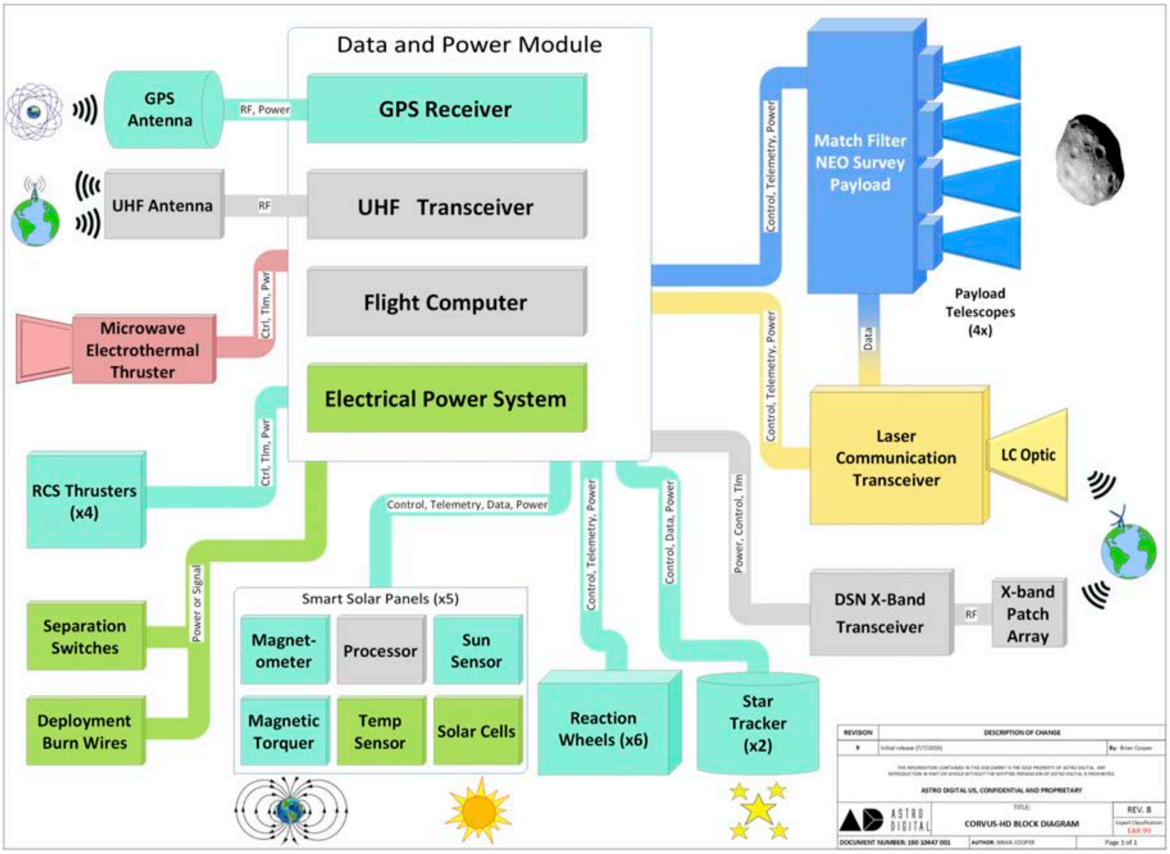


Figure 3-17— Sutter Survey Functional Block Diagram

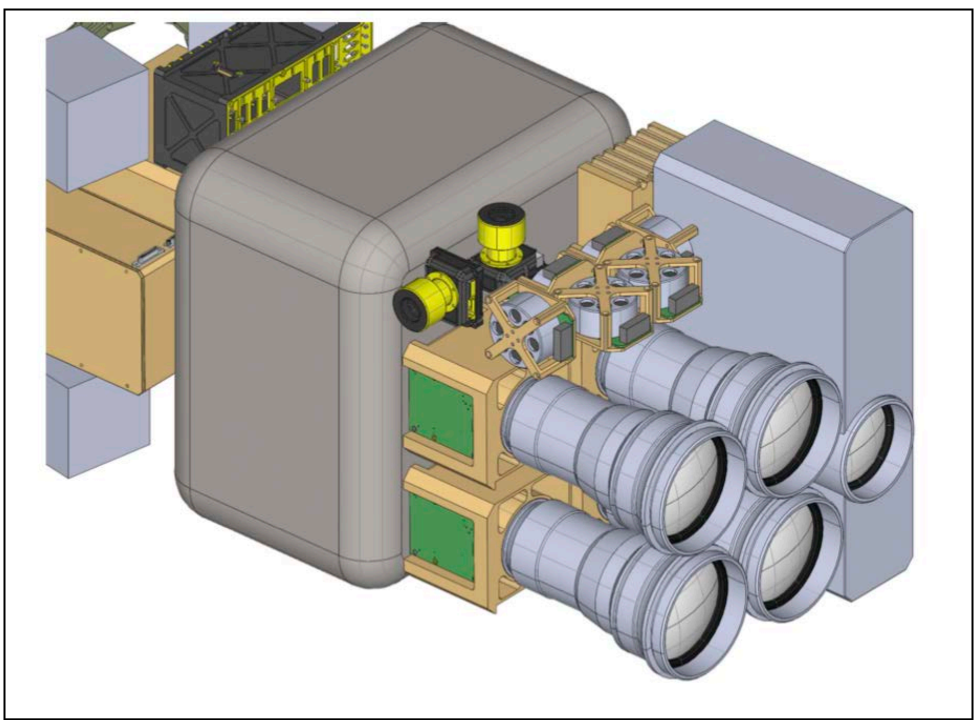

Figure 3-18— Sutter Survey Compound Telescope Layout

described in Section 2.1. The payload computer contains redundant ARM Cortex A57 , driving redundant VIRTEX-7 FPGAs. The FPGAs are responsible for the portions of the primary match filter algorithm requiring the greatest computation load. The VIRTEX-7s have been flight qualified for the NASA TESS mission currently scheduled for launch in June 2018. Given the current algorithm design a single VIRTEX-7 can process the data coming in from the telescopes at a rate greater than realtime. Excess FPGA fabric and the redundant FPGA have been included in the design to accommodate later algorithmic upgrades or additional post-processing requirements derived post launch.

### 3.3.2.2 Sutter Survey Payload Software

The Sutter Survey processing functional flow is as depicted in Figure 3-20. This is essentially identical to Sutter Demo with upgrades to be made to several image processing components as follows:

- Migration of the GPU assigned functions of matched filtering shift-and-stack plus detection/compaction, and any CPU heavy processing modules, to a FPGA chip for a more robust hardware implementation of critical runtime components.
- Single stack processing versus multi-stack processing to detect very slow movers.
- Higher fidelity frame-to-frame registration onboard the satellite using a full-image 2D phase correlation method with rank 1 subspace phase slope estimation. This will

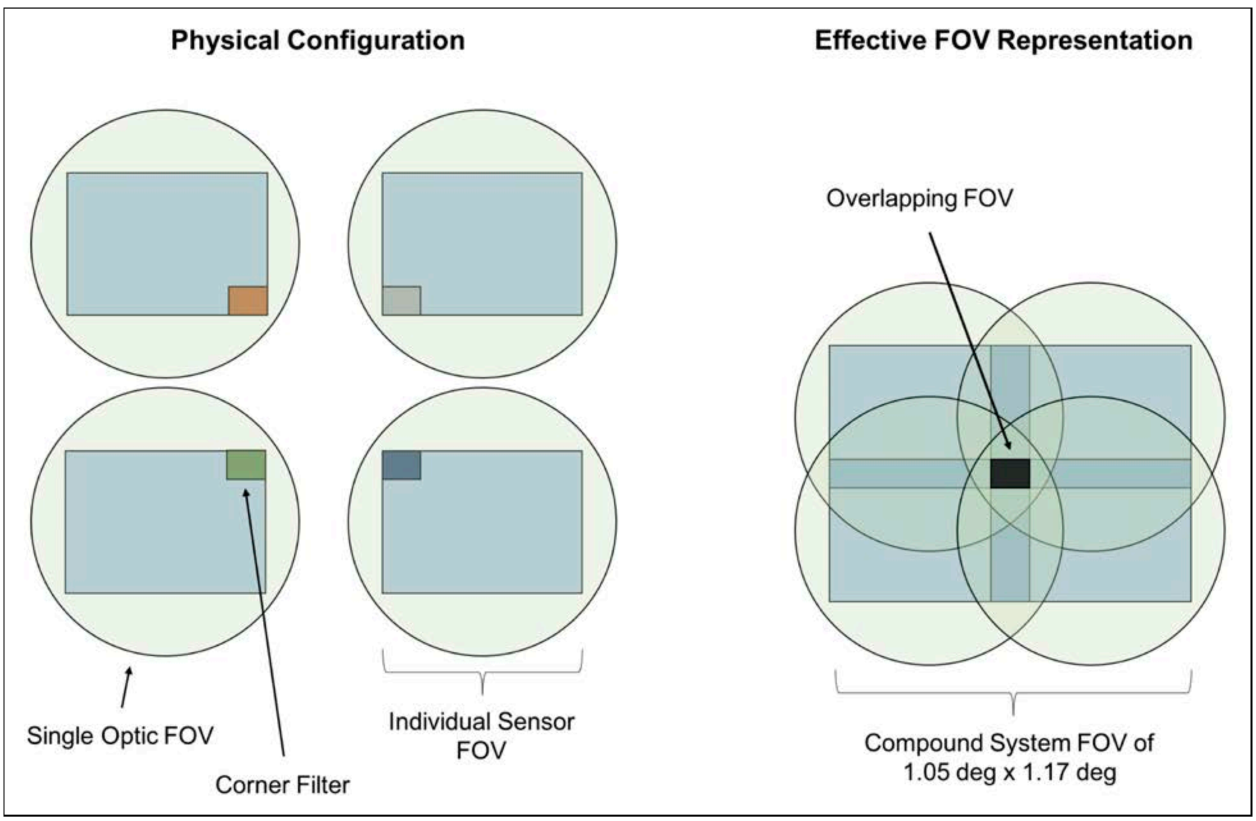


Figure 3-19 - Sutter Survey Overlapping FOV + Filter Positions estimate translation plus rotation, similarity transform, or higher order cubic warp as required for better clutter suppression (via improved alignment of the image stack).

- Introduce a non-diagonal covariance matrix that will account for any noise spatial correlation between adjacent pixels for more robust whitening.
- Provide an onboard module to locally estimate the PSF from the collected imagery and apply a spatially variable PSF across the focal plane prior to matched filtering.

Table 3-7 Noise Budget

| SNR CALCULATIONS for FIXED SNR, VARIABLE EXPOSURE | | |
|---|---|---|
| Spectral Bands | Wideband | |
| Lower Edge | 400 | [nm] |
| Upper Edge | 1000 | [nm] |
| Bandwidth | 600 | [nm] |
| Central Wavelength | 700 | [nm] |
| Transmissivity of Optics | 90% | |
| Transmissivity of Filter | 85% | |
| CMOS QE | 55.0% | |
| Target Irradiance | 471.2 | W/m2/um |
| Aperture Area | 0.0160 | m2 |
| Power of Received Light | 1.92E-10 | W |
| Energy per Photon | 2.84E-19 | J/photon |
| Photon Flux | 5.61E-01 | photons/s |
| Electron Flux | 3.09E-01 | e-/s |
| Signal Electrons | 0.00 | e- |
| Nominal Signal Electrons | 9 | e- |
| Nominal Exposure Time | 9.7 | S |
| Dark Noise | 0.00 | e- for -20ºC |
| Photon Shot Noise | 0.002 | e- |
| Read/Reset Noise | 5.0 | <2e- or <5e- Mode Dependent |
| Quant. Noise | 0.00 | e- |
| Background | 5.34 | e- |
| Total Noise | 7.32 | e- |
| Stacking | 30.00 | |
| Nominal Signal to Noise Ratio | 6.7 | |
| Saturated? | NO | |
| Fraction of Full Well | 0.03% | % |

#### 3.3.2.3 Sutter Survey Spacecraft Design

The Corvus-XL Bus, designed and developed by Astro Digital, is an evolution of the Corvus Platform product line initially developed for the Landmapper Constellation to carry payloads up to 40 kgs in LEO. It is a highly capable single string platform implementing commercial best practices with New Space technologies such as heritage subsystems from a number of recent missions including the Landmapper-BC1, 2 and 3, Sirion-1 and eight more spacecraft to be launched in 2018, as well as Rose-1, Sirion-2 and 3, and 5 additional Landmapper Spacecraft. For Sutter Survey, the Corvus-XL platform will be modified from its LEO Mission configuration to include a MET propulsion system, redundant communications as well as ACS and EPS upgrades like RCS thrusters and articulating solar arrays to support effective interplanetary operations. Table 3-8 summarizes the Mass Equipment List (MEL) for a single Sutter Survey Spacecraft.

The Corvus-XL Data Power Module (DPM) is the command and control center for the spacecraft. It houses the Flight Computer, Power Conditioning and Control Electronics, a DPM specific 96 Whr battery pack, GPS Receiver, and UHF TT&C Radio. The later two subsystems are only for use during the commissioning of the spacecraft when it is still in GTO, where GPS and UHF TT&C are possible. The Corvus-XL DPM is an evolved version of the Corvus-16 Expanded DPM, with modifications on parts selection and to the communications protocol and data bus. Specifically, the flight computer, radios and power electronics will be modified from a commercial parts selection process for LEO operations to one with an eye towards interplanetary space environments. Greater radiation ratings as

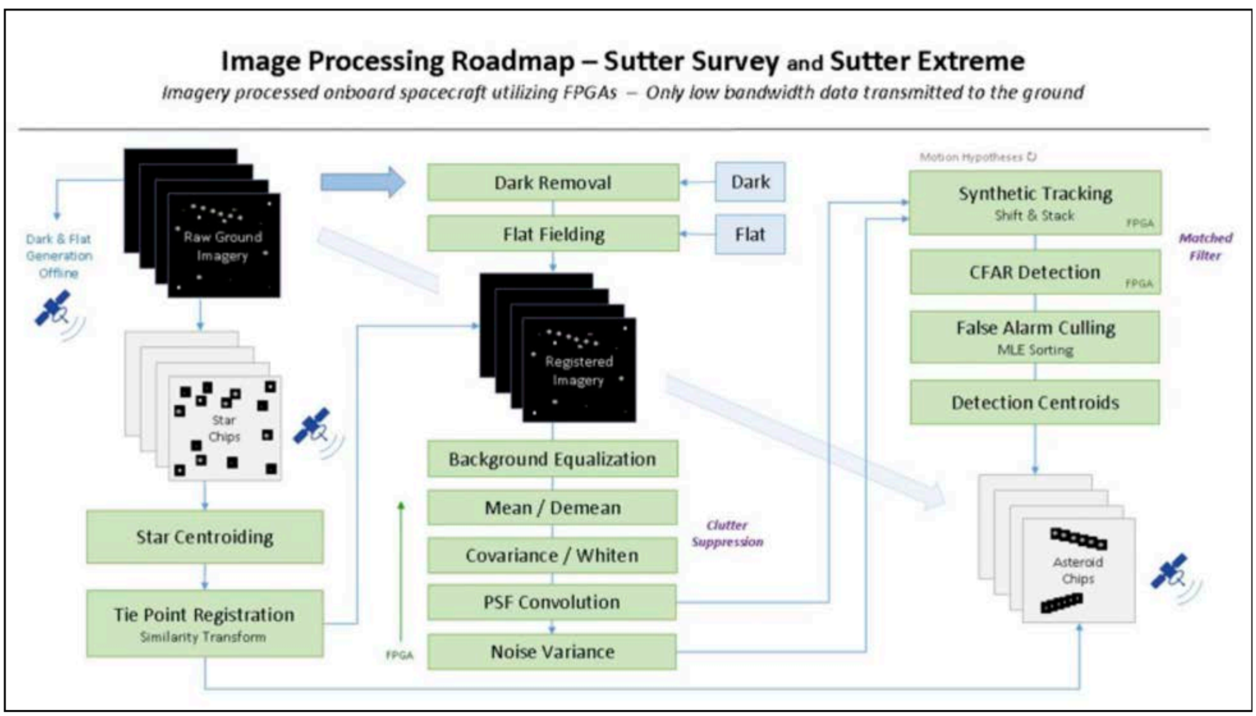


Figure 3-20 On-Board Image Processing for Sutter Survey and Sutter Extreme

Table 3-8— Survey Spacecraft MEL

| Item | CBE Mass per Unit (kg) | Qty | Current Best Estimate Total Mass (kg) | Component Contingency | Predicted Mass (kg) | Comments/Heritage/Method of Estimation |
|---|---|---|---|---|---|---|
| **Payload** | | | | | | |
| Telescope | 1.50 | 4 | 6.00 | 30% | 7.80 | Canon EF 400 mm, 14cm Optic, Light Weighted |
| Imager | 0.40 | 4 | 1.60 | 30% | 2.08 | Fairchild Imaging CIS4000, Electronics & Enclosure |
| Payload Processor | 0.40 | 4 | 1.60 | 10% | 1.76 | VIRTEX-7 FPGA, Boards, and Enclosure |
| **Structures** | | | | | | |
| Structural Panels | 15.00 | 1 | 15.00 | 20% | 18.00 | 1/2" Al Honeycomb with Al Face Sheets, Brackets, Beams, Misc. Hardware |
| Separation System | 0.50 | 1 | 0.50 | 5% | 0.53 | Mark II 11" MLB from Planetary System Corporation |
| Sun Shade | 0.50 | 1 | 0.50 | 20% | 0.60 | 1/4" Al Honeycomb Panel |
| **Thermal** | | | | | | |
| Heaters | 0.05 | 10 | 0.50 | 20% | 0.60 | 5 Watt Heaters |
| Thermisters | 0.01 | 10 | 0.10 | 20% | 0.12 | |
| **Power** | | | | | | |
| Solar Panels Fixed | 2.10 | 2 | 4.20 | 20% | 5.04 | 40 cm x 80cm Panel Substrates + 178 CICs |
| Solar Panels Deployed | 2.80 | 2 | 5.60 | 20% | 6.72 | 40 cm x 80cm Panel Substrates + 180 CICs |
| Battery Cells | 0.24 | 27 | 6.48 | 5% | 6.80 | 1300 Whr Capacity |
| Battery Enclosure | 0.20 | 2 | 0.40 | 20% | 0.48 | Al Enclosures |
| **Avionics and ACS** | | | | | | |
| Reaction Wheels | 0.23 | 6 | 1.36 | 0% | 1.36 | Sinclair Interplanetary 1 Nm Reaction Wheels (RW3-1.0) |
| Star Tracker | 0.19 | 2 | 0.37 | 0% | 0.37 | Sinclair Interplanetary (ST-16-R2) |
| Data Power Module | 1.50 | 1 | 1.50 | 5% | 1.58 | AD Space Extended DPM, Corvus-16 Based |
| **Communication** | | | | | | |
| Laser Comm Transceiver | 6.00 | 1 | 6.00 | 30% | 7.80 | Sinclair Interplanetary Deepspace Laser Comm |
| X-band Transponder | 1.20 | 1 | 1.20 | 5% | 1.26 | IRIS V2 CubeSat Deep Space Transponder |
| X-band Antenna | 0.10 | 1 | 0.10 | 30% | 0.13 | 4x4 X-band Patch Array |
| **Propulsion** | | | | | | |
| ACS Thrusters | 0.70 | 4 | 2.80 | 20% | 3.36 | DSI COMET-1000 Thruster |
| ACS Propellant | 0.75 | 4 | 3.00 | 0% | 3.00 | Water, Fixed Tank Volume Per Thruster |
| MET | 4.00 | 1 | 4.00 | 40% | 5.60 | Space Apprentices Microwave Electrothermal Thruster (MET) |
| Tank | 1.82 | 1 | 1.82 | 20% | 2.18 | Parametric Estimate of 5% of Propellant Mass |
| Propellant | 36.38 | 1 | 36.38 | 10% | 40.02 | 1520 m/s@400s = 31.1% Prop Mass Fraction + 10% DeltaV Contigency |
| **System Total - DRY** | | | **61.63** | **25.2%** | **77.16** | |
| **System Total - WET** | | | **101.01** | **16.0%** | **117.18** | |

well as functional redundancy and partial cross strapping will be implemented. The design strategy is to implement the best practices of commercial New Space in Deep Space.

The flight computer will be running an expanded version of Astro Digital's baseline Corvus Flight Software. Developed by Advanced Solutions Inc, the flight software package, called ODySSy/SOLIS, has previously been used by the military, JPL and other commercial companies in GEO and on interplanetary missions. The features and functions necessary to handle higher automation, latency tolerant communications with the ground, and interplanetary navigation are heritage, having been implemented on missions including the Mars Reconnaissance Orbiter, Juno, Orbcomm Gen 2, GOES-R and S Series, TacSat-2 and Iridium NEXT.

The Sutter Survey Electrical Power Subsystem consists of 5 solar panels, 3 battery packs, and a power distribution and control module. The power distribution and control module is contained on a set of cards within the spacecraft's DPM and is responsible for controlling battery charging, and power distribution and control to the DPM, ACS components, payload, X-band transceiver and laser communication terminal over a low voltage bus.

Sutter Survey implements 3 battery packs, one with eight 18650 lithium ion cells with a total capacity of 96 Whrs of energy storage for use by the flight computer, GPS, UHF TT&C and X-band Radios. Two larger battery packs, each with fifty-six 18650 lithium ion cells, act as the primary energy storage for the Microwave Electrothermal Thruster and Laser Comm Terminal. These large battery packs have a capacity of 1344 Whrs for a peak power draw of over a 1 kW by the MET for the 1 hr extended burns. These battery packs will be mounted thermally coupled to the spacecraft's radiators and propellant tank to ensure proper thermal dissipation during charging and use. The primary batteries are expected to undergo significant depth of discharge >90% during initial MET operations to achieve earth escape velocity, but the mission's total thruster burn time, 73 hours, means they will only undergo 73 total cycles at this depth, maintaining enough capacity through end of life (EOL) for all the spacecraft operations. See Table 3-9 for details on the spacecraft power budget.

All three battery packs are charged off a set of five solar panels. This set consists of two deployable single axis articulating panels, 2 body mounted panels, and a deployable fixed array that also acts as a payload lens cover. The system contains 403 cells total and is capable of a 185 watts of peak power generation when the deployable articulating arrays are sun pointing as planned for nominal surveying operations. The driving power modes in the system are the operation of the MET and the Laser Comm Terminal. The spacecraft will be cold biased so up to 50 watts of power has been allocated for heaters to maintain the spacecraft's subsystems within nominal operating temperatures outside of these two driving operational modes.

Sutter Survey implements a zero momentum biased attitude control system. The system includes a set of six 60 mNs reaction wheels in a fully redundant configuration providing up to 40 mNm of instantaneous torque in each axis. The required control authority is driven by the initial primary propulsion system operation at the perigee of GTO which requires an angular rotation of 2 deg/min to maintain the appropriate thrust vector. This is well below the achievable 23 deg/min maximum rate of the system given projected spacecraft mass properties. The reaction wheels are desaturated with a set of four COMET-500 water based attitude control thrusters from Deep Space Industries, mounted to the zenith deck. Each thruster consists of an integrated tank, nozzle, and control electronics for simplicity of integration and contains 300 g of water for propellant. A more detailed time evaluation of the planned surveying CONOP will help derive the total impulse necessary to desaturate the reaction wheels over the duration of the mission. Currently, the mission profile does not generate an excess of solar pressure and is well within the DSI thrusters propellant load. Solar pressure can likewise be minimized by feathering the deployable solar panels to minimize or generate torque when the power budget allows.

The GNC sensor suite consists of two ST-16RT2 star trackers, a COTS product by Sinclair Interplanetary, 6 Course Suns Sensors of Astro Digital design, and redundant MEMS based IMUs and magnetometers. During nominal operations, the ACS/GNC subsystem is able to provide <5 arcsec pointing knowledge with mission specific modifications to the star trackers, and <20 arcsec control.

Like Sutter Demo, Sutter Survey will implement a Fine Pointing Subsystem (FPS) for use during NEO prospecting operations. This system draws in data from the payload into a

Table 3-9 Sutter Survey Spacecraft Power Budget

| | | | | | Mode Power (W) | | | | | | | | | |
|---|---|---|---|---|---|---|---|---|---|---|---|---|---|---|
| Module | Component | Power (W) | Quantity | Total Power (W) | Detumble | Safe Mode | Nominal (Standby) | Thrusting | RXW Desaturation | Prospecting Primary | Heated Prospecting | UHF Downlink (GTO Only) | Laser Comm Downlink | DSN X-band Downlink |
| Panels | Sun Sensors | 0.02 | 5 | 0.10 | 0.10 | 0.10 | 0.10 | 0.10 | 0.10 | 0.10 | 0.10 | 0.10 | 0.10 | 0.10 |
| | Magnetorquers (detumble = 30% duty cycle) | | 6 | 10.00 | 3.00 | 0.00 | 0.50 | 0.00 | 0.00 | 0.00 | 0.00 | 0.50 | 0.00 | 0.00 |
| | Magnetometer | 0.00 | 7 | 0.02 | 0.02 | 0.02 | 0.02 | 0.02 | 0.02 | 0.02 | 0.02 | 0.02 | 0.02 | 0.02 |
| | Panel Processors | 0.02 | 5 | 0.11 | 0.11 | 0.11 | 0.11 | 0.11 | 0.11 | 0.11 | 0.11 | 0.11 | 0.11 | 0.11 |
| | I & V Monitors | 0.00 | 5 | 0.02 | 0.02 | 0.02 | 0.02 | 0.02 | 0.02 | 0.02 | 0.02 | 0.02 | 0.02 | 0.02 |
| | Panel Regulators | 0.00 | 6 | 0.01 | 0.01 | 0.01 | 0.01 | 0.01 | 0.01 | 0.01 | 0.01 | 0.01 | 0.01 | 0.01 |
| | Temperature Sensors | 0.00 | 9 | 0.04 | 0.04 | 0.04 | 0.04 | 0.04 | 0.04 | 0.04 | 0.04 | 0.04 | 0.04 | 0.04 |
| | H-Bridge | 0.00 | 5 | 0.01 | 0.01 | 0.01 | 0.01 | 0.01 | 0.01 | 0.01 | 0.01 | 0.01 | 0.01 | 0.01 |
| | Measured Inefficiencies | 0.37 | 1 | 0.37 | 0.37 | 0.37 | 0.37 | 0.37 | 0.37 | 0.37 | 0.37 | 0.37 | 0.37 | 0.37 |
| | Panels Total | | | | **3.66** | **0.66** | **1.16** | **0.66** | **0.66** | **0.66** | **0.66** | **1.16** | **0.66** | **0.66** |
| FCS | Avionics Board | 2.00 | 1 | 2.00 | 2.00 | 2.00 | 2.00 | 2.00 | 2.00 | 2.00 | 2.00 | 2.00 | 2.00 | 2.00 |
| | Reaction Wheels (60 mNms) | 0.50 | 6 | 3.00 | 3.00 | 0.00 | 3.00 | 9.00 | 9.00 | 0.45 | 0.45 | 3.00 | 0.45 | 0.45 |
| | GPS Receiver | 1.10 | 1 | 1.10 | 1.10 | 0.00 | 1.10 | 1.10 | 0.00 | 0.00 | 0.00 | 1.10 | 0.00 | 0.00 |
| | Star Tracker | 0.40 | 2 | 0.80 | 0.00 | 0.00 | 0.80 | 0.80 | 0.80 | 0.80 | 0.80 | 0.80 | 0.80 | 0.80 |
| | FCS Total | | | | **6.10** | **2.00** | **6.90** | **12.90** | **11.80** | **3.25** | **3.25** | **6.90** | **3.25** | **3.25** |
| Propulsion | RF Water Thruster | 1000.00 | 1 | 1000.00 | 0.00 | 0.00 | 0.00 | 1000.00 | 0.00 | 0.00 | 0.00 | 0.00 | 0.00 | 0.00 |
| | COMET-500 DSI Thrusters (2x at a time) | 25.00 | 2 | 25.00 | 0.00 | 0.00 | 0.00 | 0.00 | 25.00 | 0.00 | 0.00 | 0.00 | 0.00 | 0.00 |
| | *Propulsion Total* | | | | **0.00** | **0.00** | **0.00** | **1000.00** | **25.00** | **0.00** | **0.00** | **0.00** | **0.00** | **0.00** |
| Thermal | Heaters | 5.00 | 6 | 30.00 | 30.00 | 30.00 | 30.00 | 0.00 | 15.00 | 0.00 | 30.00 | 30.00 | 0.00 | 15.00 |
| | Thermal Total | | | | **30.00** | **30.00** | **30.00** | **0.00** | **15.00** | **0.00** | **30.00** | **30.00** | **0.00** | **15.00** |
| Imager | Imaging Sensor | 1.00 | 4 | 4.00 | 0.00 | 0.00 | 0.00 | 0.00 | 0.00 | 4.00 | 4.00 | 0.00 | 0.00 | 0.00 |
| | Analog to Digital Converter | 1.70 | 4 | 6.80 | 0.00 | 0.00 | 0.00 | 0.00 | 0.00 | 6.80 | 6.80 | 0.00 | 0.00 | 0.00 |
| | FPGA | 5.30 | 4 | 21.20 | 0.00 | 0.00 | 0.00 | 0.00 | 0.00 | 21.20 | 21.20 | 0.00 | 0.00 | 0.00 |
| | mSATA SSD | 1.50 | 2 | 3.00 | 0.00 | 0.00 | 0.00 | 0.00 | 0.00 | 3.00 | 3.00 | 0.00 | 3.00 | 0.00 |
| | Processor | 6.00 | 1 | 6.00 | 0.00 | 0.00 | 0.00 | 0.00 | 0.00 | 6.00 | 6.00 | 0.00 | 6.00 | 0.00 |
| | Payload Total | | | | **0.00** | **0.00** | **0.00** | **0.00** | **0.00** | **41.00** | **41.00** | **0.00** | **9.00** | **0.00** |
| Communication | Laser Comm Processor | 20.00 | 1 | 20.00 | 0.00 | 0.00 | 0.00 | 0.00 | 0.00 | 0.00 | 0.00 | 0.00 | 20.00 | 0.00 |
| | Laser | 100.00 | 1 | 100.00 | 0.00 | 0.00 | 0.00 | 0.00 | 0.00 | 0.00 | 0.00 | 0.00 | 100.00 | 0.00 |
| | IRIS Deepspace Cubesat Transceiver | 30.00 | 1 | 26.00 | 0.00 | 0.00 | 0.00 | 0.00 | 0.00 | 0.00 | 0.00 | 0.00 | 0.00 | 26.00 |
| | UHF Radio Tx (Beacon @ 10% Duty Cycle) | 1.00 | 1 | 1.00 | 1.00 | 1.00 | 1.00 | 0.00 | 0.00 | 0.00 | 0.00 | 10.00 | 0.00 | 0.00 |
| | UHF Radio Rx | 0.20 | 1 | 0.20 | 0.20 | 0.20 | 0.20 | 0.20 | 0.00 | 0.00 | 0.00 | 0.20 | 0.00 | 0.00 |
| | Laser Comm Total | | | | **1.20** | **1.20** | **1.20** | **0.20** | **0.00** | **0.00** | **0.00** | **10.20** | **120.00** | **26.00** |
| Total - before EPS efficiency | | | | | 40.96 | 33.86 | 39.26 | 1013.76 | 52.46 | 44.91 | 74.91 | 48.26 | 132.91 | 44.91 |
| EPS | Battery Charging Regulator Efficiency | | | | 91.00% | 91.00% | 91.00% | 91.00% | 91.00% | 91.00% | 91.00% | 91.00% | 91.00% | 91.00% |
| | Power Distribution Module Efficiency | | | | 90.00% | 90.00% | 90.00% | 90.00% | 90.00% | 90.00% | 90.00% | 90.00% | 90.00% | 90.00% |
| | EPS Total Power Dissipation | | | | **11.10** | **9.18** | **10.64** | **274.73** | **14.22** | **12.17** | **20.30** | **13.08** | **36.02** | **12.17** |
| Margin | 5% Uncertainty Margin | | | 0.0500 | 2.05 | 1.69 | 1.96 | 50.69 | 2.62 | 2.25 | 3.75 | 2.41 | 6.65 | 2.25 |
| **Total (W)** | | | | | **52.06** | **43.03** | **49.90** | **1288.49** | **66.68** | **57.08** | **95.21** | **61.34** | **168.93** | **57.08** |

Table 3-10: Sutter Survey Spacecraft Projected Pointing Performance

| Pointing Knowledge and Control Error (arcsec) | | |
|---|---|---|
| | Value (3σ) | Notes |
| Pointing Knowledge | | |
| Star Trackers | 15 | Solution frequency upgraded to 10Hz (from 2 Hz baseline in Corvus platform) to provide an estimated reduction from 40 to 15 arcseconds |
| Gyros | 0.5 | Baseline value for Corvus-XL STIM300 Gyro configuration. |
| Ephemeris | 28 | Assumes increased fidelity of orbital propogator over baseline Corvus-XL and periodic ground based ranging updates. |
| Knowledge Total (RSS) | **32** | 8 arcsec improvement over estimated Corvus-16 3-sigma knowledge driven primarily by higher frequency star field solutions. |
| Pointing Control | | |
| Jitter, Disturbance, Etc. | 70 | Estimated value driven by upgrade to Sensanor's STIM300 IMU. Baseline Corvus-16 value of 120 arcsecond with COTS mems gyro. Investigation into <50 arcsecond value with custom optical gyro. |
| Mechanical Alignment | 20 | Nominal value for commercial aerospace grade mechanical alignment followning an on orbit guide star calibration campaign. |
| Thermal Shift | 10 | May require periodic on-orbit calibration. |
| Control Total (RSS) | **80** | 20 arcsecond improvement over Corvus-16 anticipated pointing control of 100 arcseconds. |

Table 3-11 Sutter Survey Spacecraft Mission ΔV Budget

| DeltaV Requirement | Value | Unit | Notes |
|---|---|---|---|
| GTO to Earth Escape | 700 | m/s | GTO to Earth Escape |
| Apoapsis Raise to 1.575E+11 m | 439 | m/s | Apoapsis Raise (***e***= 0.024) |
| Periapsis Lower to 1.425E+11 m | 379 | m/s | Periapsis Lower (***e***= 0.05) |
| **Total** | **1518** | **m/s** | |
| | | | |
| **Propellant Load** | **Value** | **Unit** | **Notes** |
| MET ISP | 400 | seconds | Conservative Design Target |
| Vehical Dry Mass | 77.0 | kg | Margined Dry Mass |
| Propellant Mass (Unmargined) | 36.4 | kg | |
| Margin | 10% | kg | Gravity Loss on Initial Burns, Misc. |
| **Propellant Mass (Margined)** | **40.0** | **kg** | |

specific control loop designed to attain 1 arcsec pointing stability for 10 second exposures. This capability is achieved due to the primary payload's radial spatial resolution of 1 arcsec per pixel. The control loop will maintain a guide star on a single pixel for the duration of the exposure period (nominally 10 s). Isolation and fine balancing of the reaction wheels will be required to minimize high frequency dynamics. Table 3-10 provides the pointing performance of the system based on engineering analysis of the end to end system.

The main propulsion system is a plasma-based propulsion system that works with a wide variety of propellants to use thermal energy to generate thrust, much like resistojets. Its power source is a microwave generator, which converts microwave energy into thermal energy by Joule heating. This results in a compact thruster with little EMI, as well as an electrically neutral exhaust that does not require a hollow cathode neutralizer. The system also scales well to different power levels: 30 W, 350 W, 1-2 kW microwave power (not DC) have all been demonstrated as efficient systems. In general, better ISP can be expected than with a resistojet, with better thrust than other EP systems when at comparable power levels. Figure 3-21 provides a schematic view of the propulsion system. Table 3-11 provides the propellant budget for the mission, based on the ΔV required.

In most ways it resembles a cold gas thruster with an additional power supply. The system components at a high level would include a signal source, amplifier, thruster body, tank, and propellant feed system. The level of control over the impulse is going to be similar to a cold gas thruster - the actuation time of the valve will be the driving factor. Size and weight of the thruster body & amp are dictated by available DC power of the satellite. Exact thrust and ISP characteristics can be tuned within an efficient operating envelope to more precisely fit a mission's needs.

The primary payload data link for the Sutter Survey spacecraft will be a Ytterbium laser communication terminal to be developed jointly by TransAstra and Sinclair Interplanetary as part of their existing technology development roadmaps. The terminal utilizes a 14 cm F/5.4 COTS Canon optic coupled to a 20% efficient Ytterbium Doped Fiber Amplifier (YDFA) emitting 20 watts of power at 1064 nm. The optic is ruggedized in a similar fashion to the primary payload telescopes, contains no moving parts and no dichroics. The system draws 120 watts DC during operation, a majority of which is required by the 100 watt YDFA. Current analysis supports an estimated data rate of 5 Mbps at a range of 7.5 million km with appropriate link margin from earth to a 1 m ground station using High-order Pulse Position Modulation, specifically 256-PPM. An asymmetric uplink is also baselined as a component of the device to support TT&C and ranging operations. (See table 3-12_for details on the link analysis).

Current thermal analysis requires the spacecraft to be cold biased to ensure adequate thermal capacitance and radiative ability during long duration operation of both the MET and laser communication terminal. More specifically, the MET and laser communication terminal will be thermally grounded to the propellant tank, which itself will be thermally

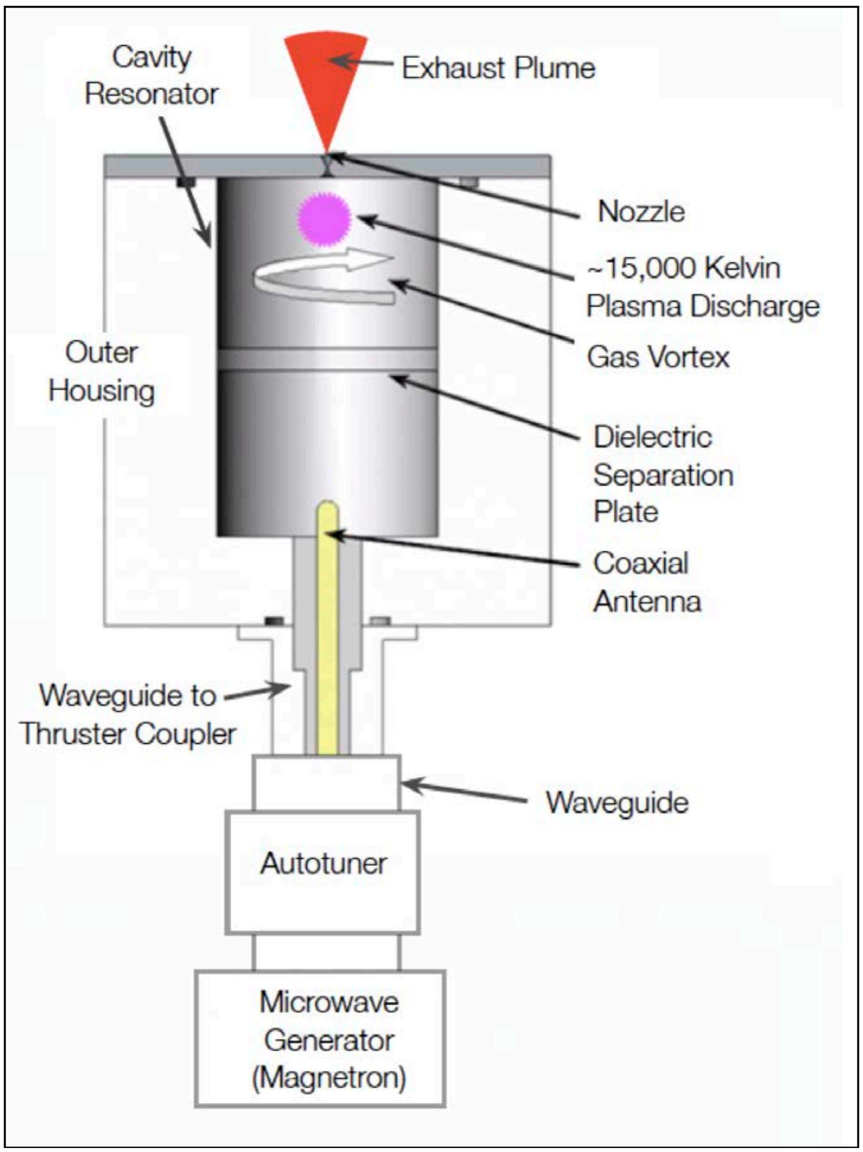


Figure 3-21 Simplified Block Diagram of Microwave Electrothermal Thruster (MET).

Table 3-12 Sutter Survey Laser Comm Link Budget

| Radiometry | | |
|---|---|---|
| Wavelength | 1.06E-06 | m |
| Plank Constant | 6.63E-34 | J-s |
| Speed of Light | 3.00E+08 | m/s |
| Photon Energy | 1.87E-19 | J |
| Photons per Joule | 5.35E+18 | Photons/J |
| | 187.29 | dB photons/J |
| DC Power | 100 | W |
| | 20.00 | dB W |
| Amplifier Efficiency | 20% | |
| | -6.99 | dB |
| Telescope Transmission | 90% | |
| | -0.46 | dB |
| **Output Power** | **199.84** | **dB photons/s** |
| | | |
| Transmit Aperture Diameter | 0.14 | m |
| Transmit Aperture Area | 0.0154 | m^2 |
| Link Range | 7.50E+09 | m |
| Transmit Fiber Mode Diameter | 6.00E-06 | m |
| Transmit Focal Length | 0.75 | m |
| First Minimum of Airy Disk | 9.27E-06 | rad |
| Image Spot Radius | 4.00E-06 | rad |
| Telescope is Diffraction Limited? | TRUE | |
| Telescope is Image Limited? | FALSE | |
| Gain Minus FSL On-Axis | 2.42E-10 | m^-2 |
| | -96.17 | dB m^-2 |
| Pointing Error | 1.00E+00 | arcsec |
| | 4.85E-06 | rad |
| ka*sin(theta) | 2.004 | |
| Pointing Loss | 0.331 | |
| | -4.80 | dB |
| Transmit Beam Quality Loss | -3.00 | dB |
| Atmospheric Loss | -2.00 | dB |
| **Receiver Power Density** | **93.87** | **dB photons/m^2/s** |

| Link Margin Calculation | | |
|---|---|---|
| Receiver Power Density | 93.87 | dB photons/m^2/s |
| Receiver Aperture | 1 | m dia |
| Receiver Primary Area | 0.785 | m^2 |
| Receiver Central Obstruction | 47% | |
| Central Obstruction Area | 0.173 | m^2 |
| Net Receiver Area | 0.612 | m^2 |
| | -2.13 | dB m^2 |
| Receiver Filter Transmission | 90% | |
| | -0.46 | dB |
| **Receiver Photon Flux** | **91.28** | **dB photons/s** |
| | | |
| Receiver Focal Length | 6.00 | |
| Fiber Mode Diameter | 6.00E-06 | |
| Fiber Projected Angle Radius | 5.00E-07 | rad |
| | 1.03E-01 | arcsec |
| Ground Station Seeing | 1.00 | arcsec |
| Fiber Couple Detector w/o Adaptive Optics? | FALSE | |
| APD Diameter | 5.00E-04 | m |
| APD Projected Angle Radius | 4.17E-05 | rad |
| | 8.59E+00 | arcsec |
| Couple APD w/o Adaptive Optics? | TRUE | |
| Bit Rate | 5.00E+06 | |
| | 66.99 | dB bits/sec |
| **Photons per Bit** | **24.29** | **dB photons/bit** |
| | | |
| Demonstrated OOK Sensitivity | 110 | photons/bit |
| | 20.41 | dB photons/bit |
| **Link Margin** | **3.88** | **dB** |

grounded to the two large body mounted radiators. Heat pipes will also be used to ensure the Fairchild focal plane arrays are kept near 0ºC to minimize dark noise and achieve the required signal to noise ratio. The positive margin in the power budget during the NEO prospecting mode will provide excess power, up to 50 watts, for heaters to ensure critical components are kept within operating temperatures. Detailed thermal analysis and design will be conducted during later phases of the Sutter Survey Design and Development program.

### 3.3.3. Ground System - Sutter Survey

#### 3.3.3.1 Sutter Survey Ground Station and Telemetry

The Sutter Survey mission is planning to use the same Astro Digital operations facility, UHF ground station, and operations software used for the Sutter Demonstration mission. These facilities will be paired with the Deep Space Network (DSN) and a set of purpose built Laser Communication ground stations at either SpaceWatch or the Iowa Robotic Observatory in Arizona for long range communication.

Primary TT&C communications will utilize the 34m High Efficiency (HEF) DSN systems coupled with the on-board IRIS CubeSat Deep Space Transponder. There are three 34 m

Table 3-13 X-band DSN Link Budget

| Downlink | | | Uplink | | |
|---|---|---|---|---|---|
| **Parameter** | **Value** | **Unit(s)** | **Parameter** | **Value** | **Unit(s)** |
| **Spacecraft:** | | | **Ground Station (GS)** | | |
| Transmitter RF Power Output | 5 | Watts | Transmitter RF Power Output | 7200 | Watts |
| Carrier Frequency | 8450 | MHz | Carrier Frequency | 7190 | MHz |
| Wavelength | 0.035 | m | Wavelength | 0.0417 | m |
| Antenna Diameter | 0.089 | m | Antenna Diameter | 34 | m |
| Antenna Aperture Efficiency | 65 | % | Antenna Aperture Efficiency | 96 | % |
| Antenna Gain | 16 | dBiC | Antenna Gain | 67.99 | dBiC |
| Antenna -3dB Beamwidth | 27.92 | deg. | Antenna -3dB Beamwidth | 0.09 | deg. |
| Line/Cable Losses | -1.00 | dB | Line/Cable Losses | -1.00 | dB |
| Switch Losses | -0.40 | dB | Switch Losses | 0.00 | dB |
| Misc. Tranmission Losses | 0.00 | dB | Misc. Tranmission Losses | 0.00 | dB |
| Spacecraft Pointing Error | 1.50 | deg. | GS Pointing Error | 0.03 | deg. |
| Spacecraft Pointing Losses | -2.00 | dB | GS Pointing Losses | -1.00 | dB |
| Spacecraft EIRP | 19.64 | dBW | GS EIRP | 104.56 | dBW |
| **Path** | | | **Path** | | |
| Polarization Loss | -0.50 | dB | Polarization Loss | -0.50 | dB |
| Range to Spacecraft (Astro. Units) | 0.050 | AU | Range to Spacecraft (Astro. Units) | 0.050 | AU |
| Range to Spacecraft (meters) | 7.50E+09 | m | Range to Spacecraft (meters) | 7.50E+09 | m |
| Path Loss | -248.50 | dB | Path Loss | -247.10 | dB |
| Atmospheric Loss | -0.10 | dB | Atmospheric Loss | -0.10 | dB |
| Ionospheric Loss | -0.10 | dB | Ionospheric Loss | -0.10 | dB |
| Rain/Water Vapor Attenuation | -1.00 | dB | Rain/Water Vapor Attenuation | -1.00 | dB |
| GS Pointing Loss | -0.10 | dB | S/C Pointing Loss | -1.00 | dB |
| Isotropic Signal Level at GS | -230.66 | dBW | Isotropic Signal Level at S/C | -145.24 | dBW |
| **Ground Station (GS)** | | | **Spacecraft (S/C)** | | |
| GS Antenna Diameter | 34.00 | m | S/C Antenna Diameter | 0.10 | m |
| GS Antenna Aperture Efficiency | 74.0 | % | S/C Antenna Aperture Efficiency | 65.0 | % |
| GS Antenna Gain | 68.26 | dBiC | S/C Antenna Gain | 16.00 | dBiC |
| GS Antenna -3dB Beamwidth | 0.07 | deg. | S/C Antenna -3dB Beamwidth | 30.74 | deg. |
| GS System Noise Temperature | 42.3 | K | S/C System Noise Temperature | 400 | K |
| GS System Figure of Merit (G/T) | 52.00 | dB/K | S/C System Figure of Merit (G/T) | -10.02 | dB/K |
| GS C/No | 49.94 | dBHz | S/C C/No | 73.34 | dBHz |
| Data Rate | 37,000 | bps | Data Rate | 850,000 | bps |
| Code Rate | 0.1667 | rate | | | |
| Symbol Rate | 221,956 | sps | | | |
| Matched Filter Eb/No | 4.26 | dB | Matched Filter Eb/No | 14.05 | dB |
| Demod. Implementation Loss | 0.45 | dB | Demod. Implementation Loss | 0.45 | dB |
| Required Eb/No | 0.80 | dB | Required Eb/No | 10.6 | dB |
| **Margin** | **3.01** | **dB** | **Margin** | **3.00** | **dB** |

X-band systems available one each at the DSN facilities in California, Australia and Spain as illustrated in Figures 3-22 and 3-23. Each transmits at 20 kW with over 68 dBI of gain depending on the configuration. As a backup, the Sutter Survey spacecraft will also carry the standard Astro Digital UHF TT&C radio implementing an omni-directional antenna. This UHF link will be utilized for backup TT&C communications as needed while the spacecraft is still in GTO at proximity to perigee. The planned Laser Communication link can also be used for TT&C as required.

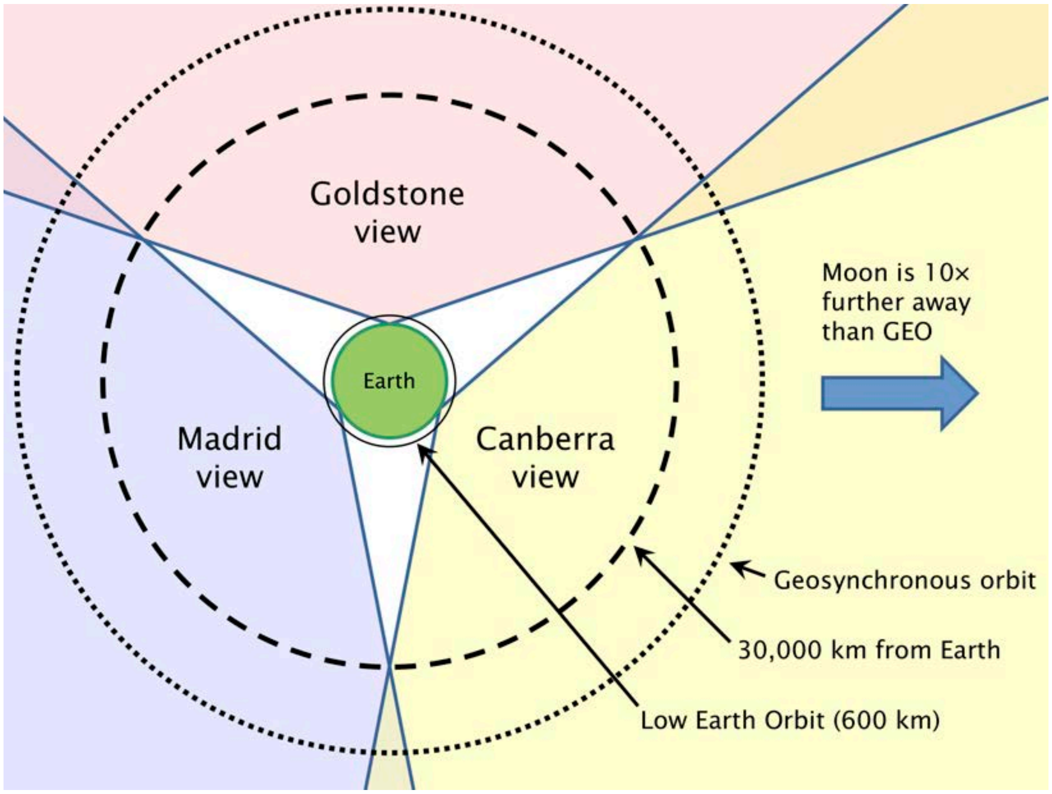


Figure 3-22 DSN Ground Station Field of View in Plane of the Ecliptic

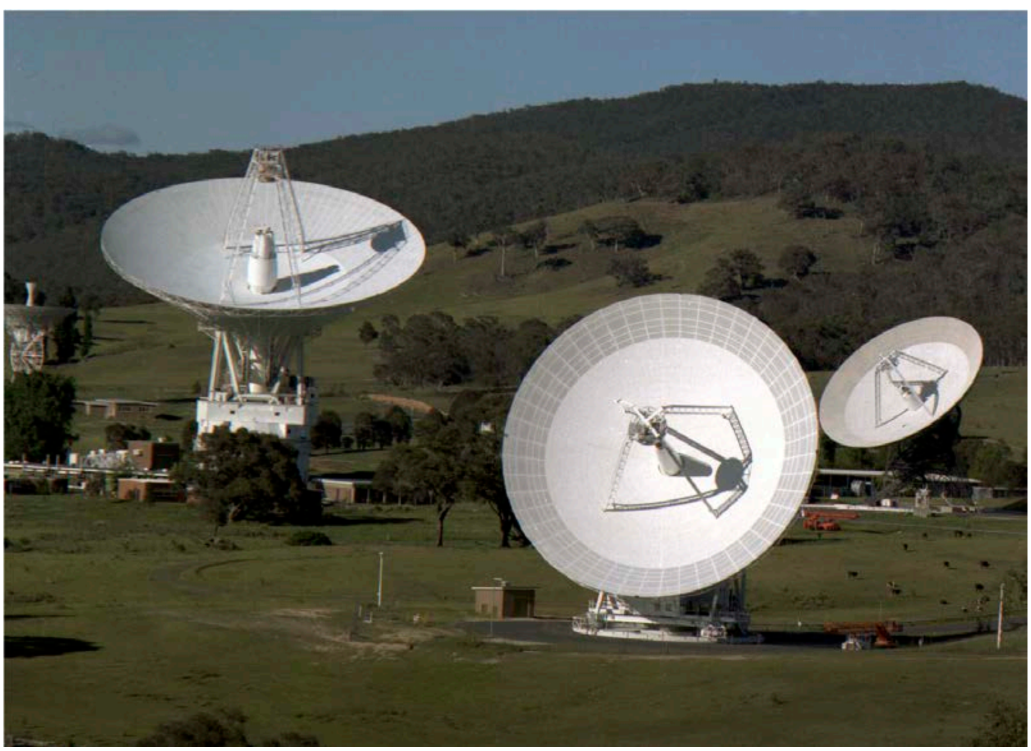

Figure 3-23 DSN Complex in Canberra, Australia

Payload data, to include TLEs and Imagery Stacks, are downlinked via a laser communication transceiver to one of two 1 m telescope ground stations located at either SpaceWatch or the Iowa Robotic Observatory Arizona. These stations, developed and operated by TransAstra will collect the payload data and push it to the cloud for easy access by the payload operations team. This ground station equipment will be developed


Figure 3-24 Our Analysis Shows that the Laser Communication Ground Station Can Be Built on Low Cost Commercial of the Shelf Telescopes Such as The PlaneWave Instruments 1 m System Shown Here

jointly with Sinclair Interplanetary and the University of Hawaii's astronomical teams. Additional duplicate stations may be erected elsewhere in the world as needed to support data budget requirements. Conceptual design of the laser communication ground system performed under this Phase 1 study shows that these stations can be based on low cost commercial telescopes such as the one depicted in Figure 2-24 which was used in our link budget analysis.

#### 3.3.3.2 Sutter Survey Science Data Processing and Distribution

The ground processing component for Sutter Survey expands upon the capabilities developed for Sutter Demo. Essentially the operations and processing pipeline have the same modules, but must handle a larger volume of imagery, since the satellite collection system has expanded from one to four optical sensing devices. The refinement of registration, astrometry resolution per sensor, matched filter tracking improvement, false alarm reduction, ISRU orbital parameter estimation, and photometric light curve estimation, all remain the same. The new wrinkle is the processing of imagery combined from the four telescopes in the overlapped viewing region. The following capabilities will be added to the ground processing pipeline:

- Expansion of processing throughput to handle four times the data volume at the ground station for one Survey satellite, and twelve times the data volume once three Survey satellites are on station,
- Improvements made to the ground processing system based on lessons learned from the Sutter Demo mission,
- Addition of new processing modules for co-registration and image analysis of the combined imagery stacks in the overlapped viewing regions of each collection,
- Integration of multiple tracklets from several Sutter Survey spacecraft with different viewing angles to refine targeted ISRU orbital parameters, and
- Optimize the processing pipeline to allow for short turn-around dynamic tasking to revisit and fine tune the characterization of any detected ISRU candidate.

The science data products will be asteroid identification and characterization in an asteroid database at TransAstra for potential commercial use, as well as provided in the appropriate data formats for eventual inclusion in the scientific databases. Objects of high importance such as PHOs that are detected will be promptly reported to the Planetary Defense Coordination Office.

## 3.4 Sutter Extreme

The Sutter Extreme Mission Flight System is based on making several upgrades to the Sutter Survey spacecraft design. It contains 6 Visible and 1 Near Infrared telescopes and upgraded imaging planes, each with a next generation GPU for running the tracking algorithm and characterization algorithms contained in a modest size (less than 2 m cube) spacecraft. It is envisioned to be compatible with a NASA New Frontiers mission in terms of cost and capability. The Sutter Extreme mission has not yet been designed to the same level of fidelity as the Sutter Survey mission and as such does not have the wealth of design detail. However the design effort to date has shown that this mission should be feasible within a cost of $500 to $600 million for all 3 spacecraft. Figure 3-25 is an artist's illustration of the Sutter Extreme spacecraft based on current CAD modeling.

### 3.4.1 Mission Design

The Sutter Extreme Mission uses the same nominal mission design as Sutter Survey.The one variation is that all three spacecraft could be launched together from one Falcon 9 to a small positive C3. At that point the spacecraft would be phased one at a time into their orbits over the next year. The prospecting strategy would be identical to the Sutter Survey Spacecraft.

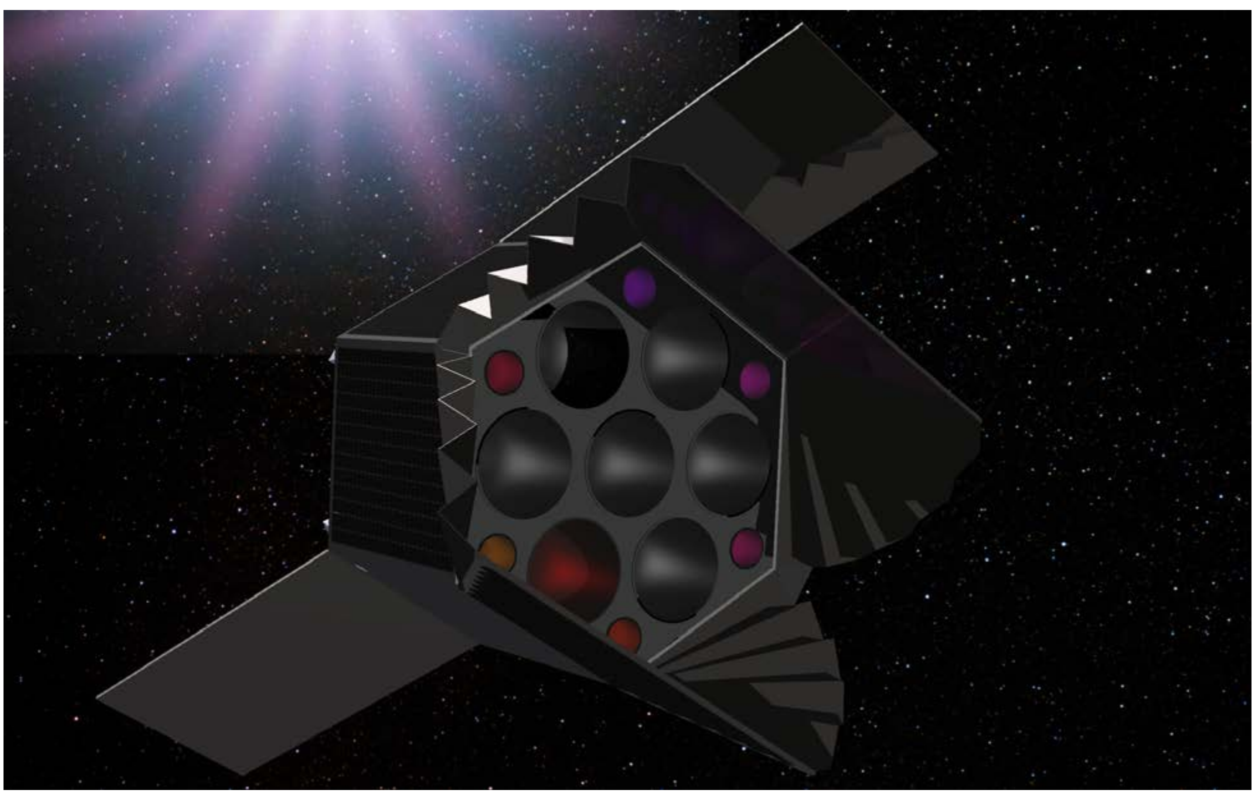

Figure 3-25 Sutter Extreme Spacecraft Design Concept

### 3.4.2.1 Payload Hardware

The major change to the Sutter Survey payload is the number, size, and type of telescopes. Sutter Extreme will have seven 50 cm aperture telescopes: 6 operating in the visible range and one in the near-infrared. This will not only provide the capability to detect an order of magnitude more objects than Sutter Survey but also increase the ability to remotely characterize, i.e., “prospect”, potential targets for ISRU. It is anticipated that improvements will likely have been made to both imaging sensors and FPGAs at this point and can be used to upgrade the payload image processing. Figure 3-26 shows a cutaway of the spacecraft showing the telescopes and other spacecraft subsystems.

### 3.4.2.2 Sutter Extreme Payload Software

The Sutter Extreme data processing functional flow is as depicted in Figure 3-20 under the Sutter Survey Ground Processing Software subsection 3.3.2.2. The main processing in Extreme is essentially identical to Sutter Survey processing. It merely involves more data

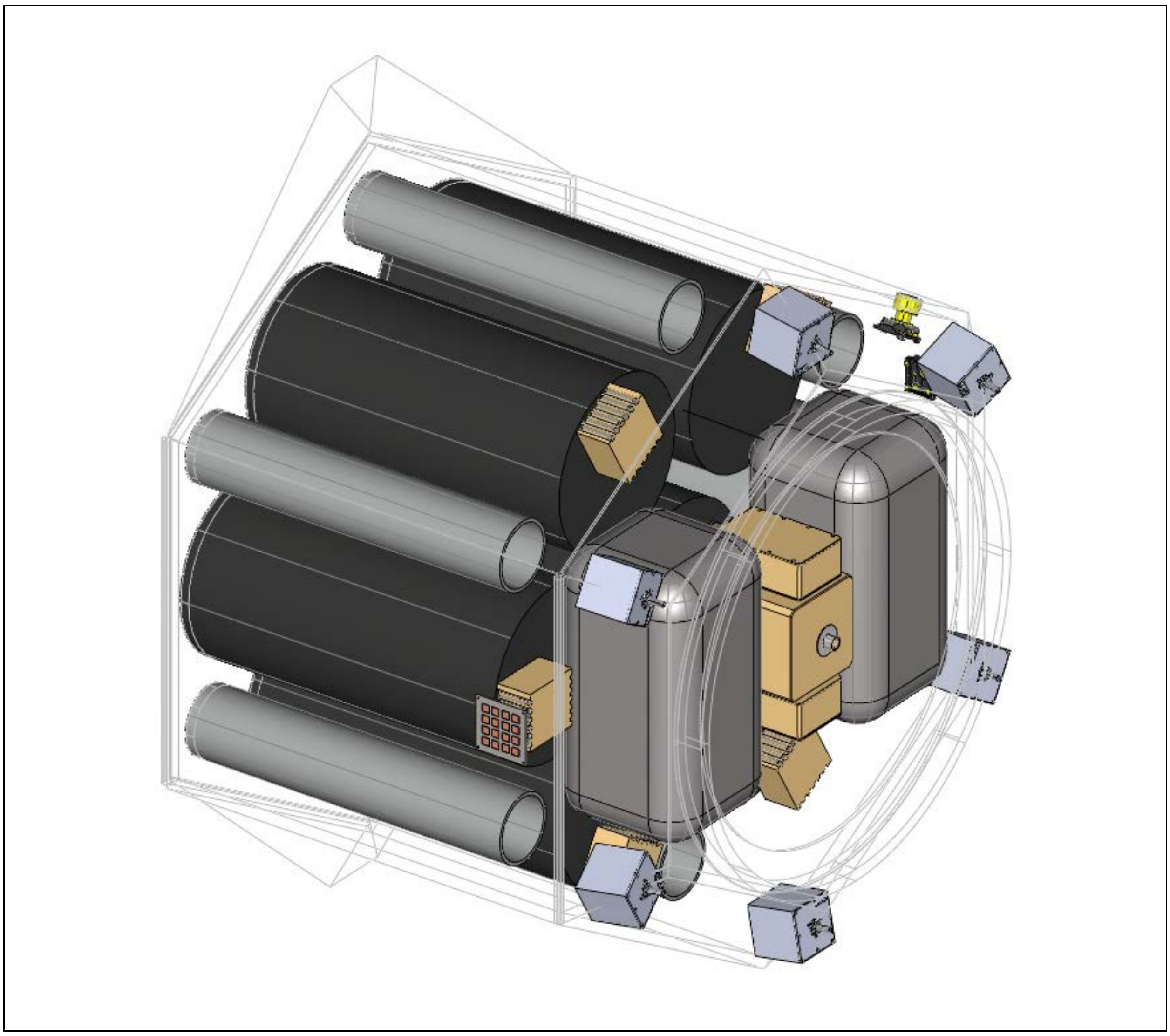

Figure 3-26 Spacecraft Cutaway with Payload

Table 3-14 Sutter Extreme MEL

| Rollup of detailed CBE | Initial Mass estimate (kg) | Average Component Contingency | CBE Mass (kg) | Comments |
|---|---|---|---|---|
| Launch Mass | | | 829.34 | Volume is ~ 2.74 m^3 so density is <1 |
| Wet Element | | | 100.00 | |
| Water | | | 100.00 | |
| Pressurant | | | 5.00 | |
| Dry Element | | | 729.34 | |
| Instruments | 339.40 | 50% | 509.10 | 6 Vis, 1 NIR telescopes + image processors |
| Power | 60.34 | 25% | 75.43 | Solar Array, Batteries, power management |
| Propulsion – RCS | 8.70 | 10% | 9.57 | 6 DSI Comet 1-750 At 1450 g each |
| Propulsion - MET | 13.00 | 30% | 16.90 | Upgraded 600 sec Isp MET Includes Tank @ 5% |
| ADACS | 23.42 | 6% | 24.83 | reaction wheels, star-trackers, sun sensors |
| C&DH | 7.87 | 13% | 8.90 | Redundant CPUs plus Comm memory |
| Comm | 27.26 | 10% | 29.99 | Upgraded Sinclair redundant laser comm + X-band |
| Thermal | 5.45 | 27% | 6.92 | radiator, heaters, temperature sensors and MLI |
| Structures and Mechanisms | | | 47.71 | @ 7% |

handling, processing distribution, and coordination across the seven collection cameras made with the various filters and pointing orientations. Additional upgrades to the processing pipeline will be made to handle the CMFA mode of operation combining multiple overlapped focal planes. Joint processing of several cameras can be combined to form initial taxonomy estimates from the multi-band photometric measurements.

### 3.4.2.3 Spacecraft Design

The spacecraft is designed as a hexagonal box to accommodate the seven telescopes in the minimum volume. The bulk of the spacecraft subsystems are located behind the telescope payload as shown in more detail in Figure 3-27. The one exception is that the laser communications telescope/terminals are placed around the corners of the hexagon. There is room for up to six laser communications devices. This can allow not only for redundancy but could also support multiple simultaneous downlinks at slightly different frequencies for improved data throughput. 1000 W of power are included in the power budget for laser communication to support such an advanced system.The laser communication ground terminals would require upgrading to take advantage of such an approach. It is assumed the propulsion subsystem has been upgraded to double the thrust available (at the cost of doubling the input power). As these spacecraft will never be in close Earth orbit, the UHF communications system has been eliminated. The spacecraft mass equipment list is shown in Table 3-14. A preliminary power analysis is given in Table 3-15. The worst case of thrusting with main propulsion under minimal sun illumination of solar arrays still allows for one hour of continuous thrust with only 90% depth of discharge on the batteries.

### 3.4.3.1 Sutter Extreme Ground Station and S/C Telemetry

The Sutter Extreme spacecraft will be designed to take advantage of improved ground stations should such facilities become available. Improvements could include larger aperture optical communication receivers or multi-frequency receivers that can handle more than one data stream at a time. This will potentially reduce the number of ground passes required to download all science data and spacecraft telemetry. The total science data volume estimated for a single spacecraft is 31 Gigabytes/day. If 8 Mbits/sec transmission is achieved, less than 45 minutes will be required for each daily ground pass.

#### 3.4.3.2 Sutter Extreme Science Data Processing (including SW) and Products

The ground processing component for Sutter Extreme expands upon the capabilities developed for Sutter Survey. Once again, most of the operations and processing pipeline modules are the same, but must handle an even larger volume of imagery, since the satellite collection system has expanded from four to seven optical sensing devices. The system includes color filters on some sensors for taxonomy estimation. The refinement of registration, astrometry solution per sensor, matched filter tracking improvement, false alarm reduction, ISRU orbital parameter estimation, and photometric light curve estimation,

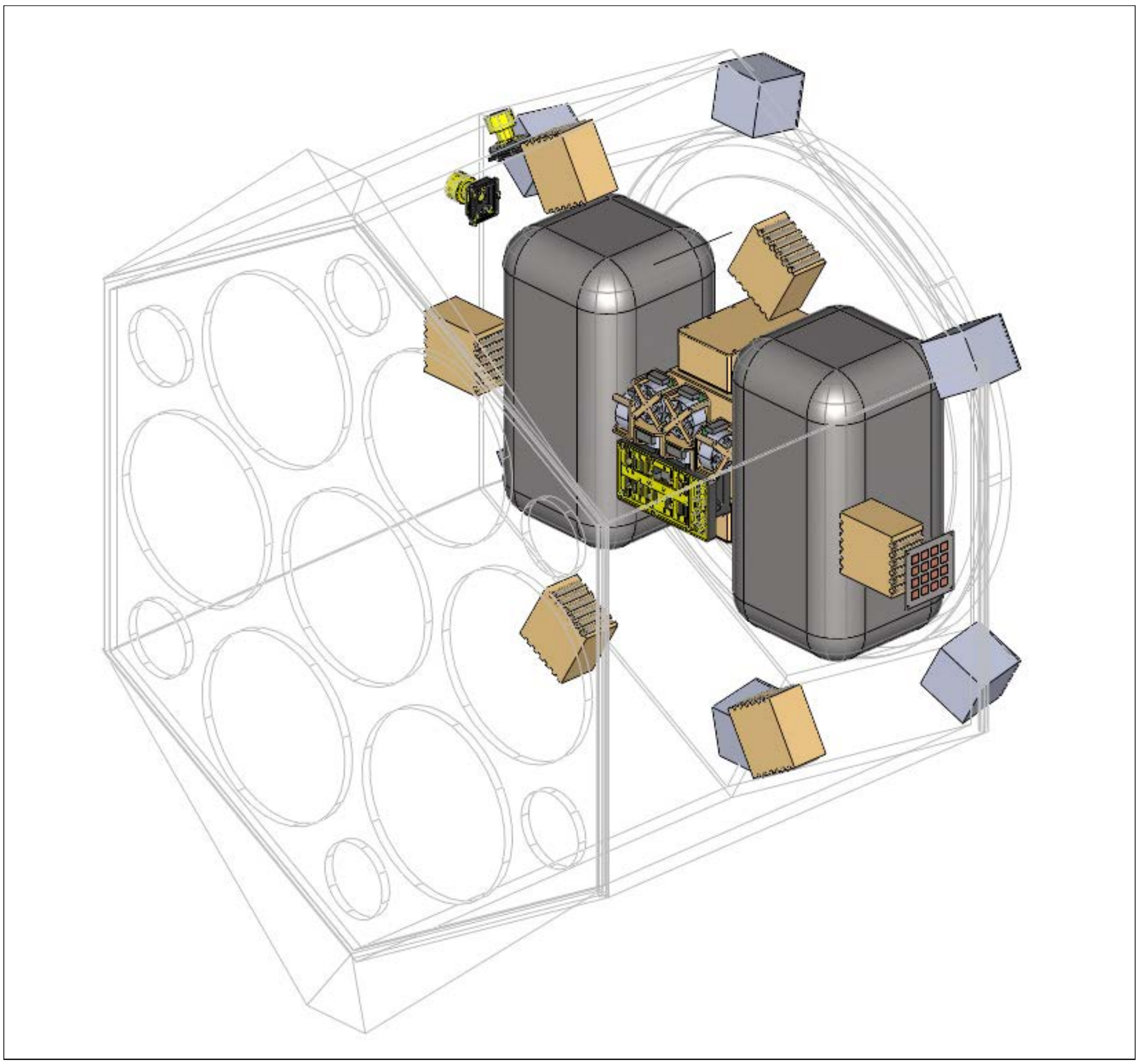

Figure 3-27 Sutter Extreme Cutaway Showing Spacecraft Subsystems

Table 3-15 Sutter Extreme Power Analysis

| | | | | | Mode Power (W) | | | | | | | | |
|---|---|---|---|---|---|---|---|---|---|---|---|---|---|
| Module | Component | Power (W) | Quantity | Total Power (W) | Detumble | Safe Mode | Nominal (Standby) | Thrusting | RXW Desaturation | Prospecting Primary | Heated Prospecting | Laser Comm Downlink | DSN X-band Downlink |
| Panels | Sun Sensors | 0.02 | 5 | 0.10 | 0.10 | 0.10 | 0.10 | 0.10 | 0.10 | 0.10 | 0.10 | 0.10 | 0.10 |
| | Magnetorquers (detumble = 30% duty cycle) | | 6 | 10.00 | 3.00 | 0.00 | 0.50 | 0.00 | 0.00 | 0.00 | 0.00 | 0.00 | 0.00 |
| | Magnetometer | 0.00 | 7 | 0.02 | 0.02 | 0.02 | 0.02 | 0.02 | 0.02 | 0.02 | 0.02 | 0.02 | 0.02 |
| | Panel Processors | 0.02 | 5 | 0.11 | 0.11 | 0.11 | 0.11 | 0.11 | 0.11 | 0.11 | 0.11 | 0.11 | 0.11 |
| | I & V Monitors | 0.00 | 5 | 0.02 | 0.02 | 0.02 | 0.02 | 0.02 | 0.02 | 0.02 | 0.02 | 0.02 | 0.02 |
| | Panel Regulators | 0.00 | 6 | 0.01 | 0.01 | 0.01 | 0.01 | 0.01 | 0.01 | 0.01 | 0.01 | 0.01 | 0.01 |
| | Temperature Sensors | 0.00 | 9 | 0.04 | 0.04 | 0.04 | 0.04 | 0.04 | 0.04 | 0.04 | 0.04 | 0.04 | 0.04 |
| | H-Bridge | 0.00 | 5 | 0.01 | 0.01 | 0.01 | 0.01 | 0.01 | 0.01 | 0.01 | 0.01 | 0.01 | 0.01 |
| | Measured Inefficiencies | 0.37 | 1 | 0.37 | 0.37 | 0.37 | 0.37 | 0.37 | 0.37 | 0.37 | 0.37 | 0.37 | 0.37 |
| | Panels Total | | | | **3.66** | **0.66** | **1.16** | **0.66** | **0.66** | **0.66** | **0.66** | **0.66** | **0.66** |
| FCS | Avionics Board | 2.00 | 1 | 2.00 | 2.00 | 2.00 | 2.00 | 2.00 | 2.00 | 2.00 | 2.00 | 2.00 | 2.00 |
| | Reaction Wheels (60 mNms) | 0.50 | 6 | 3.00 | 3.00 | 0.00 | 3.00 | 9.00 | 9.00 | 0.45 | 0.45 | 0.45 | 0.45 |
| | GPS Receiver | 1.10 | 1 | 1.10 | 1.10 | 0.00 | 1.10 | 1.10 | 0.00 | 0.00 | 0.00 | 0.00 | 0.00 |
| | Star Tracker | 0.40 | 2 | 0.80 | 0.00 | 0.00 | 0.80 | 0.80 | 0.80 | 0.80 | 0.80 | 0.80 | 0.80 |
| | FCS Total | | | | **6.10** | **2.00** | **6.90** | **12.90** | **11.80** | **3.25** | **3.25** | **3.25** | **3.25** |
| Propulsion | RF Water Thruster | 2000.00 | 1 | 2000.00 | 0.00 | 0.00 | 0.00 | 2000.00 | 0.00 | 0.00 | 0.00 | 0.00 | 0.00 |
| | COMET-500 DSI Thrusters (2x at a time) | 25.00 | 2 | 25.00 | 0.00 | 0.00 | 0.00 | 0.00 | 25.00 | 0.00 | 0.00 | 0.00 | 0.00 |
| | Propulsion Total | | | | **0.00** | **0.00** | **0.00** | **2000.00** | **25.00** | **0.00** | **0.00** | **0.00** | **0.00** |
| Thermal | Heaters | 5.00 | 6 | 30.00 | 0.00 | 30.00 | 30.00 | 0.00 | 15.00 | 0.00 | 30.00 | 0.00 | 15.00 |
| | Thermal Total | | | | **0.00** | **30.00** | **30.00** | **0.00** | **15.00** | **0.00** | **30.00** | **0.00** | **15.00** |
| Imager | Imaging Sensor | 1.00 | 7 | 7.00 | 0.00 | 0.00 | 0.00 | 0.00 | 0.00 | 7.00 | 7.00 | 0.00 | 0.00 |
| | Analog to Digital Converter | 1.70 | 7 | 11.90 | 0.00 | 0.00 | 0.00 | 0.00 | 0.00 | 11.90 | 11.90 | 0.00 | 0.00 |
| | FPGA | 5.30 | 7 | 37.10 | 0.00 | 0.00 | 0.00 | 0.00 | 0.00 | 37.10 | 37.10 | 0.00 | 0.00 |
| | mSATA SSD | 1.50 | 2 | 3.00 | 0.00 | 0.00 | 0.00 | 0.00 | 0.00 | 3.00 | 3.00 | 3.00 | 0.00 |
| | Processor | 6.00 | 1 | 6.00 | 0.00 | 0.00 | 0.00 | 0.00 | 0.00 | 6.00 | 6.00 | 6.00 | 0.00 |
| | Payload Total | | | | **0.00** | **0.00** | **0.00** | **0.00** | **0.00** | **65.00** | **65.00** | **9.00** | **0.00** |
| Communication | Laser Comm Processor | 20.00 | 1 | 20.00 | 0.00 | 0.00 | 0.00 | 0.00 | 0.00 | 0.00 | 0.00 | 20.00 | 0.00 |
| | Laser | 1000.00 | 1 | 1000.00 | 0.00 | 0.00 | 0.00 | 0.00 | 0.00 | 0.00 | 0.00 | 1000.00 | 0.00 |
| | IRIS Deepspace Cubesat Transceiver | 30.00 | 1 | 26.00 | 0.00 | 0.00 | 0.00 | 0.00 | 0.00 | 0.00 | 0.00 | 0.00 | 26.00 |
| | UHF Radio Tx (beacon = 10% duty cycle, TT&C Pass = 100% duty cycle) | 1.00 | 1 | 1.00 | 1.00 | 1.00 | 1.00 | 0.00 | 0.00 | 0.00 | 0.00 | 0.00 | 0.00 |
| | UHF Radio Rx | 0.20 | 1 | 0.20 | 0.20 | 0.20 | 0.20 | 0.20 | 0.00 | 0.00 | 0.00 | 0.00 | 0.00 |
| | Laser Comm Total | | | | **1.20** | **1.20** | **1.20** | **0.20** | **0.00** | **0.00** | **0.00** | **1020.00** | **26.00** |
| Total - before EPS efficiency | | | | | 10.96 | 33.86 | 39.26 | 2013.76 | 52.46 | 68.91 | 98.91 | 1032.91 | 44.91 |
| EPS | Battery Charging Regulator Efficiency | | | | 91.00% | 91.00% | 91.00% | 91.00% | 91.00% | 91.00% | 91.00% | 91.00% | 91.00% |
| | Power Distribution Module Efficiency | | | | 90.00% | 90.00% | 90.00% | 90.00% | 90.00% | 90.00% | 90.00% | 90.00% | 90.00% |
| | EPS Total Power Dissipation | | | | **2.97** | **9.18** | **10.64** | **545.73** | **14.22** | **18.67** | **26.80** | **279.92** | **12.17** |
| Margin | 5% Uncertainty Margin | | | 0.0500 | 0.55 | 1.69 | 1.96 | 100.69 | 2.62 | 3.45 | 4.95 | 51.65 | 2.25 |
| **Total (W)** | | | | | **13.93** | **43.03** | **49.90** | **2559.49** | **66.68** | **87.58** | **125.71** | **1312.83** | **57.08** |

all remain the same. The major change is the processing of imagery combined from the seven telescopes in the overlapped viewing region plus the color filter measurements. The following capabilities will be added to the ground processing pipeline:

- Expansion of processing throughput to handle the two times greater data volume at the ground station relative to Sutter Survey,
- Improvements made to the ground processing system based on lessons learned from the Sutter Survey mission,
- Addition of new processing modules to estimate ISRU taxonomy from the color filter measurements, and
- Combining light curves in the various color bands to reveal ISRU spin rate refinements, tumbling characterization, surface irregularities, and more completely characterize the water volume content from the all aspect viewing collections.

As with Sutter Survey, the science data products will be asteroid identification and characterization for inclusion in an asteroid database at TransAstra for potential commercial use, as well as provided in the appropriate data formats for eventual inclusion in the scientific databases. Objects of high importance such as PHOs that are detected will be promptly reported to the Planetary Defense Coordination Office.

### 3.5 Summary of Phase 1 Work: Sutter Architecture Plus Research and Development

During the Phase 1 study, several elements of the Sutter architecture have been subject to research and revision. Some elements of the architecture have been modified accordingly. There are 4 areas in particular that have been included in the architecture presented above. These are:

- Development of a new orbit design for the Survey and Extreme missions,
- Adoption of the matched filter algorithm for detection and tracking,
- Application of a Microwave Electronic Thruster (MET) as main propulsions on the Survey and Extreme missions, and
- Baselining of optical communication for science data downlink, also for the Survey and Extreme missions.

The new Pseudo Geocentric Distant Retrograde (PGDR) orbit design described in section 2.2 keeps the spacecraft in relatively close proximity to the Earth, making communications much easier and eliminating any outages due to spacecraft positions with respect to the Earth, yet still allows for surveying of the key regions for ISRU targets.

The matched filter algorithm (MFA) described in section 2.1 represents a substantial improvement over previous synthetic tracking approaches and also has an existing software baseline that has previously been used for a similar application.

The Microwave Electronic Thruster (MET) described in section 3.3.2.3 is the subject of an ongoing development effort that is separately funded, but provides several advantages over a more conventional propulsion system in that no hazardous propellants are needed, greatly simplifying spacecraft handling during ATLO.

Use of Optical Communications as described in section 3.3.2.3 is a logical emerging technology to apply for increased data communications over the distances involved for the Sutter Survey and Sutter Extreme missions. Commercial Off The Shelf (COTS) systems are currently available and it is anticipated that their capabilities will continue to increase over time as their use becomes more widespread and more ground stations become available. Sutter mission planning includes development of dedicated ground stations, if necessary, and are estimated to have modest costs, given the availability of 1 meter class telescope systems that would form the basis of such a ground station.

# 4.0 Path Forward

## 4.1 Supporting research: ISRU NEO Δ-V studies

We have begun to develop techniques for calculating ΔV for optimized round-trip trajectories with Thomas Haberkorn (U. Orleans, France) and Monique Chyba (U. Hawaii). They are mathematical experts in minimization techniques and have developed optimized missions to Earth's mini-moons (e.g., Chyba et al., 2016). Their preliminary results on optimizing the return trip ΔV from ISRU candidates confirms and improves upon the work of Jedicke et al. (2018) described above. Jedicke et al. (2018) set an upper limit on the return trip ΔV but imposed no requirements on the trip start date or duration. The new work suggests that the Jedicke et al. (2018) work overestimated the required ΔV by about 50% and hints that further reductions are possible by allowing more ΔV maneuvers and with a more sophisticated treatment of the trajectory in cis-lunar space.

## 4.2 Technology Readiness and Risk Assessment

There are some technology developments and associated risks that must be addressed as part of the path forward in achieving the goals of the Sutter Survey. Given the high maturity of the satellite platforms proposed, the preponderance of effort is on risk-reduction in payload algorithm development, payload-to-platform interface requirements definition and Interface Control Documentation (ICD), as well as updating all key system level budgets and analyses (data generation, storage and throughput, link budgets, power budget, pointing budget, mass budget, and propellant budget). These developments, risks, and mitigations are described below and summarized in Table 4-1, along with the mitigation approach. This list serves as the basis for developing a risk retirement strategy as part of the overall roadmap effort. The risks are also categorized in terms of their magnitude if not successfully overcome and the likelihood of their occurrence.

## 4.3 Technology and Mission Development Roadmap

The primary technical risks are related to the instrument and related data processing software development. Addition of a ground test development effort is a logical approach to addressing these risks early on and insuring the adequacy of the Sutter approach. This is further built upon by doing a simple, inexpensive cubesat mission in Earth orbit, so as to validate the technology.

## 4.4 Sutter Ground Test Development Plan

Based on the work performed in this Phase 1 study, therefore, the next logical step is to create a ground demonstration unit that will use almost identical hardware and software as the flight demonstration spacecraft and verify that known targets can be detected as predicted. This provides the confidence that a flight demonstration is not only practical but will actually be capable of achieving real scientific results, in addition to verifying the basic functionality of such a flight system.

Table 4-1 Technology Development Risk and Mitigation List

| Risk or Opportunity Summary | Magnitude | Likelihood | Mitigation or Capitalization |
|---|---|---|---|
| Technical | | | |
| Changes to payload(s) affect sizing of platform | Medium | Low | Freeze payload requirements and interface control documents early; adopt "one team" approach to ensure tight coordination between payload, and platform developers. |
| Final system exceeds allocated budgets (mass, volume, power) | High | Low | AD approach is to maintain robust design and performance margins throughout entire design and testing phase in all areas (mass, volume, power, link margins, propellant) in order to absorb uncertainty. As mentioned earlier, early definition of budgets and interface requirements, combined with "one team" approach ensures tight coordination and management of system configuration. |
| Instrument software development behind schedule | High | Medium | Instrument computer firmware and software are in-flight reprogrammable. Maximize flexibility post-launch in event of software delay, and embrace—rather than avoid—iterative approach to improvement in flight. Emphasis therefore shifts to functional, rather than "perfect", software pre-flight. |
| Difficulty procuring long-lead items | Medium | Low | All long-lead platform items have been identified, and lead times are known. |
| Unanticipated assembly, integration and/or test challenges | Medium | Low | Known platform and known assembly times. Principle uncertainty in instrument. Instrument constituents already chosen based on interface and electromagnetic self-compatibility considerations, and known and close relationships with vendors. |
| Platform does not meet lifetime requirements | Low | Low | Minimal lifetime requirements. Flight-proven piece parts, robust (large) system margins on power and propulsion, and functional redundancy incorporated into spacecraft to ensure mission life. |
| Fine Pointing Subsystem (FPSS) does not meet pointing stability requirement | Medium | Medium | New implementation of proven architecture from past astronomical space telescopes. Immediate engagement with best-in-class subject matter experts on pointing, spacecraft stability, telescope in the loop control, reaction wheel balancing and star tracker design. |
| EMC Issues | Medium | Medium | Proven self-compatible platform design. Otherwise mitigate preventatively. Use EMC-self-compatible subsystems, and MIL-STD-461 as guidelines for new hardware, general best practices against conducted and radiated emissions. Perform anechoic chamber testing early (dirtySat stage) at component level to evaluate emissions, receiver sensitivity, and self-compatibility. |

Table 4-1 Technology Development Risk and Mitigation List (cont'd.)

| Risk or Opportunity Summary | Magnitude | Likelihood | Mitigation or Capitalization |
|---|---|---|---|
| Programmatic | | | |
| Additional funding becomes available through Tipping Points or other investor | High | High | This will provide fundamental benefits to the mission including moving to a 16U platform with a 15 cm Aperture telescope for Sutter Demo, redundant GPUs and/or FPGA payload processors, a larger primary optic, and increase in mission capability from discovering ≈10 NEOs to ≈100 NEOs |
| NASA allows the use of a Russian launch vehicle | Medium | High | We have an offer for a free launch on a Russian launch vehicle in exchange for providing scientific data about discovered asteroids to a Russian university. If this option becomes available, it will save $500K allowing us to provide additional redundancy in electronics or substitute an FPGA for the currently baselined GPU. |
| Supplier delays in delivering key spacecraft components | Medium | Low | Multiple prospective vendors for all COTS parts identified; inclusion of penalty clauses for late delivery; procure early hardware in Phase C for risk-reduction testing. |
| Payload not delivered on time | High | Low | Strong emphasis on flight-proven COTS solution for payload hardware. Flexibility on firmware/software by virtue of in-flight reprogrammability. All constituent components have known lead-time. |
| Unavailability of key personnel on project | Medium | Low | AD has depth in all technical and managerial areas, with multiple cross-trained staff who can be substituted as needed. Backup personnel for all major areas of work already identified. AD small team approach well suited to Prospector-X development obviating the need for an excessively large team. |
| Inability to secure launch arrangements or frequencies for mission | High | Medium | AD personnel bring extensive experience working with multiple launch providers and undertaking frequency coordination on behalf of itself and others. Apply for licenses and fix launch vehicle selection as soon as possible in program. Multiple options available via third-parties. |
| Facilities unavailable when needed | Medium | Low | Multiple test facilities readily available both in house and out of house. AD has exclusive access to underutilized testing facilities at Space Systems Loral if needed. |
| Work scope becomes higher than expected, unable to meet schedule and/or cost targets | High | Low | All candidate technologies aside from payload are build-to-print of previous heritage units. Overall plan is to develop platform with "as little new as possible", such that bulk of risk is in payload. In addition, track project performance (CPI and SPI) and report bi-weekly, using earned value metrics to anticipate issues. Identify multiple different, acceptable outcomes and descoping plan at program initiation, and understand which requirements can be traded on if need be. |

### 4.4.1 Ground Demonstration

The Phase II ground demonstration has several goals:

- Actual sensor configuration characterization,
- Collection against known asteroids with Sutter Survey equivalent angular rates of motion,
- Demonstration of matched filter shift and stack operation in real-time on targeted spacecraft breadboard GPU, and
- Demonstration of software pipeline modules from raw imagery to detection products in non-real-time.

Additional tasks addressed in the development plan in Phase II are:

- Hardware specification - sensor and image dump/storage, sensor mounting, breadboard processor/GPU, offline analysis workstation,
- SpaceWatch facility - pointing slaved to asteroid recovery operations in effect at SW,
- Collection plan per pointing, typical 300 seconds of 30x10 seconds, and
- Analysis plan and products generated.

### 4.4.2 Sutter Ground Test Software

The Sutter ground test software will involve an integration of various existing or easily built components already available in the public domain. The core processing of clutter suppression and matched filtering are embedded in the baseline software suite SALTAD version 1.54. In Figure 4-1 this processing is depicted as the green colored blocks which already include interface to an NVIDIA class GPU for handling large numbers of motion hypotheses. Only minor upgrades are expected to be made to the SALTAD package for the ground test Phase II effort. Other components needed are depicted in the orange colored blocks which also exist as currently operational functional modules and/or test routines, and simply require interfacing and integrating into a processing pipeline.

Software packages and algorithm upgrades required:

- SALTAD version 1.54 with GPU interface with upgrades for:
  - Mean and covariance estimation modification to handle slow movers within a single image stack. Need to avoid mean and variance contamination (signal loss and suppression) from near stationary asteroids,
  - Add a hexagonal search grid in place of rectilinear search for motion hypothesis generation to obtain a 20% reduction in matched filter hypothesis count,
  - Alternative cosmic ray removal function,
  - Parallax template generator modifications that may arise from the curvature study.
- Dark field generator from multi-frame dark average,
- Flat field generator from multiple pointing collections using the technique and software developed for the University of Western Ontario EMCCD project,

- SourceExtractor software package for locating stars and estimating their centroids. Alternatively a very fast star extraction functional module from CAMS (Cameras for All-sky Meteor Surveillance) can be used if run time is found to be critical for SourceExtractor operating on 300 four megapixel image frames,
- Tie-point phase correction method software for estimating translational image shifts to perform frame-to-frame registration. Stand-alone functional modules for translation estimator given a list of object centroids and a bilinear interpolation warping function,
- Star and asteroid chip out function and packaging for product transmission to mimic a spacecraft broadcast of imagery products and metadata.

Current expectations are that ISRU candidate motion across the focal plane, during any given 300 second collection sequence, will be linear and non-accelerating. Thus the internal SALTAD linear search pattern hypothesis generator will be sufficient for detecting motion. However, to ensure that this assumption is correct, during Phase II a study will be done to examine encounter geometries between Sutter satellites and ISRUs within the target range of 8 million kilometers. Tracks will be examined for deviations from linear motion outside the PSF of the sensor. If significant parallax (or curvature) is found, SALTAD has a separate application that can perform non-linear and accelerating motion hypotheses given the satellite state vector in heliocentric coordinates. This is referred to as the Trajectory Generation application and already interfaces to SALTAD via an input file of motion hypotheses.

One important aspect of the ground test is to demonstrate asteroid detection in real-time on the target GPU for Sutter Demo. Thus a breadboard system containing a Tegra-X2

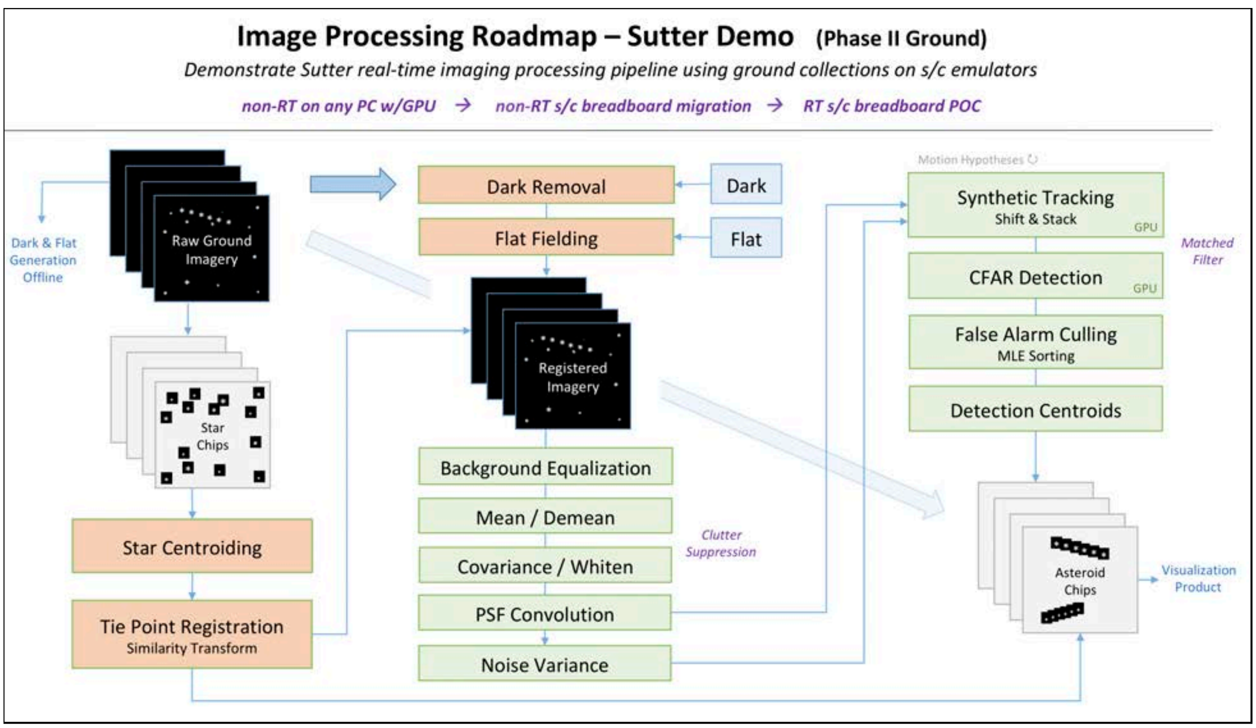


Figure 4-1 Image Processing for Sutter: Ground Demonstration

Table 4-2 Hosting Facility Trade Space

| | Iowa Robotic Observatory | SpaceWatch |
|---|---|---|
| Cost | Very cheap | cheap |
| On-site support | ✓ | ✓ |
| Site access | ✓ | ✓ |
| Machine shop access | ✓ | ✓ |
| Value-added data (e.g. all-sky monitor, weather) | ✓ | ✓ |
| Remote operation | ✓ | ✓ |
| Robotic operation | ✓ | ✘ |
| Nightly operations | ✓ | ✘ |
| High-speed internet | ✘ | ✓ |
| 100% NEO surveying | ✘ | ✓ |
| On-target acquisition signal | ✘ | ✓ |
| Camera mounting | Potential issues | easy |

GPU will be interfaced to a desktop workstation so that the matched filter shift-and-stack operation can be validated in software on the target GPU and verified to meet the real-time processing requirement. Actual star field imagery of asteroids taken with the same imaging system (lens, focal plane, readout, storage) will be fed into the processing pipeline which will have the GPU embedded in the path.

### 4.4.3 Ground Demonstration Host Facility

Hosting options for the ground-based demonstration system have been explored at several US locations. The two best options are the SpaceWatch 0.9 m telescope facility at Kitt Peak National Observatory west of Tucson, AZ and the Iowa Robotic Observatory hosted at the Winer Observatory south of Tucson, AZ. The trade space (see Table 4-2) between working with the two facilities will be explored in Phase II. Figures 4-2 and 4-3 show the SpaceWatch and IRO facilities respectively.

Figure 4-2: The 0.9 m SpaceWatch telescope from above. The dark rounded square plate would be the mounting plate for the demo telescope.

Figure 4-3 The 0.5 m Iowa Robotic Observatory (left) at the Winer Observatory south of Tucson, AZ.

# 5 Key Findings and Conclusions

This Phase 1 NIAC study has provided the analyses and engineering concept development that prove the Sutter Survey Telescope Roadmap is a key to unlocking the potential of space resources.

Named for the Sutter's Mill sawmill (Figure 5-1) where the gold was found that set off the California Gold Rush, the Sutter Survey will pave the way for human exploration, commercialization, and colonization of space. The Sutter Survey spacecraft system will discover the accessible asteroid resources needed to supply NASA's human exploration program and create new, massive, profitable, commercial industries in space including; cislunar tourism, asteroid mining, ever larger new types of robotic satellites, and space manufacturing and colonization. Figure 5-2 is an artist's depiction of a NASA astronaut exploring a small asteroid in heliocentric space supported by a Honey Bee Optical Mining system as enabled by the Sutter missions.

Sutter is a complete discovery and prospecting system. The mission roadmap approach of "walk before you run" using both ground and flight demonstrations, followed by increasingly capable systems, provides a secure and robust path forward. The Sutter Survey followed by Sutter Extreme finds thousands of low ΔV NEOs and characterizes them in terms of size, spin rate, and taxonomic type as needed to enable both asteroid ISRU and human asteroid exploration.

In our Phase II NIAC effort we will complete the ground demonstration of the Digital Matched Filter (DMF) technique to efficiently identify asteroids using a small telescope and off the shelf components. This will pave the way for the Sutter Demo mission in LEO to demonstrate the technologies needed for the Sutter Survey prospecting mission in heliocentric space.

At a cost of just $100M for three spacecraft, Sutter Survey will revolutionize asteroid astronomy and kickstart the gold rush into space by finding hundreds of low ΔV, resource rich targets for human exploration and commercial prospecting.

Sutter Extreme will be a breakthrough mission with capabilities far exceeding Sutter Survey that will find thousands of human exploration and asteroid mining targets while essentially solving the problem of identifying potential Earth impacting asteroids down to a few tens of meters in diameter. Sutter Extreme will out perform far more expensive ground based observation systems with a super high performance heliocentric telescope constellation that can be launched with a single Falcon 9 or equivalent rocket.

The NEOs in highly Earth-like orbits that are the prime targets of the Sutter Survey are our nearest neighbors in space in terms of ΔV, closer than the Moon by that measure. There are thousands of them, and yet they are virtually unexplored. They constitute a potential wealth of trillions of dollars worth of useful materials to support first space exploration and then space industrialization and settlement. It is time NASA and the private sector co-invest in prospecting this space bonanza by funding the missions of the Sutter Survey roadmap.

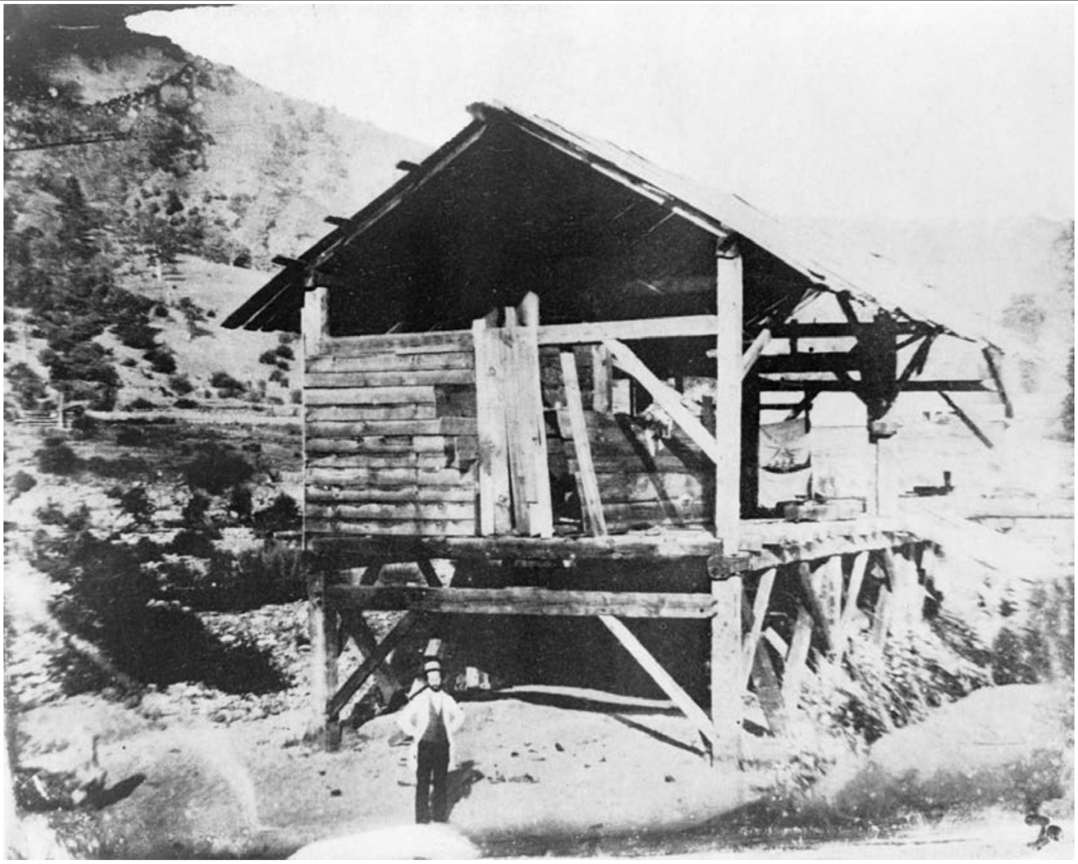

Figure 5-1 Sutter's Mill as photographed in 1850

Figure 5-2 Artist's illustration of potential of asteroid ISRU showing astronauts at asteroid as well as Honey Bee and other vehicles operating in space.

# 6 Bibliography

Beech, Martin, Brown, Peter, "Fireball flickering: the case for indirect measurement of meteoroid rotation rates", Planetary and Space Science, Volume 48, Issue 10, p. 925-932. August 2000.

Bolin, B., Jedicke, R., Granvik, M., Brown, P., Howell, E., Nolan, M. C., Jenniskens, P., Chyba, M., Patterson, G., Wainscoat, R. 2014. Detecting Earth's temporarily-captured natural satellites-Minimoons. Icarus 241, 280-297.

Chyba, M., Haberkorn, T., and Jedicke, R. (2016). Minimum fuel round trip from a L2 Earth-Moon Halo orbit to Asteroid 2006 RH120. In Special Issue of "Recent Advances in Celestial and Space Mechanics", Mathematics for Industry, Springer-Verlag, Japan. Editors: Chyba, Monique; Bonnard, Bernard.

Cyr, O. C. S., Mesarch, M. A., Maldonado, H. M., Folta, D. C., Harper, A. D., Davila, J. M., Fisher, R. R. 2000. Space Weather Diamond: a four spacecraft monitoring system. Journal of Atmospheric and Solar-Terrestrial Physics 62, 1251-1255.

Dawson et al (2016) Blind detection of ultra-faint streaks with a maximum likelihood detector.

Denneau, L., and 43 colleagues "The Pan-STARRS Moving Object Processing System. Publications of the Astronomical Society of the Pacific 125, 357. (2013)

Farinella, P., Vokrouhlicky, D., Hartmann, W. K. 1998. Meteorite Delivery via Yarkovsky Orbital Drift. Icarus 132, 378-387.

Grant et al. (2017) Report of the Near-Earth Object Science Definition Team: Update to Determine the Feasibility of Enhancing the Search and Characterization of NEOs.

Granvik, M., Morbidelli, A., Jedicke, R., Bolin, B., Bottke, W.~F., Beshore, E., Vokrouhlicky, D., Delbo, M., and Michel, P. (2016) "Super-catastrophic disruption of asteroids at small perihelion distances." Nature 530, 303-306.

Gural et al (2005) Matched filter processing for asteroid detection. A.J. 130, pp. 1951-1960

Heinze et al (2015) Digital tracking observations can discover asteroids 10 times fainter than conventional searches. A.J. 150, pp. 125-149

Jedicke, R., Sercel, J., Gillis-Davis, J., Morenz, K. J., Gertsch, L. (2018) "Availability and delta-v requirements for delivering water extracted from near-Earth objects to cis-lunar space." In review for Planetary and Space Sciences.

Mainzer, A., and 34 colleagues (2011) “Preliminary Results from NEOWISE: An Enhancement to the Wide-field Infrared Survey Explorer for Solar System Science.” The Astrophysical Journal 731, 53.

Mohanty (1981) Computer tracking of moving point targets in space. IEEE Trans. on PAMI 3, #5, pp. 606-611

Parker and Kavelaars (2010) Pencil-Beam Surveys for Trans-Neptunian Objects: Novel Methods for Optimization and Characterization. PASP 122, 549

Perozzi et al. (2017) Distant retrograde orbits and the asteroid hazard, The European Physical Journal Plus

Pohlig (1995) Spatial-temporal detection of electro-optic moving targets. ITAES 31, 608

Sanchez,P. and Shceeres, D.J. “The Strength of Regolith and Rubble Pile Asteroids”

Sanders-Reed (1998) Maximum likelihood detection of unresolved moving targets. IEEE Trans. Aerosp. Electron. Syst. 34, Issue 3, pp. 844-859

Schunova et al., 2016 (https://arxiv.org/abs/1611.03095) Meteoritics and Planetary Science, 5 March 2014

Sercel, J., “Asteroid Provided In-situ Supplies (APIS): A Breakthrough to Enable an Affordable NASA Program of Human Exploration and Commercial Space Industrialization,” NIAC Phase 1 Final Report, 2016.

Sercel, J., Jedicke, R., "Space Mission Roadmap to Prospecting Thousands of Asteroids “ NIAC Symposium, Denver, October 2017

Shao, M., Nemati, B., Zhai, C., Turyshev, S.G., Sandhu, J., Hallinan, G.W., Harding, L.K., “Finding Very Small Near-Earth Asteroids using Synthetic Tracking”, The Astrophysical Journal 782:1 (10pp), (2014 February 10), arXiv:1309.3248 [astro- ph.IM].

Skelton, R., Bhattacharya, R., Dunbar, B., Sercel,J., Longman, A., “Growable Tensegrity Artificial Gravity Habitat”, NIAC Annual Review, June 24, 2017

Shucker and Stuart (2013) Detecting asteroids with a multi-hypothesis matched filter. ACM 2008 paper 8388

Stokes et al (2000) Lincoln Near-Earth Asteroid Program (LINEAR). Icarus 148, pp. 21-28

Stramacchia, M., Colombo, C., Bernelli-Zazzera, F. 2016. Distant Retrograde Orbits for space-based Near Earth Objects detection. Advances in Space Research 58, 967-988.

Thomas, C. A., and 18 colleagues 2011. ExploreNEOs. V. Average Albedo by Taxonomic Complex in the Near-Earth Asteroid Population. The Astronomical Journal 142, 85.

Zavodny, M., Jedicke, R., Beshore, E. C., Bernardi, F., Larson, S. 2008. The orbit and size distribution of small Solar System objects orbiting the Sun interior to the Earth's orbit. Icarus 198, 284-293.

Zhai, C., Shao, M., Nemati, B., Werne, T.A., Zhou, H., Turyshev, S.G., Sandhu, J., Hallinan, G.W., Harding, L.K., "Detection of a faint fast-moving near-Earth asteroid using synthetic tracking technique", Astrophys. J. 792, 60 (2014), arXiv:1403.4353 [astro-ph.IM], doi: 10.1088/0004-637X/792/1/60

## Appendix A - Cost Estimates

Cost Estimates were developed for each of the Sutter Flight Missions using the NASA Quick Cost Model. The NASA Quick Cost Model is a parametric estimation model based on a large database of NASA uncrewed space missions. Application of the QuickCost Model uses a very basic set of cost estimating relationships (CERs). In formula terms it is:

$Y = 2.718^{-0.260} \times DryMass^{0.585} \times 2.718^{2.6*BusNew} \times 2.718^{0.231*Destination} + 2.718^{-1.46} \times InstDryMass^{0.475} \times InstAvgWatts^{0.223} \times InstDesLife^{0.386} \times 2.718^{1.44*InstNew}$ .

The Parameter definitions for the formula are:

- $2.718^{-0.260}$ - Scaling factor for Spacecraft Bus
- DryMass – Spacecraft Bus Dry Mass
- BusNew - % of Spacecraft Bus considered new development
- Destination – 0 for Earth Orbit, 1 otherwise
- $2.718^{-1.46}$ - Scaling factor for Instruments
- InstDryMass – Instrument Dry Mass
- InstAvgWatts – Average Instrument Power Usage in Watts
- InstDesLife – Instrument Design Life in months
- InstNew - % of Instruments considered new development

For the Sutter Survey and Sutter Extreme missions, an 80% learning curve was assumed on the 2nd and 3rd flight units. The results of this modeling is presented in Table A-1.

Comparing the cost estimate given by Quick Cost to a ground up estimate for the Sutter Demo mission, it is possible that the actual cost may be closer to 87% of the Quick Cost Model Cost. Applying that correction factor, The Sutter Survey mission comes in at around $87 million while the Sutter Extreme mission is estimated at $450 million. This does not include launch costs.

Table A-1 Result of Cost Model Analysis

| **2016 QuickCost Model with 80% learning curve on Survey and Extreme** | **Sutter Demo** | **Sutter Survey** | **Sutter Extreme** | **Comments** |
|---|---|---|---|---|
| Dry Mass (kg) | 10 | 77 | 673 | Spacecraft Dry Mass |
| BusNew (%) | 0% | 30% | 50% | % New Systems in Spacecraft |
| Destination | 0 | 1 | 1 | 0 for Earth Orbit, 1 otherwise |
| INSTDryMass (kg) | 1.7 | 12 | 35 | Instruments Dry Mass |
| InstAvgWatts (w) | 15.5 | 32 | 59 | Average Instrument Power Use |
| InstDesLife (months) | 12 | 60 | 60 | Instrument Design Life in Months |
| InstNew (%) | 0% | 20% | 50% | % New Instruments |
| Learning Curve for multiple units (%) | NA | 80% | 80% | Based on industry best practices |
| First Protoflight Development Unit Cost (M$) | 4.37 | 38 | 192 | Model results |
| 2nd Unit Cost (M$) | NA | 30 | 154 | Based on learning curve |
| 3rd Unit Cost (M$) | NA | 24 | 123 | Based on learning curve |
| Total Cost (M$) | 4.4 | 91.5 | 468.4 | Sum |
| Operations Cost @ 10% | 0.4 | 9.2 | 46.8 | |
| **TOTAL Mission Cost (M$)** | **4.8** | **100.7** | **515.2** | |
| First Unit $/kg | 445,681 | 487,106 | 285,223 | |
| First Unit $/lbm | 202,582 | 221,412 | 129,647 | |